Modeling cytokine signaling pathways for the study of autoimmune disease

Inna Pertsovskaya

Universidad de Barcelona

Facultad de Biología

Programa de Doctorado de Biomedicina

Línea de Biología molecular i celular de cáncer

Modeling cytokine signaling pathways for the study of autoimmune disease

Memoria presentada por

Inna Pertsovskaya

para optar al grado de Doctora en Biología por la Universidad de Barcelona.

Esta tesis doctoral ha sido realizada en el El Programa de Neuroinmunología del Centro de Investigación Biomédica August Pi i Sunyer (IDIBAPS) bajo la dirección del Dr. Pablo Villoslada y la tutoría de la Dra. Marta Cascante

Dr Pablo Villoslada Diaz	Dra Marta Cascante Serratosa	Inna Pertsovskaya
Director	Tutora	Doctoranda

Barcelona, Abril 2014

On the cover: “View of a Skull”, Leonardo da Vinci, c. 1489

Modeling cytokine signaling pathways for the study of autoimmune disease

Modelos de vías de señalización de citoquinas para el estudio de enfermedades autoinmunes

Inna Pertsovskaya

2014

I dedicate this thesis to my mother,
the most inspiring example of an outstanding person

Acknowledgements

I would like to thank my PhD advisor, Dr Pablo Villoslada, for constant support during last 5 years. Dr Villoslada is not only an excellent researcher but also a helpful and supportive supervisor who always finds the way to inspire me to climb the career stairs and achieve new levels of understanding of nature.

I'm grateful to Prof. Marta Cascante for her tutorship of this PhD thesis. I would like to thank the committee members, Prof. Patrick Aloy, Prof. Carlos Rodrigues and Prof. Blas Echebarria, for finding time to review my thesis and attend the defense.

I would like to thank Prof. Andrey Mironov, my University supervisor, with whom I was born as a scientist.

I also would like to thank my collaborators: Prof Jordi Garcia Ojalvo Dr Elena Abad from Universitat Pompeu Fabra, Dr Julio Saez Rodriguez and his fellows from European Bioinformatics Institute, Prof. Jesper Tegner and Dr Narsis Kiani from Karolinska Institutet and others.

All our supportive lab members contributed to this thesis come true. I would like specially to mention Dr Beatriz Moreno and Dr Ekaterina Kotelnikova. I would like to thank Gemma Vila and Begoña Fernandez for their direct involvement in projects and hand-on help with experimental procedures.

I would like to thank my all-time best friend and supervisor Dr Alexander Favorov for recommending me as an UEPHA-MS trainee in Dr Villoslada's lab. Sasha is a friend who gives the confidence in the world. I'm also grateful to many and many of my friends who were directly and indirectly involved in my life during the last 5 years, especially Encarna Busquet, Evgenia

Redkozubova, Vesna Prčkovska, Ekaterina Nevedomskaya, Natalia Timakova and many-many others.

I would like to thank my mother for her lifelong help and support; for her love and example; for the great starting push she gave to my career and me.

I would like to especially thank my husband, Alex Virgili, for his incredible support during all the time and especially in the last hard months of my PhD. Thank you, Alex, for your constant love and moral and physical support during this time. Thank you for being such a great partner and father (and sometimes mother). I would like to thank my daughters, Olesya and Patricia, for bringing joy and happiness to my life and giving sense to each and every day.

Funding

This work was supported by the EU 7FP – Marie Curie initial training network UEPHA*MS (ITN-212877), Fundacion Cellex, by the Spanish network of excellence in MS of the Instituto de Salud Carlos III, Spain (RD07/0060), by EMBO Short term fellowship (EMBO ASTF 308-2012) and by EU 7FP CombiMS network (HEALTH-F4-2012-305397).

Summary

Systems Biology opens new frontiers in the studies of complex diseases such as Multiple Sclerosis (MS). The questions that couldn't be addressed before due to lack of understanding and methodological base, such as the molecular mechanism of action of many drugs on the signaling pathways, were resolved using new Systems Biology vision of nature. Signaling pathways have dual biological and mathematical nature. Modern Systems Biology developed various methods to model signaling pathways and predict their behavior in different conditions.

This dissertation is focused on some of the key molecular mechanisms of signal transduction in MS development and progression, which are important in order to explain the mechanism of action of the common MS drugs.

My main hypotheses are based on the assumption that the most important art of the biological system are the connections between molecules rather than the molecules themselves (e.g. edges rather than nodes of the model graph). For example, the immune cell subtypes have different response to the external stimulus because the molecules regulate different activities of each other inside the cell rather than the components of the cells are different. Another examples of it are the kinetic changes driven by the changes in the translocation activity of the Stat1 protein.

To prove my hypothesis, I developed two different mathematical models of IFNbeta pathway: Boolean and ordinary differential equations (ODE). The combination of two modeling approaches allowed us to look at the same pathway from two perspectives: in connection with other related pathways and as a

kinetic system. We identified oscillatory and damped oscillatory regimes in the IFNbeta signaling and the key sensitive parameters, which determine the switch of the regimes. Both model were validated experimentally and leaded to several predictions, which could be important for the development of new drugs or drug combination. For example, the bifurcation analysis of the kinetic model revealed the importance of the features of the nuclear translocation of the Stat1 protein for the correct functioning of the signaling pathway. Sgk/Akt-Foxo3a is another pathway described, modeled and validated in my dissertation. The nuclear translocation is a known key element of this system, but we focused on the on/off circuit mechanisms and the importance of the combination of different phosphorylation sites for signal transduction.

The main outcomes of this work are:

1. New models of IL6, IFNbeta and Akt/Sgk signaling pathways
2. Predicted prevalence of translocation parameters over the phosphorylation rates on the IFNbeta pathway
3. New method of the application of the Boolean model workflow to the clinical data

As a conclusion, the Systems Biology is a powerful tool to predict new properties of the biological systems, which can be used in clinical practice, such as dynamical biomarkers or differential signal transduction. Thus, Systems biology provides a new approach to search for new treatments and biomarkers of autoimmune diseases.

Preface

"Every object that biology studies is a system of systems"

Francois Jacob, [1]

The complexity of life and molecular processes underneath it is an exciting topic of research that shows the limitations of human brain that struggles to analyze the whole picture. That's where the models and modern computational power come to hand and help to reach the higher level of understanding. The traditional biological approach of "dissection" of the object of interest and analyzing parts doesn't provide new knowledge due to its obvious limitations. During the last several hundred years we learned a lot about the parts but still lack the knowledge about their functioning as a whole. Another traditional biological method is categorizing. The organisms, cells, molecules were categorized in different groups and subgroups (based on evolutional, phenotypic, genetic or other characteristics) and analyzed based on the differences and commonalities.

Biologists and clinicians face more and more complicated challenges trying to answer modern medical questions. One of these topics is neuroimmunological disease, such as Multiple Sclerosis (MS). The complex nature of MS combines genetic and environmental factors and the cause of the disease remains unclear [2]. Classical approaches are not able to capture the complexity of the interactions between different species involved in the development of the disease. For this reason, scientific community intends to develop and put in practice new methods of clinical research based on the interdisciplinary approach. For example, CombiMS consortium (http://www.combims.eu) aims to develop

new combination therapies for MS by combining phosphoproteomics studies with Systems Biology approach.

Systems Biology approach in molecular biology, although has its own limitation, is a new way to capture the sense of biological processes and analyze the interaction network in all its complexity. This dissertation aims to develop new methods and workflows to put together theoretical Systems biology and practical drug discovery.

This thesis is organized in several parts: general introduction, hypothesis, objectives, materials and methods, results and general discussion. It also includes references and supplementary data sections. The results are organized in several chapters representing separated but interconnected parts of my work:

Chapter 1. Theoretical considerations on pathway dynamics in individual cells and cell populations

Chapter 2. The Boolean model of IFNbeta signaling in human cell lines and a new approach to analyze clinical experimental data for the drug combinational therapy

Chapter 3. Kinetic model of the IFN-beta signaling pathway in macrophages

Chapter 4. Nuclear translocation as a modulator of the pathway kinetics. IFNbeta pathway example

Chapter 5. AKT/SGK-Foxo pathway model

Table of content

Introduction **3**

Mathematical modeling approaches in biomedicine **3**

Most common patterns in signaling **9**

Different methods of modeling in Systems biology **13**

Models as logic systems 14

Models as dynamical systems 15

Populations of cells versus single-cell modeling **17**

Signaling pathways involved in Multiple Sclerosis **19**

IL6 signaling **22**

IFNbeta signaling **24**

Sgk/Akt-Foxo3a signaling **28**

Systems biology approaches in the development of new biomarkers and drug combinations for autoimmune diseases **33**

Hypothesis **35**

Objectives **39**

Materials and methods **41**

Materials and reagents **41**

Human samples **41**

Cell culture and stimulation **41**

RT-PCR **43**

Western blot and quantification **44**

ELISA and xMAP multiplexing assays **44**

Mathematical modeling **46**

Boolean model 46

ODE model 49

Parameter space exploration for Foxo-Akt model 50

Results **51**

Chapter 1. Theoretical considerations on pathway dynamics in individual cells and cell populations **51**

Chapter 2. Differential role of IFNbeta signaling in T cells and macrophages modeled with Boolean networks **58**

Boolean modeling of IFN pathways in Jurkat and THP1 cell lines.....58

The pipeline to apply Boolean modeling to the clinical data 63

Chapter 3. Kinetic model of the IFN-beta signaling pathway in macrophages **67**

Chapter 4. IFNbeta model analysis and nuclear translocation as a modulator of the IFNbeta pathway kinetics **75**

Chapter 5. Nuclear translocation dynamics of Foxo3a orchestered by Sgk/Akt balance **83**

Discussion **87**

Conclusions **97**

List of figures **99**

References **105**

Supplementary data **114**

Resumen en castellano **121**

Annex 1. Curriculum vitae **140**

Annex 2. Published work **143**

Introduction

Mathematical modeling approaches in biomedicine

Cell is a complex system with millions of elements working together as a whole. To understand the grade of complexity of the living organism, scientists developed a new field, Systems biology.

The understanding of the idea that the organism is not just a sum of its elements is not new. It was known and acknowledged from the ancient times with Aristotle's famous "the whole is something over and above its parts and not just the sum of them all''. Nevertheless, later on in the middle ages the reductionists approach was the mainstream paradigm of biological research. The prevalence of reductionism was favored by the development of physics and ideas of Rene Descartes in the 17th century. The prevalence of the reductionism was based on the idea that all complex systems can be explained by explaining their parts. The mechanistic biology was based on the reductionism theory. Its ultimate expression was expressed in the book "The mechanistic conception of life: biological essays" by Loeb Jacques (1912) [3]. He summarized the paradigm of the mechanistic biology stating that the biological behavior was predetermined, forced, and identical between all individuals of a particular species. He concluded that the organisms were merely complex machines. In the beginning of the 20th century the holism concept was proposed to oppose the reductionism. Whole systems such as cells, tissues, organisms, and populations were proposed to have emergent properties. It was impossible reassemble the behavior of the whole system from the properties of the individual components. [4]. Even though the holism and reductionism

theories were generated in oppose to each other they can be used together. The two approaches answer different questions and can complement each other.

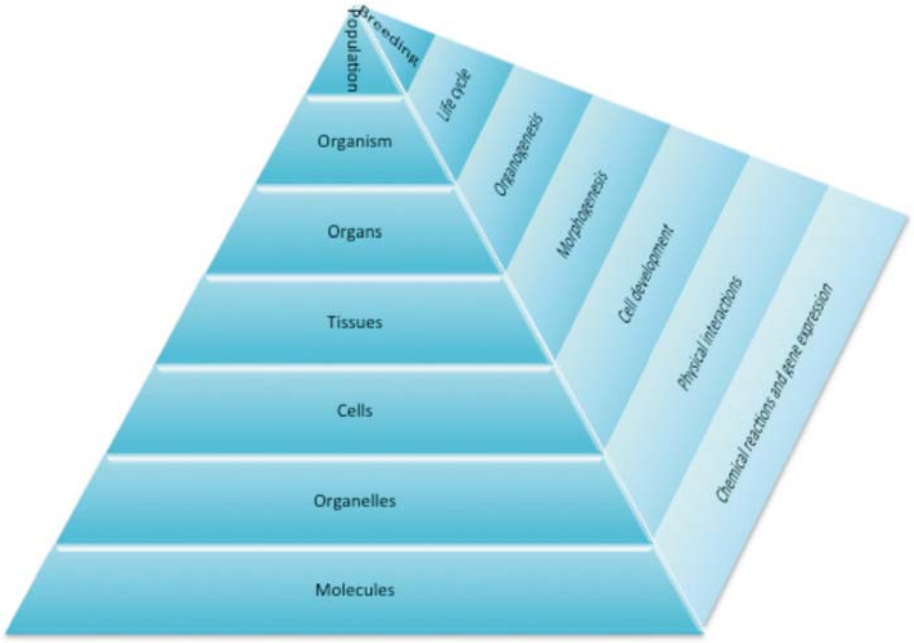

Figure 1 A simplified hierarchical structure of a living system. The system is composed by the components with increasing complexity. On one edge of the pyramid are the physical entities and on the other their functional properties.

The turning point in the history of Systems biology is the 1950s. At this time the breakthrough book was published by Roger Williams [5]. Williams showed huge differences in physiological parameters and even organ size of normal healthy humans. Thus, it's the systems balance that creates independent biochemical and physiological pattern and adopts and tolerates that variation. The tolerance and the resistance to variation is what differ living organism from mechanical machines. The victory of systematic, holistic theory promoted various studies, which leaded to the

establishment of Systems theory. Systems theory states that two basic emerging features of any system are hierarchy and interconnectivity.

The recognition of the hierarchical organizational properties of the system represented an important advance in understanding of the properties of biological phenomena [6]. A simplified example of hierarchy on living system is show on the fig. 1. Each level in the hierarchy is an emerging property of the complex interactions inside the lower level. At the same time, each level is consisted of several subsystems each representing an emergent properties on its own, which can also be arranged in the hierarchical organization [7]. One of the main recognized features of the biological system is interconnectivity. Interconnectivity is a more complicated concept. It includes different connections between systems, networks and individual components (fig.2). Interconnectivity between different layers of the hierarchy was first recognized in the late 60s. Polanyi (1968) first clarified the relationship between levels in a hierarchy. He showed that adjacent levels mutually constrain but do not determine each other and emphasized that the upper level harnesses the constituents of the lower level to carry out behaviors that they would not perform on their own [8].

At the same time scientific community identified numerous example pointing that the layers of the hierarchy are highly connected in a more complex system rather than working as independent blocks. This recognition led to the formulation of the general systems theory by Von Bertalanffy [9].

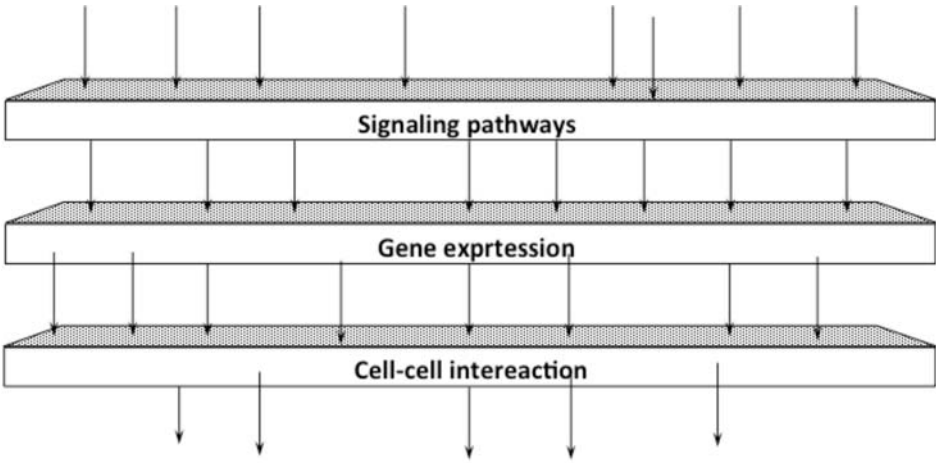

Figure 2 The interconnection between different layers of cellular system. This figure represents only the connections between different layers of signaling. The interconnections create increasing complexity systems of intersections and relationships between subsystems in the same layer and between different layers of the hierarchical system.

Bertalanffy argued that all systems shared the similar properties and were composed of interconnected components; therefore they should share similarities in detailed structure and control design. Nowadays the theory received strong evidence based on the studies of mathematicians, physicists, biologists, and physiologists. It's believed that hubs and connectors represent a common stable structure of a real system. Hubs are the central components, which are linked to many other nodes in the system, while connectors are connected to a few other nodes (fig. 3) [10].

In the 20th century Systems biology evolved from molecular biology in two parallel historical roots [11]. On one side the most acknowledged root is based on the technological breakthroughs in the genomics and other "omics" disciplines.

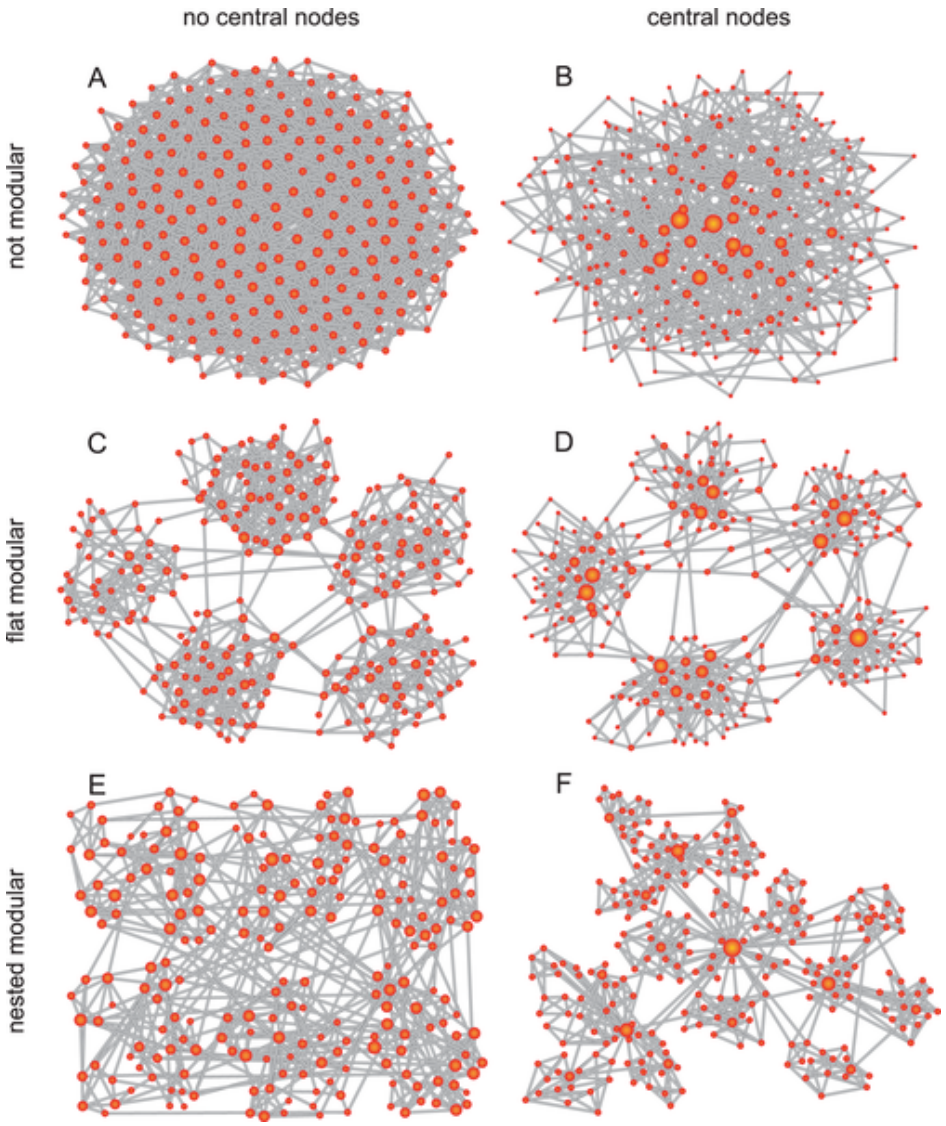

Figure 3 Basic graph models representing different combinations of both modular and hub characteristics from [12]**. Most real Systems are both modular and contain hubs (central nodes), e.g. D or F graphs of the figure.**

While new technologies increased exponentially the amount of biological information, new methods were needed to comprehend and analyze them. This root led to the big networks of connections and was more "statistical" in character. These networks can explain and describe a system as whole but lack

dynamical dimension.

The other root of the historical development of Systems biology is much less known. It consisted of the effort, which was constantly focused on the formal analysis of new functional states that arise when multiple molecules interact simultaneously. These approaches were historically called nonequilibrium dynamics and may be seen as an ancestor of the modern Systems biology. The main characteristic of this discipline raised from this root was the focus on the discovery of general principles rather than descriptions. The nonequilibrium dynamics was interested in such traditionally physics concepts as oscillators, chaos, noise, steady state and symmetry of the systems.

Until the end of the 20th century the dynamical and theoretical biology was highly rejected by the biological community as "unuseful" for answering "real" biological questions. The beginning of the 21st century marked the phenomena of the convergence of the two paths in to one mainstream Systems biology approach. The reductionism is now giving its way to the holistic tendency in biology under the pressure of growing amount of big data. As a result the convergent Systems biology unites the dynamical methods and high-throughput statistical models creating impressive mathematical constructs to explain increasingly complex systems. For example in the work of Karr et al. the whole-cell model predicts the behavior of the entire simple organism [13].

The main difference between Systems biology and traditional Molecular biology is the focus on the connections rather than on the molecules forming them. Systems biology takes the cell as a

complex interacting system and analyzes the connections and common patterns of this system. What seemed to be the universe of different structures and patterns at the end was shown to be the combination of several commonly repeated circuits, which lead to several classes of behavior responses [14]. Evolutionary chosen circuits are sharing similar characteristics: resistance to noise and perturbations, stabilizing power together with sensitivity to the external factors. These features are critical for the survival of the living organism and its functional stability in the complex environment. Natural selection selected the best evolutionary adapted to the environment circuits, which are both functional and stable. These circuits are responsible for all the variety of responses and behaviors of the cell, which includes, among others, oscillatory and overdamned oscillatory behaviors, exponential and sigmoid curves, pulse generators, bi-stable motifs and more complex combinations of different patterns and circuits.

Most common patterns in signaling

The building blocks of complex networks are called network motifs. In other words network motifs are the patterns that appear significantly more frequently in real networks than in randomized networks [15]. The network motifs are persistent in the regulatory networks. It was speculated that this persistence is a result of evolution and the motifs are derived from the constant selective pressure that means their structures provide advantages in natural selection. Nevertheless, many studies suggest that the the common subgraphs within network may be selected by nature a posteriori to their appearance and the abundance of motifs is a

byproduct of the network construction process [16]. In any case, motifs are useful tools to construct biological networks.

There are several common network motifs, which are also present in the models described in this dissertation:

1. Single input and regulatory chain
2. Feed-forward motif
3. Positive and negative feedback loops

The graphical representation of different motifs is shown on fig. 4.

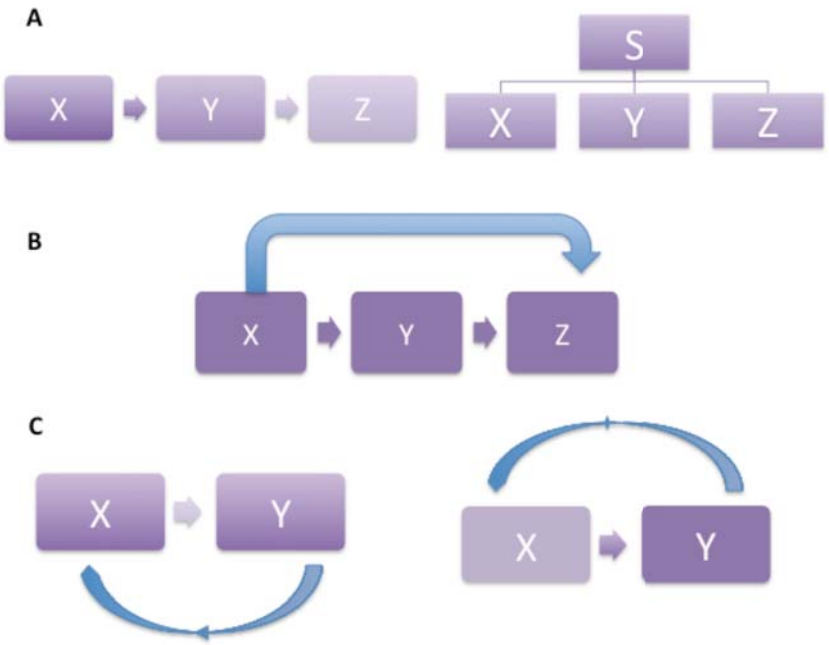

Figure 4 Most common network motifs. A – regulatory chain (left) and single input (right); B – feed-forward motif; C – Feedback loops: positive (left) and negative (right).

Different motifs produce different dynamics of the system. For example, negative feedback loop leads to oscillatory behavior of the system. Oscillators are very common in signaling systems and commonly appear when the product of some transcription

factor (TF) activity inhibits the activation of this TF thus producing a negative feedback loop (fig. 5).

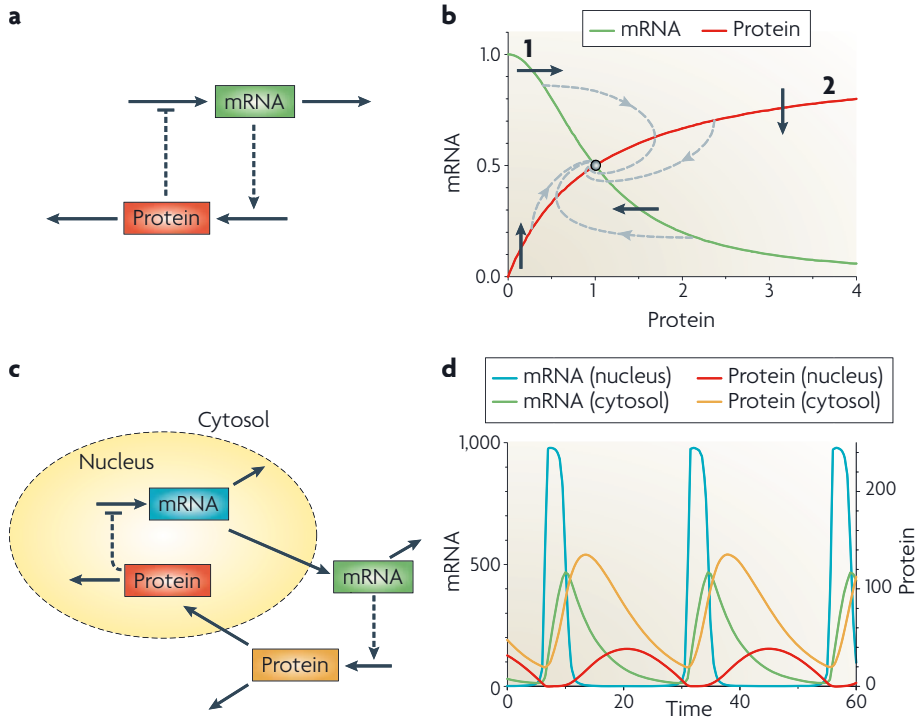

Figure 5 Multi-component negative-feedback oscillator. A. Negative feedback between mRNA and protein, as described by kinetic equations in the text. B. Representative solutions (dashed curves) of equations in the text, for parameter values: $p = 2$, $K_m/K_d = 1$, $S/K_d = 1$, $k = k = 0.1$ min^{-1}, $k = k\,E\,/K = 1$ min^{-1}. Notice that every trajectory spirals into the stable steady state located at the grey circle. C. The negative-feedback loop, taking into account transport of macromolecules between the nucleus and the cytoplasm. D. Sustained oscillations for the four-component loop in panel. From [17]

The negative feedback showed on the fig. 5 can be represented by the following equations [17]:

$$\frac{dX}{dt} = k_1 S \frac{K_d^p}{K_d^p + Y^p} - k_{dx}\,X$$

$$\frac{dY}{dt} = k_{sy}X - k_2 E_T \frac{Y}{K_m + Y}$$

where X and Y are mRNA and protein concentrations, k_{dx} and k_{sy} for degradation of mRNA and synthesis of proteins, the term

$$k_1 S \frac{K_d^p}{K_d^p + Y^p}$$

is the rate of the RNA synthesis and the term

$$k_2 E_T \frac{Y}{K_m + Y}$$

is the term for protein degradation.

So with only 2 (or even one with explicit time delay) equations we may reproduce the oscillatory behavior that we see so frequently in the biological systems.

Bistability is a situation in which two possible steady states are both stable. In general, these correspond to a "low activity" state and a "high activity" state. There are several patterns that may produce bistability (fig. 6). Each of them produces bistability only in the certain range of parameters, e.g. it's not mandatory for the systems containing mutual activation or mutual inhibition circuits to lead to bistability.

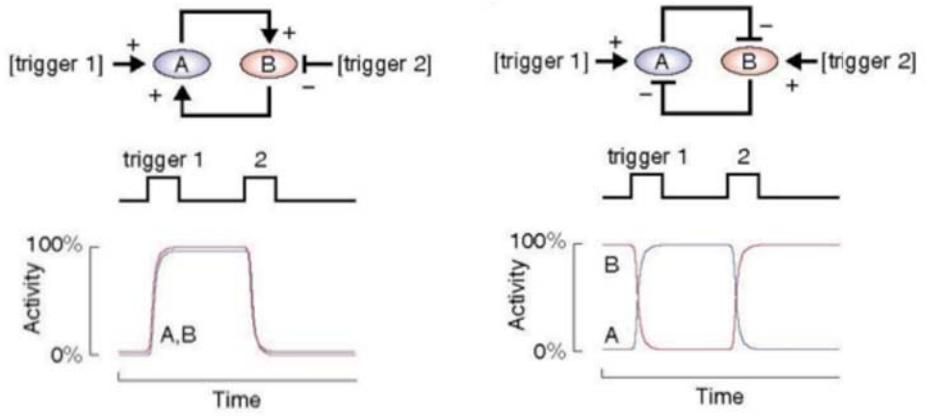

Figure 6 The circuits, which may produce bistability: mutual activation (on the left) and mutual inhibition (on the right). From [18]

In the bistable system the multiple steady states are possible and the initial conditions determine which steady state is reached [19] The examples of bistable systems include lac operon in E. coli [20] and MAPK cascade [21]. In our model of IFNbeta we also found bistability and analyzed the bifurcation (see chapter 4 of the results section).

Different methods of modeling in Systems biology

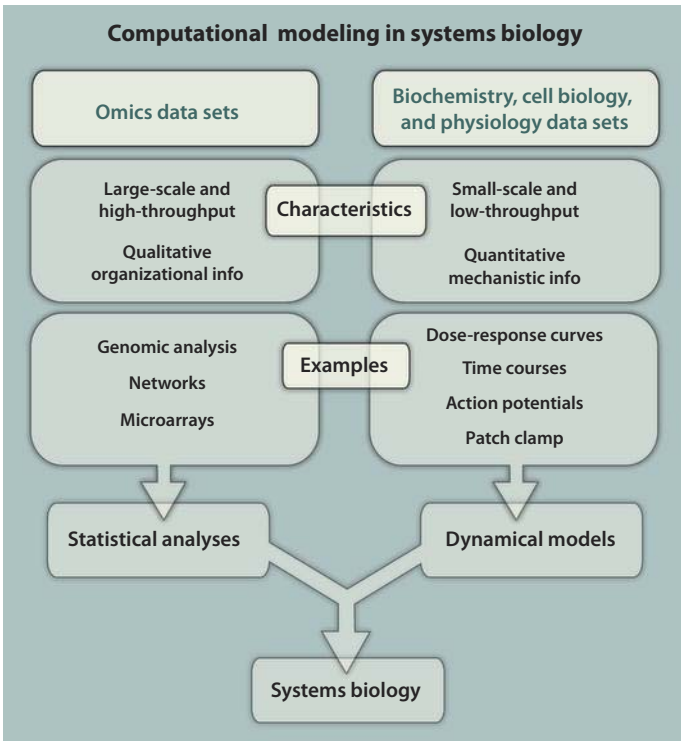

Figure 7 Data sets can dictate the computational approaches used in systems biology. (Left) Omics technologies generate extremely large data sets that can be analyzed and organized into networks by using statistical modeling techniques. This strategy can be considered "top-down" modeling. (Right) When high-quality data are available, smaller-scale systems can be represented by dynamical models, and simulations with these models can generate quantitative predictions of system behavior. This strategy is sometimes called "bottom-up" modeling. Both approaches are important in systems biology, and a few cutting-edge studies combine the positive aspects of both. From [22]

There are two basic approaches in Systems Biology, which rose from the two historical paths of the scientific field development we discussed above. The first one evolved from statistical methods and is called "Top down" and the other one, dynamical, is called "Bottom up" (fig. 7) (from Coursera "Dynamical modeling methods for Systems biology" course by Eric Sobie).

Models as logic systems

"Top down" method commonly involves following steps:

1) Begin with data set (often very large scale)

2) Use statistical methods to find patterns in the data.

3) Generate predictions based on the structure within the data

The amount of data and the size of the networks obligate the researchers working in this area of Systems biology to propose the simplified approaches to assess large-scale data. One of the approaches is to design logic, static or semi-static models, which are qualitative or limited in terms of quantifying time-dependent changes. One of the common methods is logic modeling which treats the connections between molecules as logic variables [23]. The logic modeling consists of building a Boolean network where nodes are connected with binary edges (the values on the edges can be only ON or OFF). The nodes can be AND or OR logic functions. There are many deviations and add-ons to make this simple models more flexible, include time or stochastic inputs [24].

In this dissertation we used the software designed by Dr Saez group in EBI and called CellNoptR [25]. The R package is available in Bioconductor and depends on RBGL and graph packages (http://bioconductor.org/packages/2.10/bioc/html/CellNOptR.

html). CellNoptR package does optimization of Boolean logic networks of signaling pathways based on a previous knowledge network (PKN) and a set of data upon perturbation of the nodes in the network. The detailed information on the usage of the package can be found in the package manual and the methods section of this dissertation.

Models as dynamical systems

"Bottom up" approach is based on the following sequence of steps:

1) Begin with hypothesis of biological mechanism.

2) Write down equations describing how components interact.

3) Run simulations to generate predictions.

The classical method to model dynamical biological system is by set of ordinary differential equations (ODE). ODEs describe the model as variable changes in time:

$$\frac{dy}{dt} = f(y, p)$$

where y – is a variable and p – a vector of parameters. Depending on the number of variables the system may have multiple dimensions. Each new dimension leads to increasing number of possible dynamical outcomes of the system. While one-dimensional reactions are able to produce only steady state dynamics, the three-dimensional systems produce several different kind of dynamics, e. g. steady state, limit cycles and chaos [26].

Many signaling pathway events are explained by using a modified Hill function. Hill function is typically used in

biochemistry to describe ligand-binging reactions based on Michaelis-Menten dynamics:

$$\frac{d[P]}{dt} = \frac{V_{max}[S]}{K_m + [S]}$$

Hill function describes many real gene input functions, which are usually monotonic S-shaped functions. The Hill function for an activator is a S-shape curve that rises from zero and approaches a maximum saturated level:

$$f(y) = \frac{\beta x^n}{K^n + y^n}$$

where K is an activation coefficient, β is a maximum expression level and n is a Hill coefficient, which corresponds to the steepness of the function [14].

One of the main challenges in ODE modeling approach is the number of parameters. The parameters should be assigned or fitted to achieve the desired simulation outcome. There are different ways to fit the parameters:

1. Manual fit. This way the parameters are obtained from the experimental papers and adopted to the model [27];
2. Automatic fit. There are various algorithms and methods to automatically fit the parameters to the data [28–31]. Most of them are based on the exploration of the multi-dimensional parameter space to find the combination of parameters, which corresponds to the maximum model fit to the data (fig. 8); We used manual fitting and literature search to obtain parameters for IFNbeta ODE model (see results).
3. Exploration of the parameter space. The other approach to solve the parameter problem in the dynamic systems is the exploration of the all possible qualitative outcomes of the big

range of parameters. The workflow we use here to explore the parameter space of Foxo3a pathway models was developed by Gomez-Cabrero et al. [32].

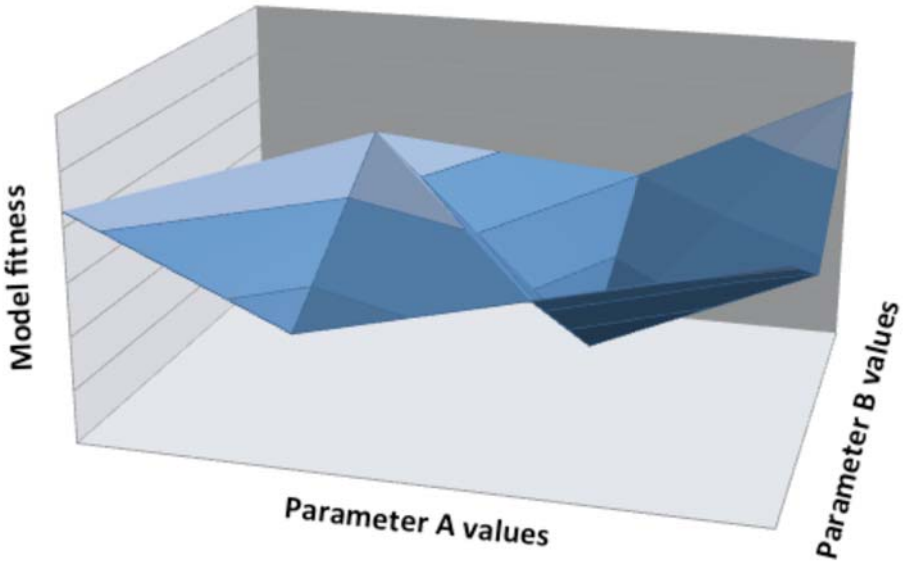

Figure 8 The 2-dimensional parameter space vs model fitness to the data. Most of the algorithms search for the combination of parameters to maximize model fitness.

Populations of cells versus single-cell modeling

Most experimental data are coming from the analysis of cell populations (Western blot, RT-PCR, Elisa, Luminex and other methods are working with cell lysates). Population level measurements may not only average out the variation in the response and mask heterogeneity, but also hide important biological phenomena (fig. 9).

Nowadays the advanced technologies allow several techniques to measure the protein concentrations and phosphorylation on a single-cell level. These methods include, among others, Flow cytometry and derived from it flow imaging

ImageStreamX (Amnis co.) system. Flow cytometry measure the fluorescence signal from each individual cell on a high-throughput manner [33]. The standard analysis of flow cytometry data averages the signal from the single-cell measurements, but we can use the raw data to verify the behavior of the pStat3 on a single-cell level.

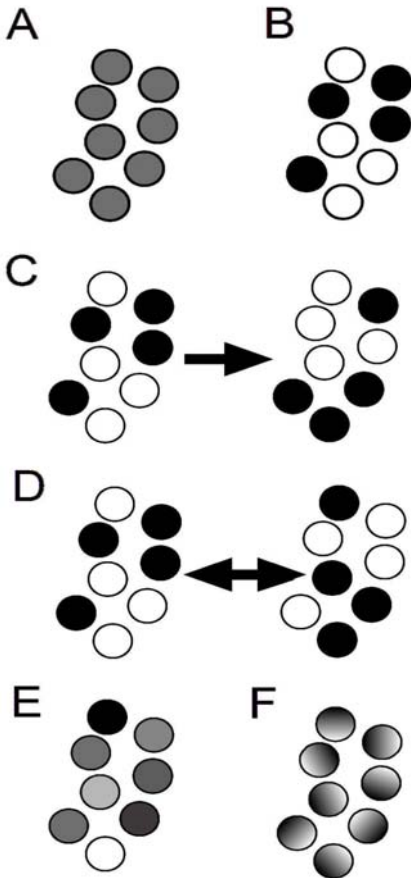

Figure 9 Examples of single cell behaviors that produce the same average population behavior. Individual cells are shown as circles with each cell's signaling activity denoted by its color; black denotes 100% signaling and white denotes 0% signaling. The population average for each panel is 50%. In panel A, each cell signals at 50%. In panel B, half of the cells are in the 100% state and half of the cells are in the 0% state. In panel C, cells are as in panel B, but individual cells may switch states in time without affecting the population average. The switching may occur stochastically, or result from

oscillatory signaling activity whose phase and frequency vary from cell to cell. In panel D, cell signaling is distributed between 0 and 100%. In panel E, signaling within a cell is spatially heterogeneous such that the average signaling within each cell is 50%. From [34]

Classical ODE modeling is based on assumption that there are enough of molecules of the modeled species to justify the usage of the concept of concentrations as a smooth function. This assumption is often inaccurate for signaling in single cells [34]. Signaling within individual cells often behaves probabilistically and requires stochastic simulations. The formal way to represent a stochastic system is commonly used chemical master equation which represents the probability that the system contains a certain number of molecules evolves over time [35].

Signaling pathways involved in Multiple Sclerosis

Multiple Sclerosis (MS) is an autoimmune disease affecting more than 2 million people worldwide. MS is an autoimmune inflammatory disease of the central nervous system (CNS). MS is chronic and the progression depends significantly on the individual, but it nearly always culminates in the increasing disability. MS normally begins in the young adulthood and is driven by inflammatory attacks against myelin protein, which covers the axons of the neurons. The zones of the brain affected by demyelination process are visualized on the MRI scans as plaques [36]. The symptoms vary depending on the zone of a new immune attack.

There are several different types of the MS: relapsing-remitting (the most common), primary progressive, secondary progressive and progressive-relapsing forms (fig. 10).

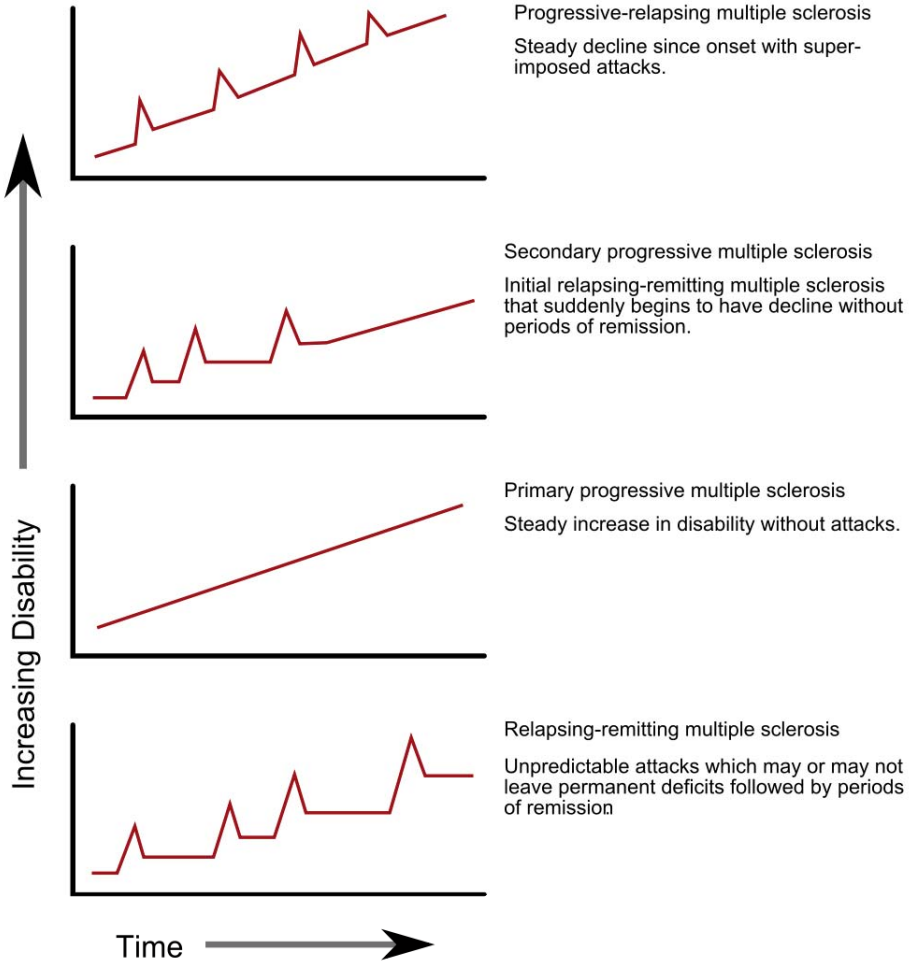

Figure 10 Different types of MS produce different clinical course.

All forms of MS are characterized by abnormal immune activity both in the blood and in the brain. The T cells are the main drivers of the immune attack on the myelin. Normally the immune attack occurs during a short period called relapse followed by a longer period of remission and partial recovery due to the reparation ability of the brain driven mainly by glial cells. The neuroinflammatory period of the disease is often followed by increasing neurodegenaration. Neurodegenaration is characterized

by axonal damage and brain volume reduction and no partial recovery (fig. 11).

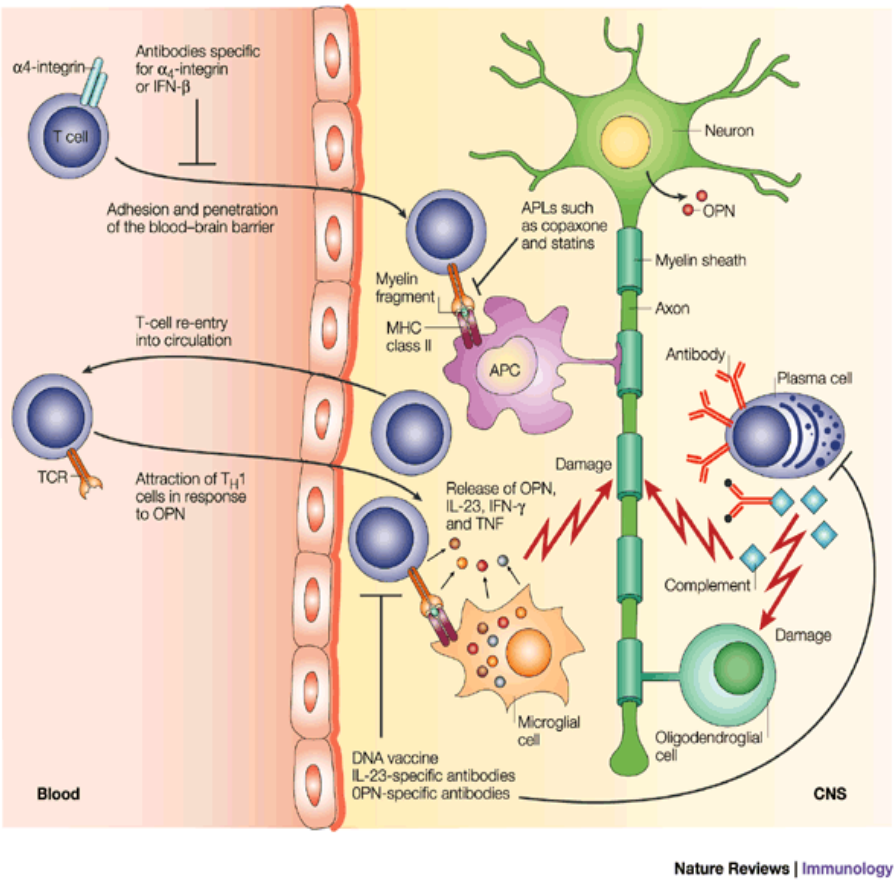

Figure 11 The inflammatory phase of multiple sclerosis. T cells, B cells and antigen-presenting cells (APCs), including macrophages, enter the central nervous system (CNS), where they secrete certain chemicals known as cytokines that damage the oligodendroglial cells. These cells manufacture the myelin that insulates the neuronal axon. The injured myelin cannot conduct electrical impulses normally, just as a tear in the insulation of a wire leads to a short circuit [37]

The cause of MS is unknown but it's believed that both genetic and environmental factors are involved. There are more than 100 SNPs recognized as associated with MS by recent genome-wide association studies [38]. The environmental factors include, among others, infections (associated with EBV, HHV6,

MSRV), vitamin D and sun exposition, smoking, diet and western style of life.

The treatment options of MS are limited to disease-modifying therapies primary targeting the inflammatory part of the disease, but not neurodegenaration. Immunomodulatory drugs currently used in the treatment of MS are divided in first line therapy (Interferon beta (IFN-beta), glatiramer acetate (GA)) and second line therapy (natalizumab, fingolimod or mitoxantrone).

There are several key signaling pathways, which are crucial either in disease progression or treatment efficacy. The list of known MS-related pathways include IFNbeta signaling, S1P signaling, TLR, different interleukin-modulated pathways, vitamin D signaling, PI3K signaling, TrkA and TrkB and others.

In this dissertation we are focused on the several of these pathways: IL6 signaling pathway, IFNbeta signaling pathway and PI3K-Foxo pathway.

IL6 signaling

IL-6 is a pleiotropic cytokine with important role in immune regulation, hematopoiesis, inflammation and oncogenesis. IL-6-type cytokines exert their action via the signal transducer gp130 that associates with IL6R in a cooperative manner to form a hexameric signal transducing complex, capable of activating the down stream mediators of this signaling pathway. This mechanism of signal transduction is shared by other members of the IL-6 type cytokines like IL-11, leukaemia inhibitory factor, oncostatin M, ciliary neurotrophic factor and cardiotrophin-1 that use gp130 as a common subunit of the signal transducing complex [39]. IL-6 stimulation leads to the activation of Jak/Stat pathway

[40] (fig. 12) . Stat3 protein is phosphorylated and is able to form homodimers after activation leading to their its localization and subsequent regulation of transcription of respective target genes.

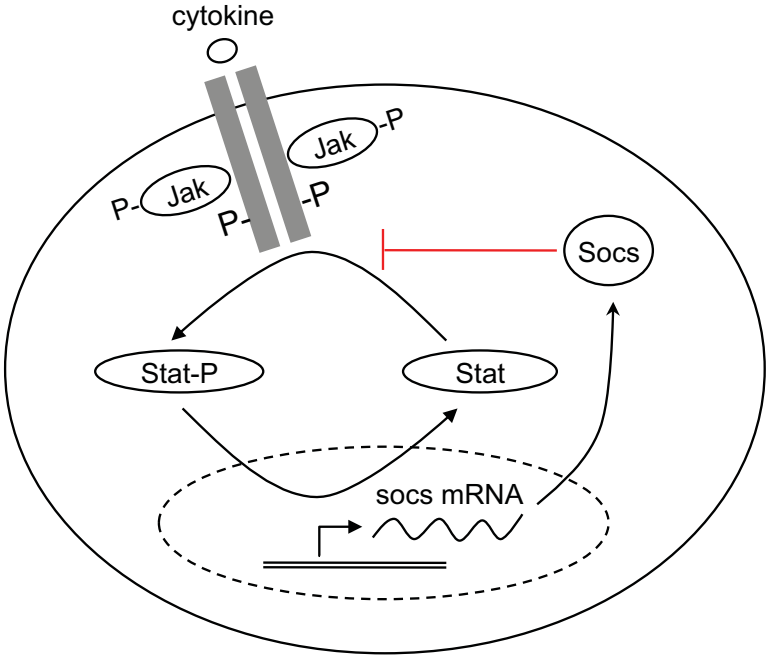

Figure 12 The main events of IL6 signaling and pathway self-regulation. Schematic representation of the circuit. Cytokines bind their membrane receptors, causing a cascade of phosphorylation reactions that triggers Stat activation. Active Stats upregulated the transcription of the repressors SOCS, which inhibit Stat phosphorylation

SHP-2 is one of the ubiquitous tyrosine phosphatases and IL-6 stimulation leads to the SHP2-dependent activation of MAPKs, it also links the Grb2–SOS complex and Gab1 to gp130. Phosphorylated Gab1 acts as an adapter and is involved in the indirect association of SHP-2 and PI-3 kinase. Downstream activation of Vav1, Rac-1 and MAP2K4 is necessary for the IL-6-mediated Stat3 phosphorylation and transactivation to accomplish its effects. PTPN11 and SOCS3 exert inhibitory function and thus lead to down regulation of the signaling cascade.

IFNbeta signaling

One of the most studied prototypical signaling pathways in MS is type I interferon pathway. This is a pathway driven by Jak-Stat signaling. It is able to integrate environmental information related with infection (virus and bacteria) through the ligation with more than 15 different IFNα and one IFNβ. The canonical type I interferon (IFN) pathway involves different signaling cascades, one of which is the Jak/Stat pathway. This pathway is composed by several steps, which include receptor binding, transformation of the latent transcription factor (a protein of the Stat family) into its active form by phosphorylation, nuclear migration of the transcription factor (TF), binding of the TF to target promoters, and expression of their corresponding genes [41]. Type I IFNs bind to IFNAR1 receptors, phosphorylation of Jak1 and TYK2 proteins transmit the signal downstream, phosphorylation of Stat1 and Stat2 proteins allows to form the ISGF3 complex (pStat1-pStat2-IRF9) which binds to the ISRE binding sites in the nucleus. Previous studies have shown that phosphorylated Stat1 forms other TF complexes in response to type II interferons, the most important of which is a Stat1-Stat1 homodimer, known as GAF, that binds to IFN Gamma-activated sequence (GAS) elements [42].

It was shown that at the same time that the ISGF3 complex is formed due to the stimulation, there is also formation of other transcription factors containing activated Stat1 [43]. The main one of them is GAF (Stat1-Stat1 homodimer), the primer complex for the type II IFN pathway (fig. 13). There are different activator and inhibitor molecules, which regulate the Stat1 tyrosine

phosphorylation. One of the most important inhibitors of Stat1 phosphorylation is Socs1. Its expression is regulated by GAF transcription factor (pStat1-pStat1) binding to GAS elements, which are presented in Socs1 promoter (fig. 13).

Dynamical models of IFN induction of the Jak/Stat signaling pathway based on nonlinear ordinary differential equations, have been previously used to study the effect of IFN pre-treatment on the response of the immune system to virus infection [44, 45] and the robustness of the pathway to noise and parameter fluctuations [46], among other problems. Previous studies suggested that a combination of positive and negative feedback loops, together with the eventual degradation of the IFN signal in the medium, leads to a transient oscillatory response in several components of the pathway.

Type I interferons, such as interferon alfa and beta, are cytokines that represent a first-line endogenous defense mechanism in response to viruses and bacterial infections, and are secreted by many cell types (e.g. lymphocytes, macrophages and endothelial cells). Because type I interferons play a key role in both innate and adaptive immunity, they are frequently used as a therapy in Multiple Sclerosis (MS) treatment.

Stat1 is a protein of the Signal Transducer and Activator of Transcription (Stat) protein family. Stat1, as other Stats of the protein family, is activated by cytokines binging to the appropriate receptor, mainly IFNAR1 or IFNGR. The activation is produced mainly by tyrosine phosphorylation. The phosphorylation of Stat1 causes immediate dimerization of the protein in its SH2 domain. [47] Stats tend to form both homo- and heterodimers. In case of

Stat1 the main dimers are Stat1-Stat1 and Stat1-Stat2, which are produced in different amounts by activation of different receptors. The engagement to form homo- and heterodimers are regulated by the balance in the concentrations of external inputs (cytokines). On the other hand, there are numerous regulators of Stats activity both inside and outside the nucleus, including Socs1 and Irf1 [43].

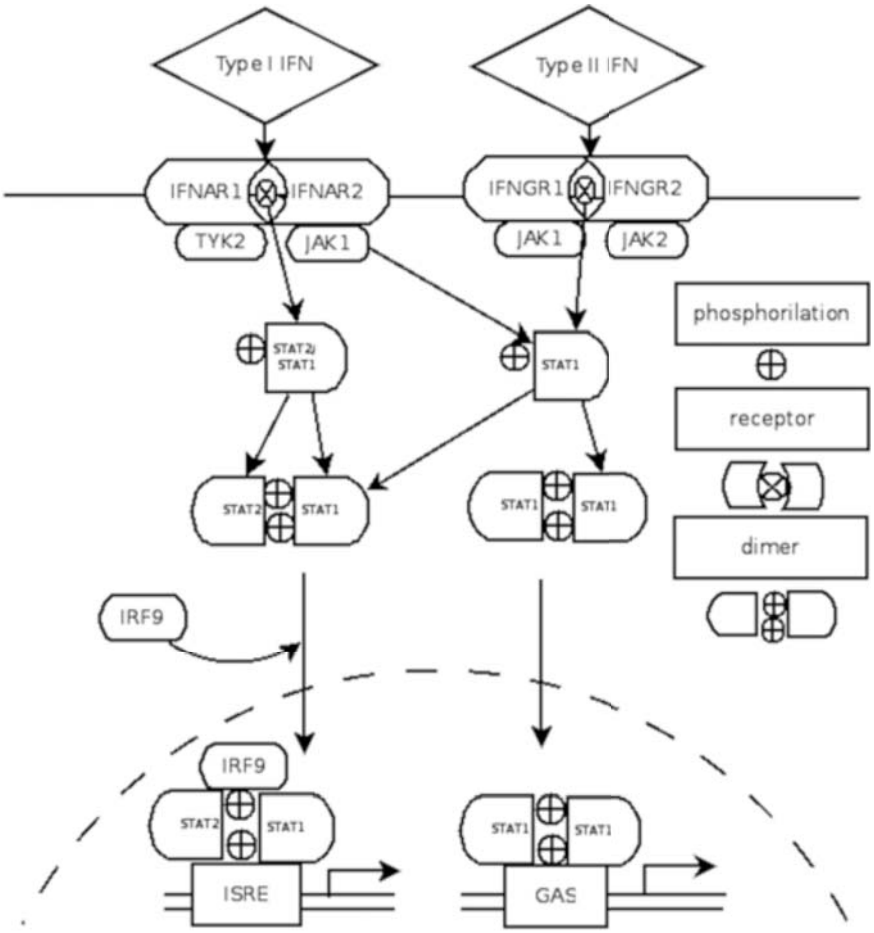

Figure 13 The canonical type I and type II IFN signaling pathways. The plot represents the canonical IFN pathways and the cross-talk between them, including the different pStat dimers formed after stimulation. [48]

The target genes of the IFN-beta pathway can be divided into three categories according to the type of activating transcription

factor: 1) the ISGF3 complex activates genes containing an ISRE binding site in their promoter (e.g. ISG15, Mx1, OAS1, IRF7). These genes are known to be upregulated in T-cell populations of immune cells upon IFN-beta stimulation or virus-induced IFN-beta production. 2) The GAF complex activates genes containing a GAS binding site in their promoter, such as Socs1 and IRF1. Early studies found Socs1 and IRF1 to be up-regulated mainly upon IFN-gamma induction, but recent work has shown their importance in IFN-beta pathway regulation in macrophages [49, 50]. 3) A third class of Stat protein complexes activates other canonical pathways that exhibit crosstalk with the Jak/Stat pathway (such as PI3K, NFkB, MAPK) [51]. Recently it was shown that different immune cell subtypes respond differently to IFN-beta induction through activation of these different types of genes [52].

Different proteins regulate Stat1 phosphorylation. Importantly, a negative feedback loop upon Stat1 activation coexists with a positive feedback mechanism. First, the phosphorylation of Stat1 is inhibited by its inhibitor Socs1 [53]. The Socs1 protein then inhibits Stat1 phosphorylation at the kinase level. Besides this negative loop based on Socs1, Stat1 is a subject to positive regulation via the TF IRF1, whose transcription is induced by activated Stat1. IRF1 promotes the expression of the Stat1 gene at the transcriptional level. Given the existence of these multiple feedback loops, a mathematical modeling of the system would help provide an understanding of the response to type I IFN-beta.

Sgk/Akt-Foxo3a signaling

Another well-known pathway critical for the trophic factor signaling is Pi3K. PI3K-Akt pathway is a key signaling pathway in apoptosis that plays an important role in longevity and cancer. It is activated by growth factors such as Insulin Growth Factor (IGF1). IGF1 binds to the external domain of the Receptors of tyrosine kinase (RTK). The phosphorylation of the inner domain of the receptor leads to the binding of PI3K. Activated PI3K binds to PIP2 membrane phospholipid transforming it to the activated PIP3 form. PIP3 activates Pgk1 signaling kinase, which activates Akt by phosphorylation. pAkt triggers many different cellular processes promoting cell growth and preventing cell death. The main mechanism of PI3K-Akt signaling is an activation of protein synthesis and translation by mTOR. The other mechanism is the inhibition of Foxo3 apoptotic activity by phosphorylation.

While the well-studies kinase acting downstream of PI3K is Akt, there are other kinases involved in the regulation of downstream TFs. One of the families of these kinases is the serum- and glucocorticoid-inducible protein kinase (Sgk). Sgk proteins are phosphorylated by PI3K-dependent mechanism, but not through PIP3 phospholipid. SGKs are serine/threonine kinases that are related to Akt. In common with Akt, these proteins are activated by the PI3K pathway and translocate to the nucleus in cells stimulated with survival factors. SGK1 phosphorylates FoxO3a at the same sites as those phosphorylated by Akt, likewise leading to the cytoplasmic localization and inhibition of FoxO3a. However, SGK1

preferentially phosphorylates serine 319 whereas Akt prefers serine 256 [54].

The Foxo (Forkhead Box, type O) family of transcription factors (TFs) cause changes in gene expression to implement a cellular stress response program, and an increase in their activity leads to the genetic interventions that extend lifespan in model organisms. Foxo are conserved in all animals from worm to human. There are four closely related Foxo proteins in mammals, Foxo1 (FKHR), Foxo3 (FKHRL1; Foxo3A), Foxo4 and Foxo6. All Foxo proteins are widely expressed in different tissues, but Foxo3 is especially highly expressed in the brain. Foxo factors contribute to the regulation of various processes such as cell cycle progression, cell size determination, cell death, cell differentiation, resistance to stress, and energetic metabolism. [55] Phosphorylation of Foxo proteins in response to growth factors such as IGF-I, erythropoietin, epidermal growth factor or nerve growth factor causes exclusion from the nucleus [56] For many growth factor-activated protein kinases, the specific phosphorylation sites are known. These include Akt and serum and glucocorticoid inducible kinase (Sgk), which are activated mainly through the PI3K pathway [57, 58]. Phosphorylation of Foxos in response to oxidative stress involves JNK and results in Foxo import in the nucleus. Foxo residues targeted by these kinases are different from those targeted by growth factor-regulated kinases [59–61]. The effect of oxidative stress appears to prevail on the effect of growth factors [62]. Probably, a more important determinant of Foxo protein expression is its rate of degradation [63].

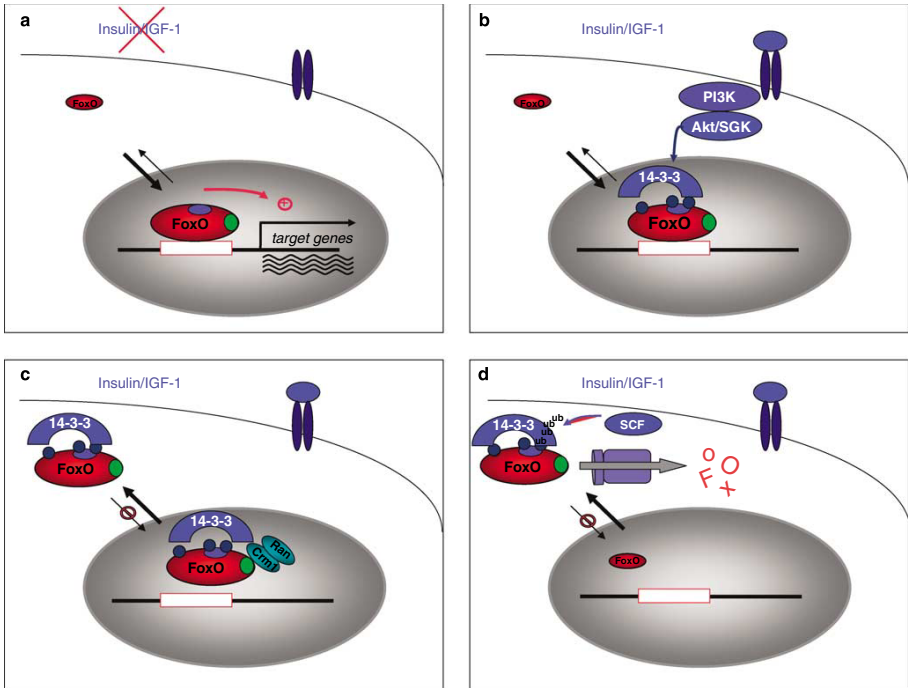

Figure 14 Some of Foxo3 inhibition mechanism from [64]**. Note the alternative IGF1 activator - Sgk**

New implication of Akt-Foxo3 signaling in neuronal and behavior response [65, 66] opens a new field of possible drug targeting of Foxo TF for autoimmune and neurological diseases.

The PI3K-Akt pathway is critical for growth factors signaling to promote cell survival through phosphorylation of Foxo3. In this pathway, nuclear translocation of Foxo3 after phosphorylation is the key step for modulating gene expression pattern (fig. 14). This pathway can be impaired in patients with neurodegenerative diseases leading to neuronal loss. Moreover, neuroprotective therapies targeting this pathway are promising therapeutic approaches for brain diseases. For this reason, understanding the dynamics and bottlenecks of this pathway will be useful for monitoring and predicting the response to these drugs. A previous

mathematical model on dynamic features of Foxo TF was described before [67]. The model is focused on the post-translation modifications and their implication in the Foxo fate (fig. 15).

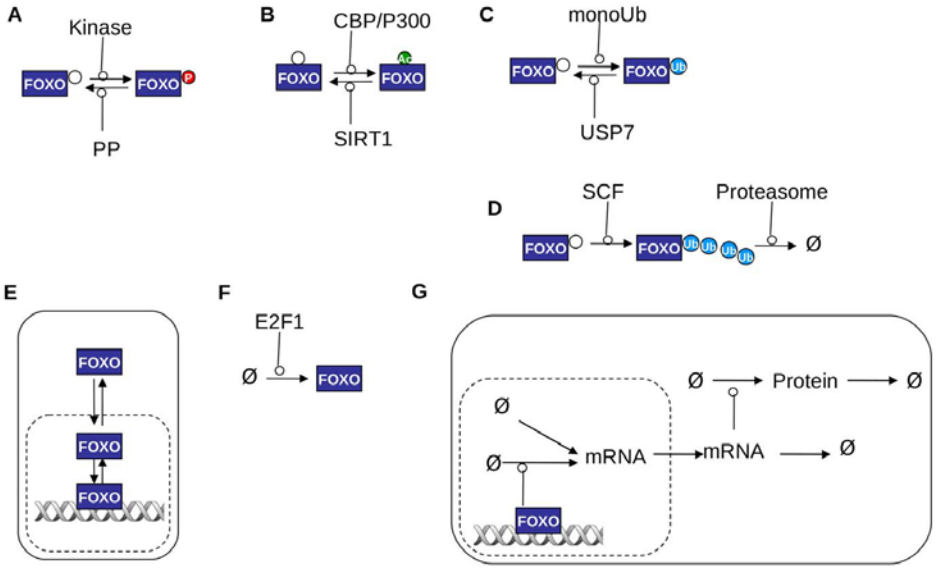

Figure 15 Fundamental reaction types of Foxo translocation (from [67]**)**

The regulation pattern of Foxo3a is highly conserved through all vertebrates. The pathway is regulated by an inhibitor loop Pten--|PI3K (fig. 16). This loop may lead to the alternative behavior of the system that is important for our kinetic model. Foxo3a TF directly regulates Pten gene expression. Therefore, the inhibition of Fioxo3a leads to activation of Pten and inhibition of PI3K phosphorylation. This work can be helpful in order to identify some of the important parameters for Sgk/Akt-Foxo3a signaling model.

Target	Up- or downregulation	FOXO	Pathway	References
Cyclin D	–	FOXO3, FOXO4	Cell cycle	84
Cyclin G2	+	FOXO1, FOXO3, FOXO4	Cell cycle	17, 58
P130	+	FOXO1, FOXO3, FOXO4	Cell cycle	17, 54
P15	+	FOXO1, FOXO3	Cell cycle	47
P19	+	FOXO1, FOXO3	Cell cycle	47
P21	+	FOXO1,FOXO3,FOXO4	Cell cycle	65, 88
P27	+	FOXO1, FOXO3, FOXO4	Cell cycle	24, 61, 92
Plk	+	FOXO1	Cell cycle	106
Manganese superoxide dismutase	+	FOXO3	Stress resistance	53
catalase	+	FOXO3	Stress resistance	66
Peroxiredoxin III	+	FOXO3	Stress resistance	18
Sterol carrier protein	+	FOXO3	Stress resistance	21
Gadd45	+	FOXO3, FOXO4	DNA repair	30, 100
Bim	+	FOXO3	Apoptosis	23, 33
Fasl	+	FOXO1, FOXO3	Apoptosis	13, 19
Tumor necrosis factor receptor-associated death domain	+	FOXO1	Apoptosis	81
Tumor necrosis factor-related apoptosis inducing ligand	+	FOXO1, FOXO3	Apoptosis	63
p53 upregulated modulator of apoptosis	+	FOXO3	Apoptosis	105
Bcl 6	+	FOXO3, FOXO4	Apoptosis	28, 98
PTEN-induced kinase 1	+	FOXO3	Apoptosis	62
Glucose-6-phosphatase	+	FOXO1, FOXO3	Metabolism	69, 78
Phosphoenolpyruvate carboxykinase	+	FOXO1	Metabolism	86
PGC1	+	FOXO1	Metabolism	20
adiponectin	+	FOXO1	Metabolism	79
Agouti-related protein	+	FOXO1	Metabolism	49, 51
proopiomelanocortin	–	FOXO1	Metabolism	49, 51
neuropeptide Y	+	FOXO1	Metabolism	49
Apoliprotein C-III	+	FOXO1	Metabolism	2
Pdx1	–	FOXO1	Metabolism	52
B-cell translocation gene 1	+	FOXO3	Differentiation	5
Id1	–	FOXO3	Differentiation	10
Atrogin-1	+	FOXO3	Muscle atrophy	83
Bnip3	+	FOXO3	Muscle atrophy	57, 107
LC3	+	FOXO3	Muscle atrophy	57, 107
Garabl12	+	FOXO3	Muscle atrophy	107
Interleukin 7R	+	FOXO1	Inflammation	70
C/EBPβ	+	FOXO1	Inflammation	43
Interleukin 1β	+	FOXO1	Inflammation	94
4E binding protein 1	+	FOXO1, FOXO3	Insulin signaling	76
InsR	+	FOXO1	Insulin signaling	77
trible 3	–	FOXO1	Signaling	59
Caveolin-1	+	FOXO1, FOXO3, FOXO4	Signaling	82, 102
Protein phosphatase 2A	–	FOXO1	Signaling	67
FOXO1	+	FOXO1, FOXO3	Signaling	27
FOXO3	+	FOXO1, FOXO3	Signaling	27
P110α	+	FOXO3	Signaling	42
Collagenase	+	FOXO3	Extracellular matrix degradation	60
Matrix metalloproteinase 9	+	FOXO4	Extracellular matrix degradation	55
Mxi1	+	FOXO3	Tumor suppression	22
Estrogen receptorα	+	FOXO3	Tumor suppression	35
Myostatin	+	FOXO1	Differentiation	1
Endothelial nitric oxide synthase	–	FOXO1, FOXO3	Vessel formation	75
Multidrug resistance protein 1	+	FOXO1	Drug resistance	36
CBP/p300 interacting transactivator 2	+	FOXO3	Angiogenesis	6

Listed are transcriptional targets that have been reported to be directly regulated by FOXO1, FOXO3, or FOXO4. FOXO target genes are grouped by cellular function. The effect of FOXO activation on the expression level: upregulation and downregulation are indicated by – and +, respectively.

Table 1 The list of Foxo target genes from [68]

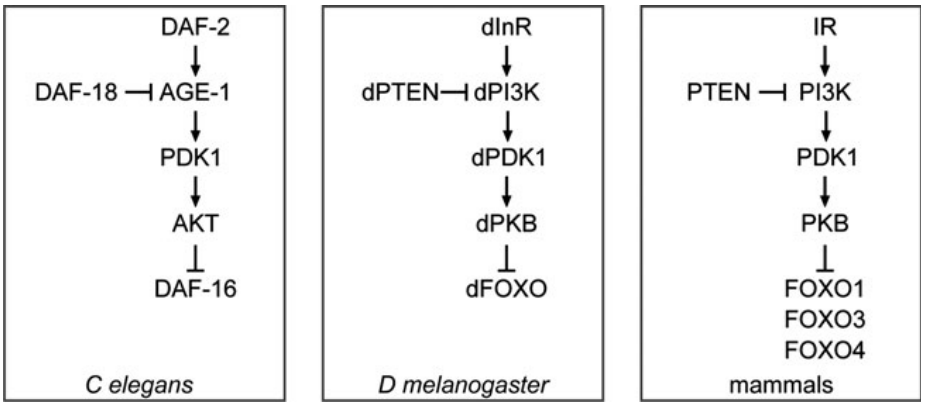

Figure 16 Regulation of Foxos is conserved between Caenorhabditis elegans, Drosophila melanogaster, and mammals. Activation of the insulin receptor (DAF-2) activates PI3K (AGE-1) resulting in the formation of PIP_3. These phosphorylated lipids form docking sites for PDK1 and PKB (AKT) resulting in their activation. PKB phosphorylates and inhibits Foxo transcription factors. While C. elegans and D. melanogaster have a single Foxo isoform, in mammals three distinct Foxos are regulated by PKB: Foxo1, Foxo3, and Foxo4. From [69])

Systems biology approaches in the development of new biomarkers and drug combinations for autoimmune diseases

Extracellular molecules, such as cytokines, play a crucial role in signal transduction. Cytokines mechanism of action is a complicated network of closely connected intracellular signaling pathways. In general, binding of cytokines to the cell receptors forces the activation of different pathways to provide a systematic response. Although significant knowledge has been acquired in the last decades regarding the molecular components in the signaling pathways, how the cell computes information is not well understood. For this reason, the combination of biochemistry, molecular biology and systems biology approaches may provide new insights about this critical cell process.

Systems biology is achieving an outstanding level of understanding of complex processes. A hot topic in clinical research actively using Systems biology approach is drug combinations discovery for complex diseases such as type II diabetes [70], breast cancer [71], MS (CombiMS FP7 project) and others. There is a number of new methods and tools to identify effective drug combinations based on the big data networks (for example, [71, 72]).

Clinical studies call for interdisciplinary efforts to confront the challenges of the autoimmune and neurological disorders such as MS [73]. With the increasing amount of produced data and little progress in the therapy of these diseases the Systems Biology approaches are the key to break the wall of misunderstanding of the deep mechanisms of the pathogenesis of MS.

Hypothesis

The main players of the biological systems are the interactions between the molecules rather than the molecules themselves. It's rather connections then nodes, which determine the behavior of the whole cell. From this perspective I'm going to determine several hypothesis examining different layers of hierarchical living system: population of cells, entire cell and particular signaling pathway.

Questions that we discuss in this dissertation are:

1. Should we treat populations as a group of single cells or as an interconnected social system?

The populations are a higher layer of the systems hierarchy than single cells and therefore, according to the general systems theory, possess the features directly derived from the lower layer of single cells. But can we derive all the features of the cell populations from a sum of single cells features? The holistic philosophy is based on the assumption that the higher hierarchical system possesses the properties that derive from the lower layers but can't be directly represented as a sum of them. Our hypothesis is that the population dynamically behaves differently from the single cells in response to same stimuli and produced a coordinated response, which is an emergent property of the population. This behavior has evolutionary importance at the populational level because provides more robust responses.

2. How do different cell types respond differently to the same signal?

All cell types share the same genetic background but possess different phenotypic feature and are responsible for different

functions within the body. There are various mechanisms to achieve this variety, including epigenetics and posttranslational modifications among others. At the end, the cells obtain different transcriptional profile according to their functions. I propose that it is mainly through the connections in their molecular networks, which make the difference. The signal transduction networks operate differently because they are constructed with the same nodes but different dynamic parameters (e.g. epigenetic regulation of specific kinases). In other words, the signal from certain external signals passes through the same molecules but by different signaling pathway routes or with different kinetic properties.

3. Why does negative feedback loop is such a common motif in cytokine signaling and how the oscillatory dynamics is regulated?

Frequently the kinetics of the pathway is dependent on the positive and negative feedbacks, which orchestrate oscillatory dynamics of the cascade that regulates the translocation of TF and modulate gene expression. Oscillatory behavior has evolutionary advantages in the noisy environment the cells have to analyze the signal. I propose that the kinetic oscillations are the mainstream behavior of cytokine signaling in mammals and are insensitive to the ODE model parameter variations.

4. How do nuclear translocation parameters may influence the kinetic behavior of a signaling pathway?

The nucleus of eukaryotes is separated from the cytoplasm by the nuclear membrane. The membrane regulates the import and exports to and from the nucleus by creating the gradient and act as a mechanical barrier. As part of the iterative cycle of systems

biology research (from theory to experiments and back), I realized that dynamical features of the nuclear transport of TFs are important variables in the signal transduction kinetics. The nuclear transport may be a kinetic buffer for the signal transduction events. I hypothesize that these parameters of the nuclear transport may determine the dynamics of the systems, including oscillatory/damned oscillatory regimes. The dynamic analysis of TF translocation is a readout of the activation of the pathway and can be used as a biomarker of the activation of the pathway and the effects of therapies targeting this pathway.

In this work we examine these hypotheses and provide proof of concept studies to validate them.

Objectives

Information transmission through signaling pathways is a dynamic process in which signals of activation are transmitted through phosphorylation reactions. The general goal of the thesis is understand how the information is transmitted through prototypic signaling pathways which are relevant for the pathogenesis and therapy of MS, namely the IL-6, IFNbeta and PI3K (Sgk-Akt-Foxo3a) pathways, with different layers of system complexity. A second goal is to make use of these pathway models for translational research, in order to understand how drugs target these pathways and for identifying biomarkers of the response to therapy of MS.

The specific objectives are:

1. To model the dynamical features of IL-6 pathway at population and single cells level in order to assess the emerging properties of cell population signaling.
2. To assess the differences of cytokine signaling pathway in the two main immune cell subtypes T cells and macrophages, by building and validating a Boolean network of IFNbeta signaling;
3. To analyze the oscillatory dynamics of IFNbeta signaling by developing a kinetic model of Type I IFN signaling which can explain the observed dynamics from our experiments and determine the properties that are crucial for the oscillatory dynamic
4. To evaluate the role of nuclear translocation of TF (Stat1 for IFNbeta pathway and Foxo3a for PI3K pathway) as modulators of the pathway kinetics and the possibility to

use it as a potential drug target or dynamical biomarker of response to therapy.

Materials and methods

Materials and reagents

Cells were obtained from ATCC library, mouse recombinant IFN-beta was purchased from Cell sciences, lipopolysaccharide from *Escherichia coli* and poly(I:C) salt was purchased from Sigma-Albrich, lipofectamine 2000, Hiperfect transfection agent were purchased from QIAGEN, Taqman PCR master mix, VIC-dye GAPDH endogenous control, IRF1, Socs1, Stat1, Stat2, MX1, OAS1a pre-designed FAM-dye assays were purchased from Applied Biosystems, total Stat1 and Stat1(pTyr701) antibodies and beads, cell detection kit for xMAp assays were purchased from Merck Millipore (Billerica). Alexa Flour 647 Stat1 (pTyr701) and PE Stat1 N-terminal anti-Mouse antibodies and all buffers for cytometry were purchased from BD biosciences. APC-labeled IFNAR1 antibody was purchased from Biolegend.

Human samples

The blood samples were obtained from MS patients and healthy controls according to the informed consent. These studies were performed under the frame of CombiMS project and approved by Ethic committee of the Hospital clinic of Barcelona . The blood was used to extract PBMCs using standard Ficoll gradient protocol. PBMCs were maintained in full medium (RPMI+5%SBF+penicillin/streptomycin) for 6-24 hours and stimulated with appropriate stimulator for indicated times (see results).

Cell culture and stimulation

Mouse leukemic monocyte macrophage cell line RAW 264.7 and mouse fibroblasts 3T3 cell lines were purchased from ATCC

and maintained in DMEM medium complemented with 10% fetal bovine serum and 1% antibiotics at 37ºC and 5% CO2. The cells were passed every 2-3 days and maintained in 20-80% surface coverage. One day before the stimulation the cells were seeded in 12 well plates in concentration 1 x 10^6 cells/well. The cells were stimulated with 1000 units of recombinant mouse IFN-beta, 15 μg of LPS for different times or 15 μg of poly (I:C) solution. At the end of stimulation supernatants or cells were collected for further analysis. The same amount of PBS was added at the corresponding time-points to the control samples. For the Boolean model we used Jurkat and THP-1 human cell lines obtained from ATCC cell bank. PBMCs from healthy controls and patients with MS were obtained and processed according to standard protocol. 3T3 fibroblasts were cultured in 24-well tissue culture plates in DMEM containing 10% fetal bovine serum (FBS). Prior to stimulation, the cells were serum-starved for two hours by replacement of media with DMEM alone. At t=0, IL-6 (BD Biosciences) was added to wells at 100 ng/ml, 10 ng/ml and 1 ng/ml. To separate 3T3 cultures, IFN-γ (BD Biosciences) was added at 100 ng/ml and 1 ng/ml. Control 3T3 fibroblasts were cultured without IL6 or IFNγ. To assess intracellular signaling pathways, cells were removed at regular intervals during the course of eight hours from the wells by the addition of cold 0.25% trypsin (Invitrogen) and fixed at room temperature for 10 minutes with a PBS solution containing 1.6% paraformaldehyde (Electron Microscopy Sciences). Following fixation, cell suspensions were washed with PBS and ice-cold methanol was directly added to a final concentration of 90% methanol.

RT-PCR

Cell lysates were prepared with QiaShredder columns and total RNA was isolated using standard Qiagen Rnaesy Mini kit protocol. Equal amount of total RNA was added to each reverse transcription reaction tube (High-Capacity cDNA Reverse Transcription Kit from Applied Biosystems and cDNA was used for a second step of RT-PCR. Results were analyzed using relative 2CTT method normalized to a GAPDH endogenous control (VIC-dye primer-limited control from Applied Biosystems) as described before [74]. All the qRT-PCR experiments were performed in triplicates and repeated three times independently. For 3T3 cell line, frozen cells were thawed, disrupted and homogenized using QIAshredder spin column and RNA were extracted using standard manufacturer spin protocol for animal cells with DNAse digestion using RNeasy mini kit (QIAGEN). The amont of total extracted RNA was measured by nanodrop and used for reverse transcription (High Capacity cDNA Archive kit from Applied biosystems 4322171) in concentration 100 ng/mcl. The second step of real-time PCR was performed using designed primers and probes for Socs1 and Socs3 were ordered from SIGMA. Predeveloped VIC-dye TaqMan Endogenous control for mouse GAPGH (Applied Biosystems) was used to normalize the expression of Socs genes. 50 ng/mcl of cDNA obtained from reverse transcription was used for each real-time PCR reaction. The standard $2^{-\Delta\Delta Ct}$ method [75] was used to calculate the results.

Western blot and quantification

Western blot (WB) was performed using polyclonal rabbit anti-mouse pStat1 and Stat1 N-terminal antibodies (Abcam) using standard WB protocol. Western blot results were quantified using ImageJ software (http://rsb.info.nih.gov/ij/index.html) using the method of Luke Miller (http://www.lukemiller.org/journal/2007/08/quantifying-western-blots-without.html)

ELISA and xMAP multiplexing assays

IFN-beta in culture supernatants and Socs1 protein concentration in cell lysates were measured by standard sandwich ELISA with anti-mouse Socs1 antibodies (Abcam). IRF1 protein concentration in cell lysates was measured by in-cell ELISA using the kit (Thermo Scientific) Stat1 total protein and phosphorylated state (Tyr701) concentrations (nuclear and cytoplasmic together) were measured using xMAP assays and read in Luminex 201 platform using standard vacuum separation protocol (Millipore). xMAP experiments were repeated twice.

Flow cytometry and ImageStreamX imaging system

Cells for flow cytometry were stimulated with 1,000 Units/ml of IFN-beta as stated before and fixed immediately after stimulation. IFNAR1 receptor on the surface of the RAW 264.7 cells was marked using APC-labeled anti-IFNAR antibody. The mean fluorescent intensity was calculated using FlowJo software. For Stat1 staining cells were fixed immediately after stimulation in order to preserve phosphorylation and then permeabilized using

Perm III buffer (BD biosciences). Samples were stained simultaneously with anti-Stat1 (pTyr701) and anti-Stat1 total (N-terminus) antibodies. The mean fluorescent intensity, the percent of staining-positive cells, the medians and the standard deviation were calculated using FlowJo software and the raw single-cell data were extracted to plot the histograms and further analysis. To determine the quantity of pStat1 shuttling to the nucleus after IFNbeta injection in patients in MS we used ImageStreamX imaging system that allows visualizing the co-localization of two different molecules using flourchrome-conjugated antibodies (fig. 17). The nucleus was labeled with DAPI and pStat1 with mouse anti-human Alexa Flour 488 pStat1 (Y701) antibody.

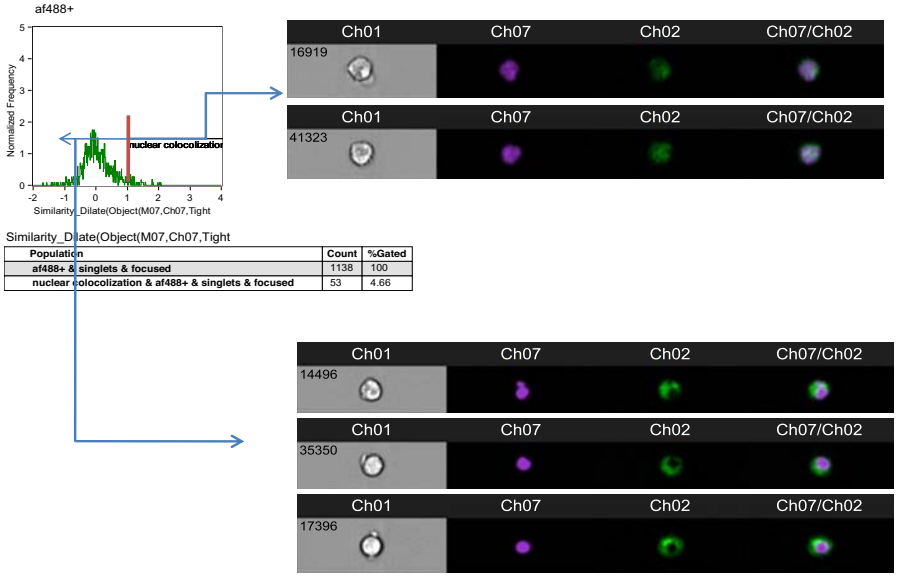

Figure 17 ImageStreamX technology. The method allows to quantify the nuclear translocation in single cells.

Mathematical modeling

Boolean model

To build the Boolean network of antiviral and antibacterial immune response we used the workflow developed by Dr Saez-Rodriquez and described in [76]. In brief, we developed a Preliminary Knowledge Network (PKN) based on text-mining, databases and previous studies. This PKN was represented as a topology is Cytoscape using "sif" file (tab-separated file with 1 and -1 assigned to each link between connected molecules). The experimental results were transformed in the MIDAS files and used to refine and fit the PKN using the CellNoptR software. The workflow is present on the fig. 18.

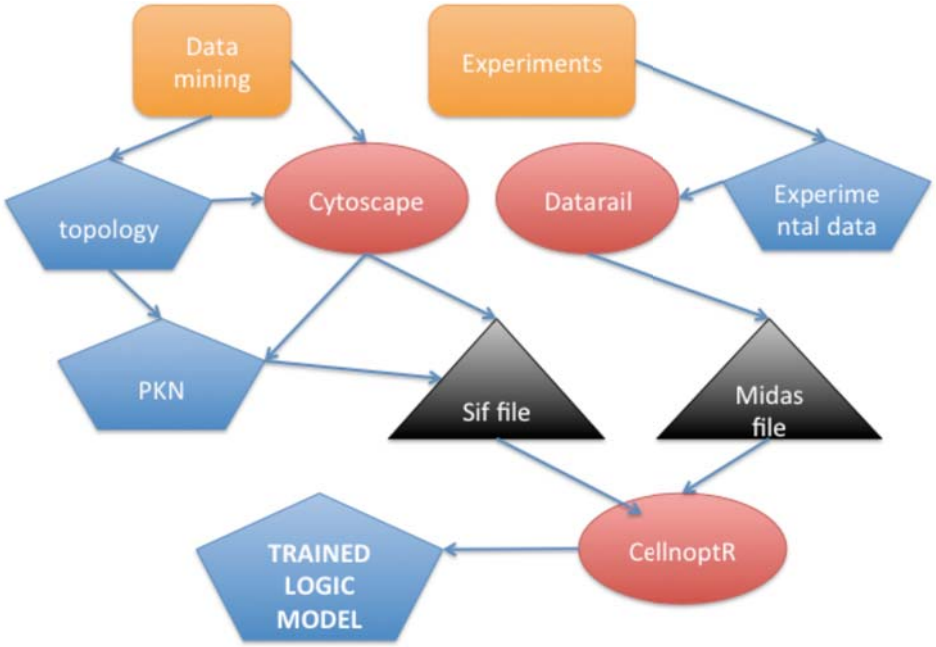

Figure 18 The simplified workflow to obtain the specific logic model based on the experimental data. See details in the text.

The experiments were designed to fit the requirements of the CellNoptR software. The stimuli, inhibited and measured

molecules are labeled on fig. 19. The PKN was evenly covered by inhibitor perturbations and available for measurements phosphoproteins. The experiments were performed for 2 timepoints (15 and 60 min) and analyzed using two-timepoint algotirhm. The experimental data were normalized to endogenous control (GAPDH) and to the time 0 measurements according to the package manual.

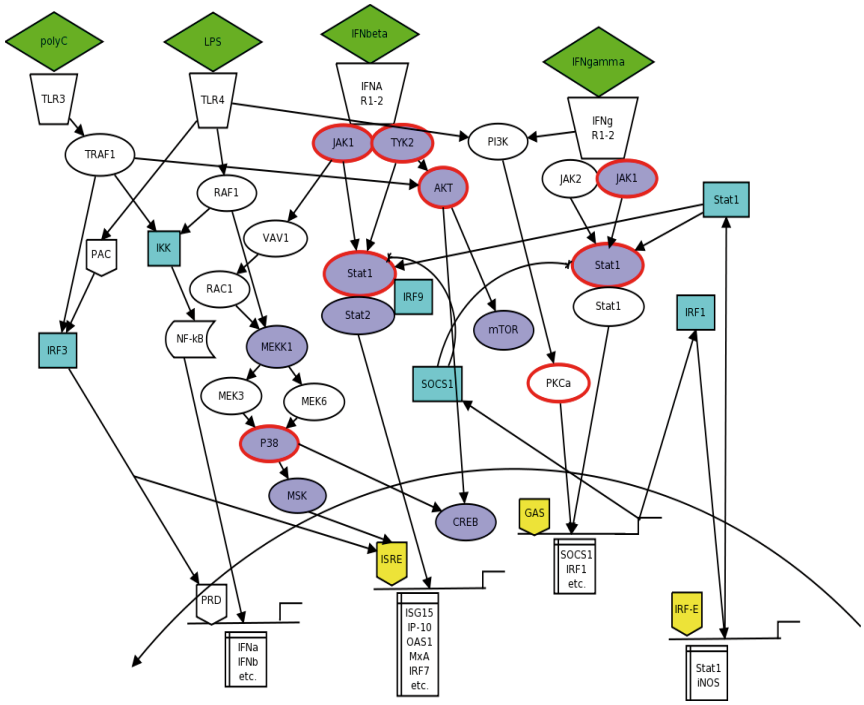

Figure 19 The PKN used for the Boolean modeling of immune response network in THP1 and Jurkat cell lines. Stimulus marked in green, measured phosphoproteins – in purple, inhibited proteins in red rounds, transcription factors in yellow, measured total proteins - in light blue. The analytes are labeled as following Green – stimulus: IFNbeta, IFNgamma, LPS, polyC, Blue – phosphoproteins: p38, Mekk, Stat1, Stat2, mTor, AKT, Jak1, Yellow – Lueferase reporter assay targets: GAS, ISRE, IRF-E, Red circles – the proteins to inhibitor: Stat1, p38, PKCa, AKT, Jak1, TYK1

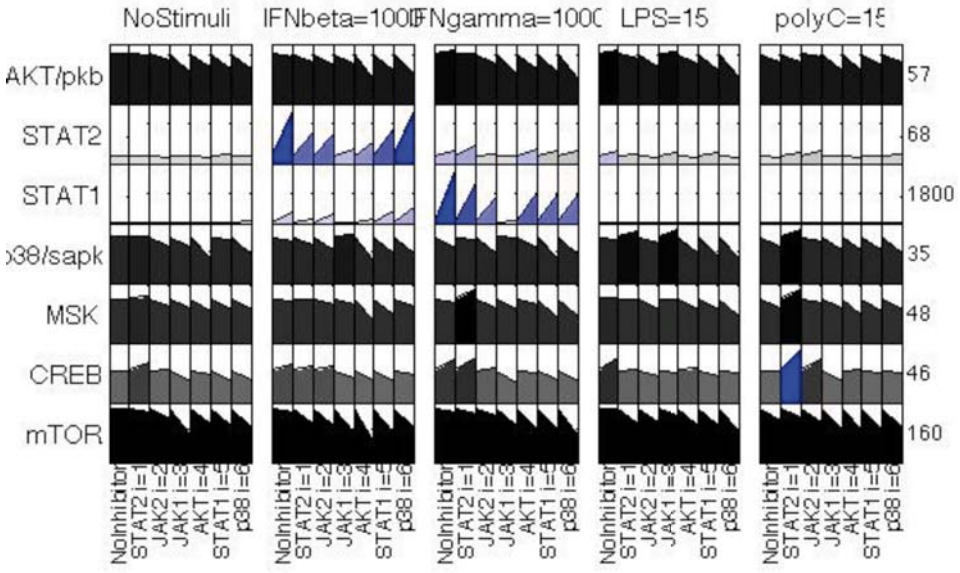

Figure 20 The example of the experimental data visual representation by DataRail. Rows - measured phosphoproteins. Columns: up - stimulus, down - inhibitors used during the experiment. The graph inside represents the change in the signal over time (from 0 to 15 minutes)

The following workflow was proposed to fit the models to the data (adopted from [77] with modifications):

1. Build the PKN
2. Map available stimulus/inhibitors and targets
3. Design the experiments
4. Perform first set of trial experiments
5. Represent the data in MIDAS format
6. Normalize data to use in Boolean logic models
7. Perform simulations predesigned PKN against experimental data with CNO
8. Use preliminary data to add new links and refine the network
9. Repeat stage 7 with refined network
10. Refine the experimental design according to the

preliminary results

11. Perform the all the experiments
12. Repeat stages 5-9 with each dataset

We converted our data to MIDAS file format accepted by DataRail (fig. 20) and described out PKN in a sif file that can be visualized using Cytoscape. We use DataRail software (http://code.google.com/p/sbpipeline/) to preprocess the data and CNOptR software to fit the model to experimental data. All the scripts and functions were written in R. The CellNoptR and other packages were downloaded from Bioconductor. Graphviz and Cytoscape were used for visualization of the models. The best fit was compared manually to each other to determine the differences between cell subtypes.

ODE model

The ODE model of IFNbeta and IL6 pathways and simulations were run in MATLAB using the ODE15s solver (Matlab codes are provided in the supplementary data). The stability analysis of the dynamical system was performed with custom-made Matlab codes.

To establish the ordinary differential equations (ODE) model, which explains the behavior of the model, we need to minimize the number of parameters. We used Matlab scripts for model stimulation.

We used different methods to obtain the parameters for the model. Some of the parameters were estimated using experimental data from previous knowledge (table 2) [48] while others were fitted manually according to the experimental results from RAW 264.7 cell line.

Parameter	Value	Reference
b_{deph}	15 min half-life	[78] [79]
n	3	[80]
u	1	[81]
λ_r	2.82 hour half-life	This work
λ_f	1.23 hour half-life	[82]
A initial	10^5 molecules/cell	[83]
S initial	700-900 receptors/cell	[84]
$\lambda_{Stat\ protein}$	24 hour half-life	[85]
λ_F	30 min half-life	[86]
f initial	1 molecule/cell	[87]

Table 2 Parameter values obtained from the literature

For IL6 model we used stochastic simulations by Gillespie's algorithm to simulate heterogeneity in cells by varying randomly initial conditions for STAT3 molecules and the number of active receptors available/ or stimulated by cytokine.

Parameter space exploration for Foxo-Akt model

The model of Sgk/Akt-Foxo3a was simulated in Matlab. Additionally we used the workflow explained in the paper by Gomez-Cabrero et al. to explore the whole parameter space of the system [32]. The workflow was implemented in MATLAB. The certain parameters were fixed according to the previous knowledge (see sup. table 6), and the others were explored in the all positive parameter space. The initial conditions were fixed according to sup. table 5.

Results

Chapter 1. Theoretical considerations on pathway dynamics in individual cells and cell populations

The models designed in the other chapters of this thesis are examining the behavior of the system in the presence of certain stimuli without taking into account the variations of the response of single cells. The other side of the coin is the population behavior that we actually see in most of the experiments.

There are three aspects affecting the population behavior as a whole:

1. The kinetics of the behavior of each member of the population (each cell) (fig. 21). The cells may be synchronized in time or have desynchronized oscillations, which won't be seen on the populational level;
2. The effects of the members of the population (cells) on each other;
3. The environmental noise affecting the population (stochastic inputs).

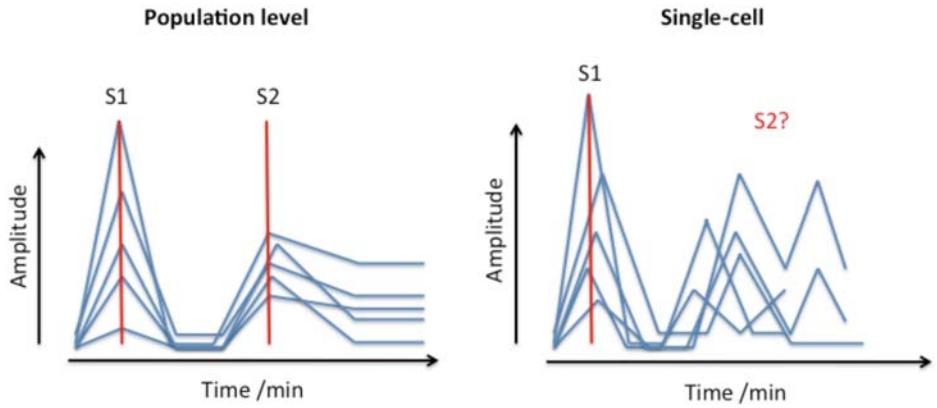

Figure 21 Population versus single cells oscillations. The second peak may be present in single cells, but missing in populational level due to desynchronization.

Using the dataset from Prof Garcia-Ojalvo group from UPF we performed a case study of the dynamics of the population versus single cells in IL6 signaling pathway (manuscript in preparation). We explored a dynamic feature of the Stat/Socs system that has been reported as ultradian oscillations by Yoshiura et al [88]. Yoshiura et al. showed that serum stimulation triggers oscillations due to the interplay between active Stats and Socs alone. That is, oscillations in Socs3 levels required cyclic phosphorylation of Stat3 and vice versa, periodic activation of Stat3 depended on Socs3 oscillations.

The dataset we used consists of time-resolved measurements of Socs3 RNA by RT-PCR and Tyr-phosphorylated Stat3 (Stat3-P) by Flow Cytometry in serum-stimulated fibroblasts for extended time intervals (fig. 22). Oscillations showed a period of approximately two hours. Oscillations of the repressor, Socs3, affected both its mRNA and protein concentrations. In particular, approximately in-phase oscillations of Stat3-P and Socs3 mRNA were followed by one hour-delayed oscillations in the levels of Socs3 protein..

The fact that oscillations exist at the population level indicates that cells acted in a synchronized fashion after serum treatment (otherwise, averaging would have rendered oscillations unobservable).

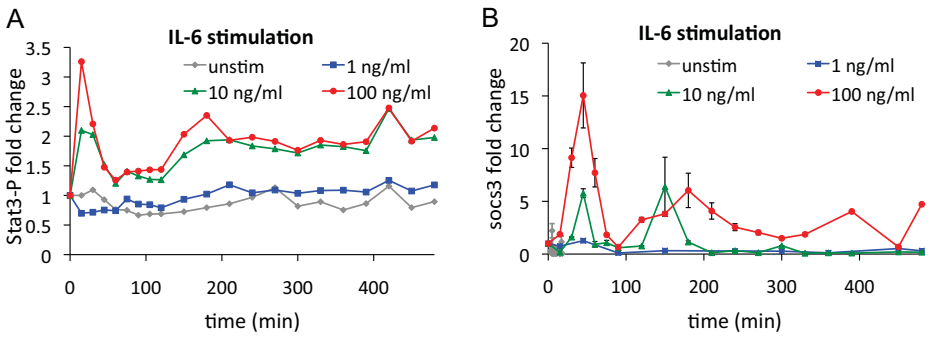

Figure 22 Median levels of phosphorylated Stat3 (A) in mouse 3T3 fibroblasts measured by flow cytometry in the absence of stimulation (grey), stimulated with IL-6 (1 ng/ml: blue, 10 ng/ml: green, 100 ng/ml: red). Standard errors (SE) are smaller than 0.02 in all cases, therefore error bars have been omitted. Mean fold change in the expression of Socs3 (B) in response to IL-6 is also shown, as measured by RT-PCR, with error bars corresponding to the SE of two experimental replicates.

The experiments show that the oscillation period is insensitive to cytokine levels (fig.22). The experimentally observed oscillations, however, were reported only at the cell population level and were not self-sustained: a few hours after stimulation the oscillations in the population were seen to disappear. In order to verify that this behavior is consistent with our model, we now consider a population of independent cells reacting to identical environmental conditions.

From experimental results of pStat3 after IL6 stimulation, we derived a histogram of single cells distribution (fig. 23), which shows that not only the mean (black dots over the green plots), but also the distribution differs in different timepoints. To better understand the nature of the distribution we calculated the coefficient of variation (CV) from the single cell flow cytometry data (fig. 25).

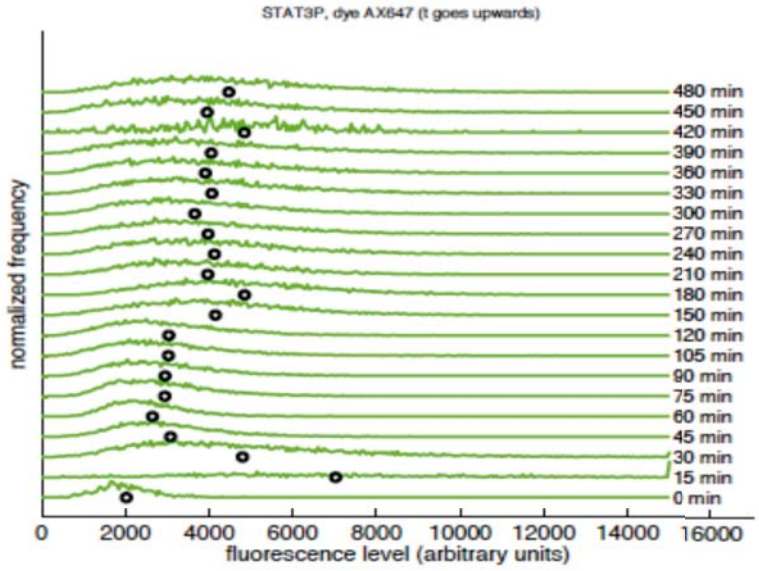

Figure 23 The single-cell distribution histogram for pStat3 after IL6 stimulation of 3T3 fibroblasts. Based on single-cell flow cytometry results

We developed an ODE model of the IL6 pathway graphically represented on the fig. 24. Our ODE model consists of key signaling processes:

- the activation of IL6 receptors by cytokine
- the subsequent phosphorylation of Stat3 and its translocation to the nucleus
- the dephosphorylation inside the nucleus and the export to the cytosol in the dephosphorylated state, closing the loop for Stat3 in cytosol.
- At same time, we have considered the repressor module from SOCS3 gene expression as a negative feedback loop, which inhibits the phospho cascade from the active receptor.
- All species of subject of degradation

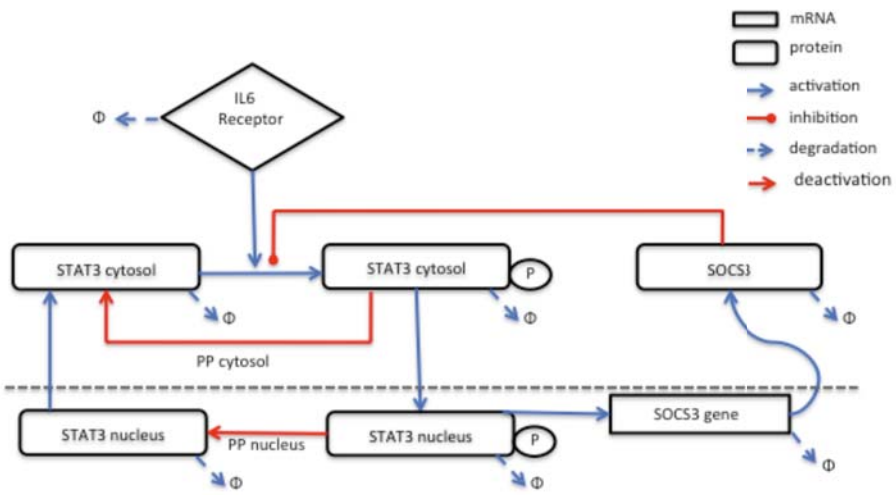

Figure 24 Graphical reppresentation of IL6 signaling pathway model

Our model displays the following features: i) the model leads naturally to a stable limit cycle with period and phase profiles that match the values experimentally observed, (ii) the limit cycle exists with a markedly robust period for a large range of parameter values, such as the amount of cytokine and of total Stat proteins, and (iii) stimulation of the pathway by the sudden addition of inducer leads to the synchronization of a population of already-oscillating cells, in a dose-dependent manner.

The model from fig. 24 can be represented by a system of differential equations (ODEs):

$$\frac{dAc}{dt} = b_{\exp} * An + b_{deph} * Apc - b_{ph} * S * (Ac/k_A)/(1 + (Ac/k_A) + power(R/k_I, q)) - \lambda_{STAT3} * Ac$$

$$\frac{dApc}{dt} = b_{ph} * S * (Ac/k_A)/(1 + (Ac/k_A) + power(R/k_I, q)) - b_{imp} * Apc - b_{deph} * Apc - \lambda_{STAT3} * Apc$$

$$\frac{dApn}{dt} = b_{imp} * Apc - b_{deph\_nucleus} * Apn - \lambda_{STAT3} * Apn$$

$$\frac{dAn}{dt} = b_{deph\_nucleus} * Apn - b_{\exp} * An - \lambda_{STAT3} * An$$

$$\frac{dr}{dt} = b_r * power(Apn/k_r, n)/(1 + power(Apn/k_r, n) - \lambda_r * r$$

$$\frac{dR}{dt} = b_R * r - \lambda_R * R$$

We simulated the model dynamics on a populational levels (fig. 25 in black).

CV is calculated as standard deviation divided by the mean for each measured timepoint (fig. 25 on the right) CV is a measure of the difference in the response of the cells to stimuli at the same timepoint. It shows that the desynchronization of the cells occur in 15 minutes after stimulation. So all cells get activated at the same time, but at the different level (amplitude of response). Then CV drops down and goes up again. The second minimum of the CV at 200 min corresponds to the second peak of the median response. It means that the cells get more synchronized at the second peak then at the first one. After the second peak the cell desynchronize again and get to a steady state of desynchronization. This kinetic profile remains the same with different concentrations of IL6.

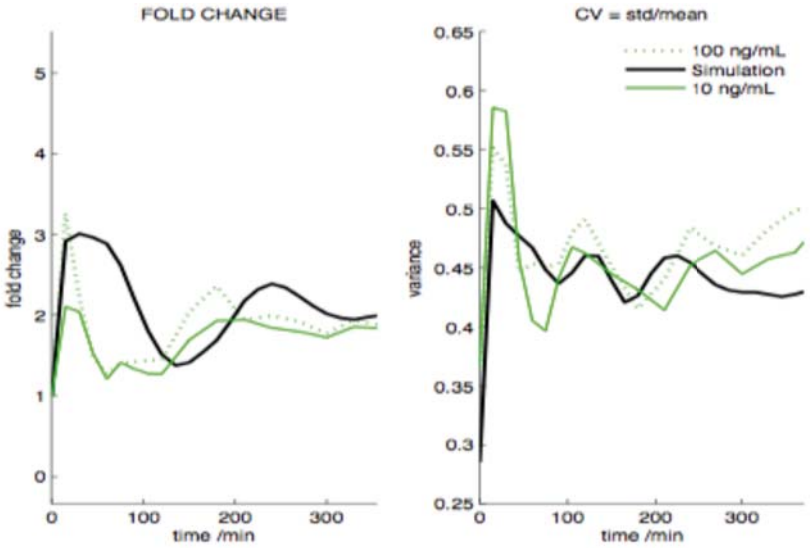

Figure 25 Model simulations versus experimental data for pStat3. Fold change of phosphorylation levels (on the left) and coeffecient of variation (right). Green lines correspond to experimental data and black – to the simulation of the model.

This observation proofs that all the cell are strongly activated shortly after the stimulation (at 15 min), but the amplitude of the activation vary a lot from cell to cell (high CV on fig. 25 right). On the second peak the response is lower (lower peak at 200 min on fig. 25 left), but the CV is also reaches local mínimum (200 min on fig. 25 right). The model could reproduce this variability changes (fig 25 in black).

Biologically speaking, the second round of cells activation corresponds greatly to the cell synchronization and the population acts as an entire system rather than a collection of differently responding cells. It may be important for the correct immune response.

Chapter 2. Differential role of IFNbeta signaling in T cells and macrophages modeled with Boolean networks

Boolean modeling of IFN pathways in Jurkat and THP1 cell lines

IFNbeta signaling pathway interacts with many antiviral and antibacterial response pathways, becoming a part of a bigger molecular network. To answer the question on how this network is organized in different immune cell subtypes we used the workflow developed by Prof Saez-Rodriquez (see introduction and methods sections). We developed a simplified topology of the interactions between IFNbeta, IFBgamma, TLR3 and TLR4 pathways based on previous studies and data-mining. This topology is called the Preliminary Knowledge Network (PKN) (see methods and fig. 19). In this PKN we labeled the stimuli, the intermediates and the genes as well as feedback loops and crosstalk between different pathways in the network. The aim of Boolean modeling approach is to predict the interactions between the molecules in the network in the concrete conditions or cell types. In short, our objective was to build cell-specific networks of type 1 IFNs and inflammation signaling pathways in T cells and macrophages. We used the T cells (Jurkat) and macrophage-like (THP1) cell lines to obtain the experimental data. The cells were challenged with the combinations of different stimuli and inhibitors and different phosphoproteins, which were measured by XMAP bead assays under these conditions (labeled in fig. 19). See methods sections and [89, 90] for more details.

The data obtained from the cell lines and the goodness of fitness of the model is shown in the figures 26 and 27.

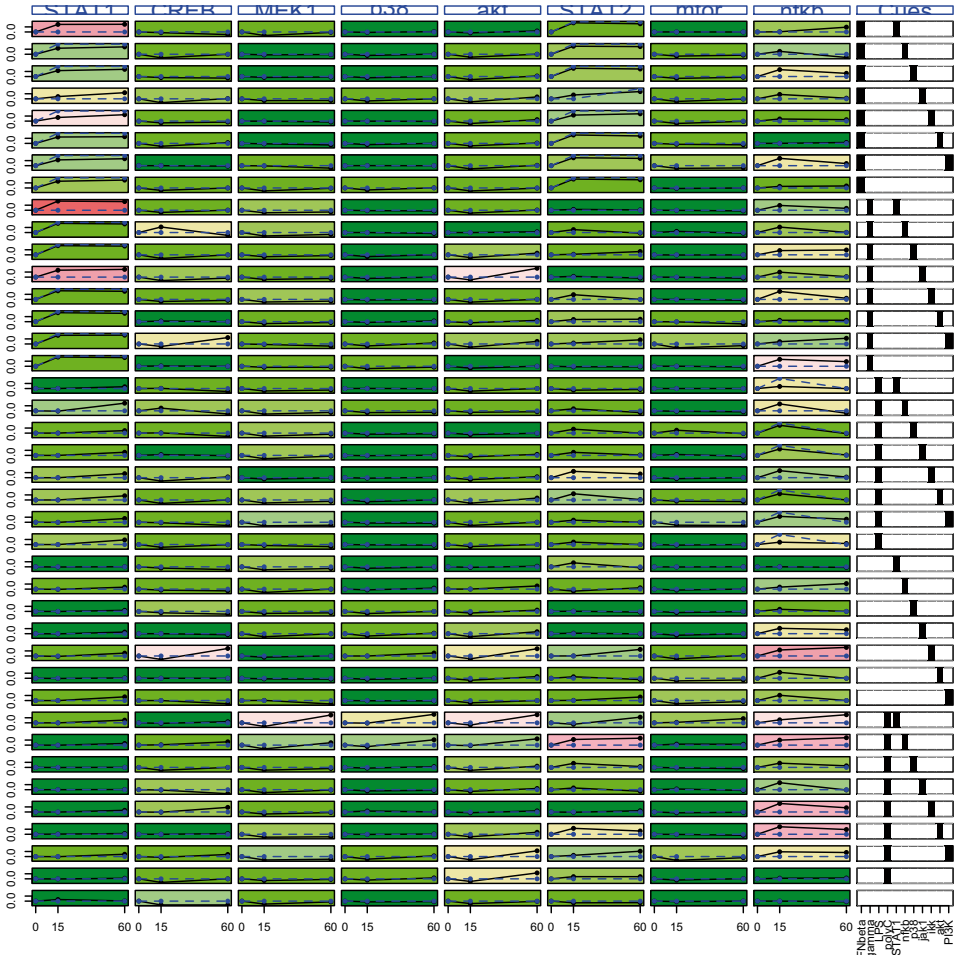

Figure 26 Experimental results and model fit for Jurkat cell line. Fit of model predictions (dashed blue lines) to data. The color of cells represents the quality of fit (green - perfect fit, red - the model couldn't explain the data).

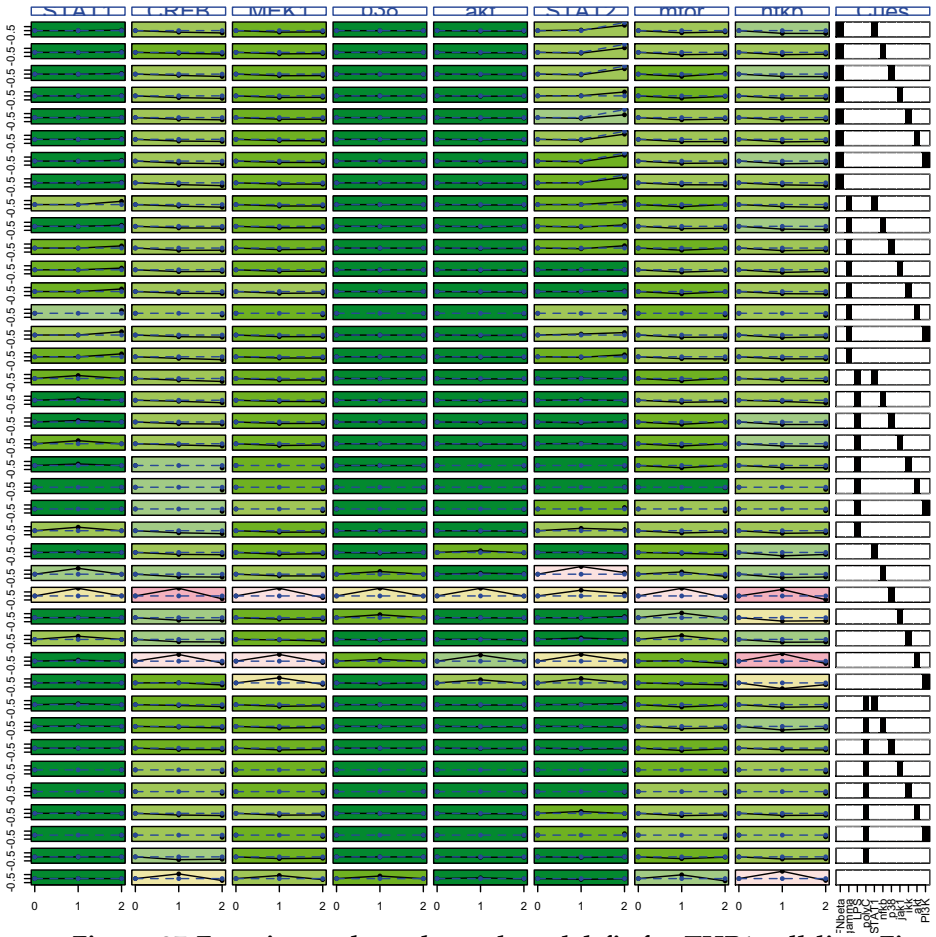

Figure 27 Experimental results and model fit for THP1 cell line. Fit of model predictions (dashed blue lines) to data. The color of cells represents the quality of fit (green - perfect fit, red - the model couldn't explain the data).

After applying the CellNoptR algorithm (see methods) to the PKN and experimental data for two different cell lines, we obtained the logic models and topologies for each cell line (fig. 28 and 29).

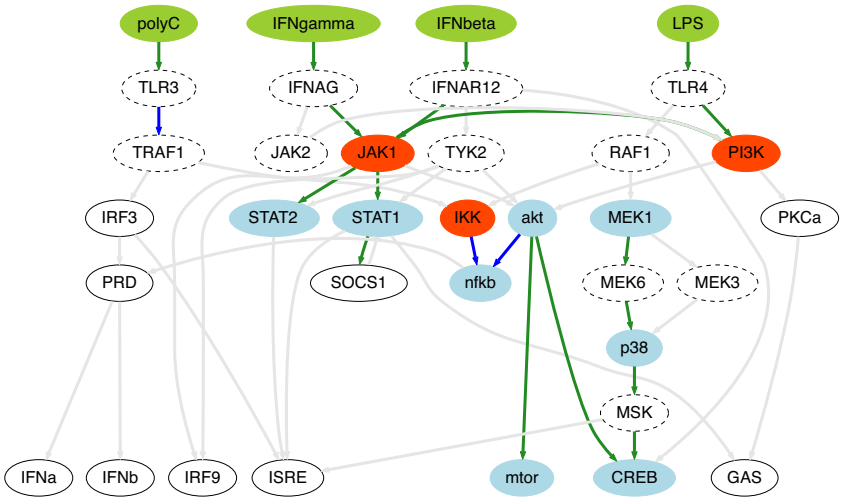

Figure 28 Logic model fitting the data from Jurkat cell line. Confirmed links are in green and blue.

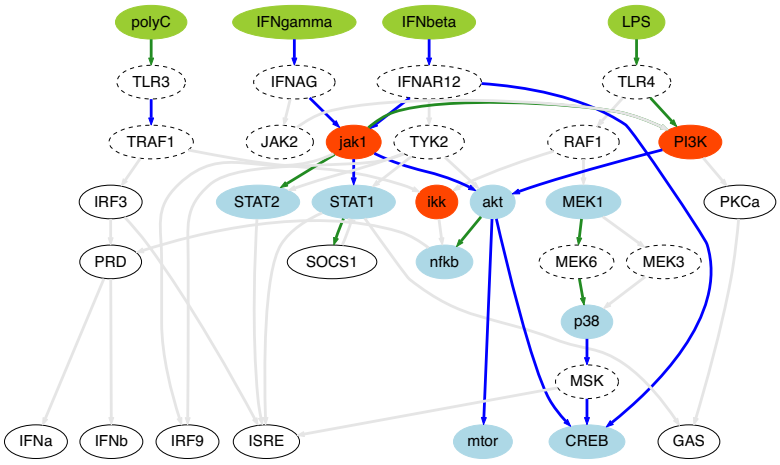

Figure 29 Logic model fitting the data from THP1 cell line. Confirmed links are in green and blue.

The models can be represented as scaffolds (fig. 30) that allow assessing the differences in the signaling between Jurkat and THP1 cell lines.

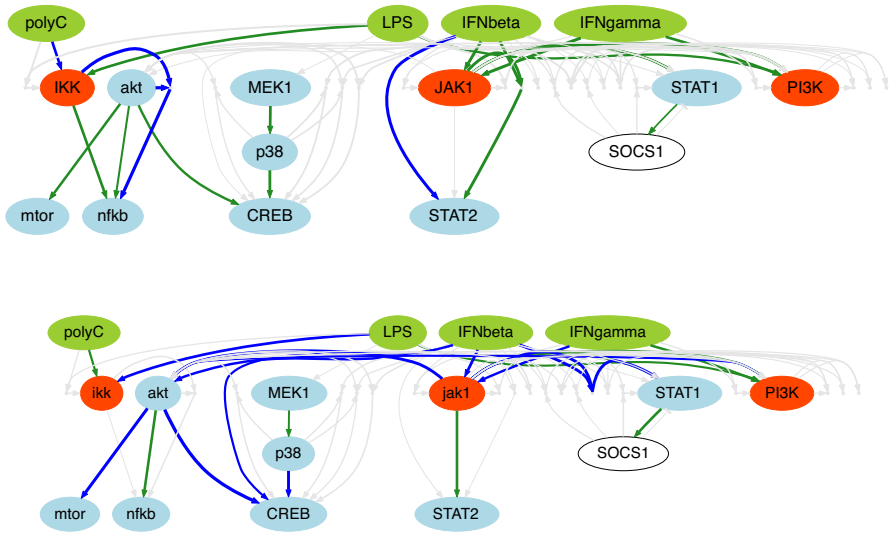

Figure 30 Scaffolds obtained from logic models for Jurkat cell line (up) and THP1 cell line (down)

As many of the main signaling channels are the same (it can be expected due to the close relationship between all immune cell subtypes), there are clear differences between the two scaffolds. For THP1 the connection IFNbeta-Jak1-Stat2 is direct. In Jurkat cell line the Jak1 is not directly triggering Stat2 activation. The activation in this case is due to other intermediates. In THP1 we see the activation CREB by IFNbeta, while in Jurkat we could not detect this effect. IKK is directly activating NFkB in Jurkat cells, but not in THP1 cells. There are other differences in signaling which may explain some of the difference in the response of immune cell subtypes in vivo (see discussion).

The pipeline to apply Boolean modeling to the clinical data

The approach was applied to the stimulated human PBMCs from healthy individuals to validate the clinical application of logic modeling.

The difference in type I IFN signaling pathway between immune cell subtypes may be crucial for the IFNbeta treatment cell response. For this reason we developed a method to apply the same approach for clinical data from individual patients. The challenge of the clinical data is the diversity between individuals in the cohort that produce noisy data.

For this reason we proposed the following algorithm for the analysis of 2 groups of individual clinical readouts of homogenous data. We applied the CellNoptR package to the simulated experimental results from [91] mimicking patients' dataset. The PKN and the simulated datasets were used to optimize the method of averaging and comparing resulting network topologies.

The method was based on averaging bitstrings corresponding to each model generated from each dataset. The bitstring is a vector consisted of 0 and 1 values corresponding to not-confirmed and confirmed by the experimental data links between different species. After CellNoptR simulation a bitstring was assigned to each toy set corresponding to an "individual".

The average model bitstring for each cohort was calculated using the following formula:

$$<n> = 1/SUM(MSE_i)*SUM(1/MSE_i*bs_i)$$

where <n> is the resulting average bitstring vector, N – number of models in the dataset, MSE – mean squared error of the

best model based on the i-dataset, bs – the best model bitstring for the i-dataset. The resulting normalized average bitstring <n> was used to build the graphical representations of the models. The difference was calculated using the following formula:

<dif> = abs (<n1>-<n2>)

where <n1> and <n2> are the bitstrings for average group models calculated previously and the <dif> is the resulting bitstring, graphically represented on fig. 31 with numbers on the edges meaning the "strength" of the differences

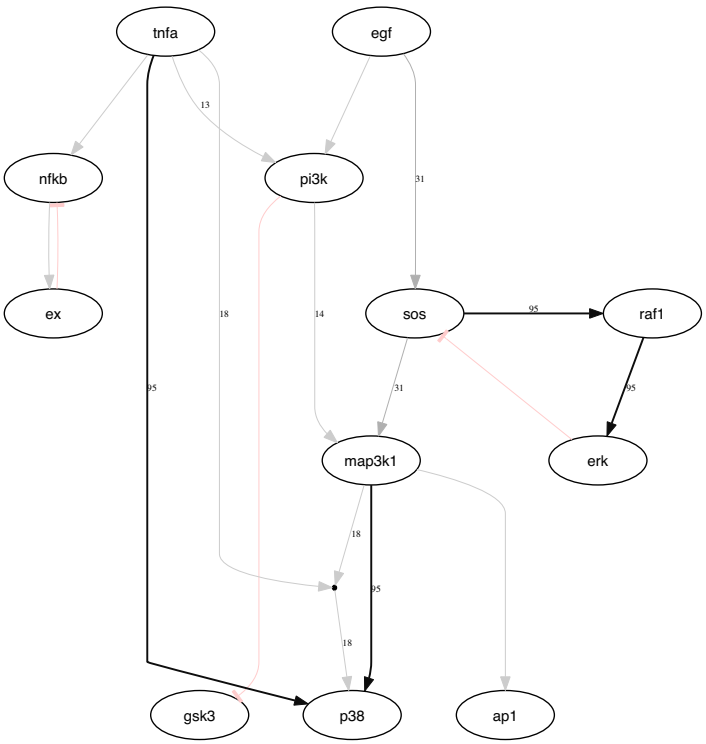

Figure 31. Differences between two average networks of simulated patients cohorts

The graph representing the differences between two dataset groups (20 datasets each) is shown on fig. 31. I found that the main difference were the links between TNFa and p38 and map3k and p38 (solid lines with the weight of 95 on fig. 31).

The developed approach can be used on the data from a big cohort of patients when it's necessary to see differences in the logic model between two groups. We are applying this method to the data from over 250 human samples with different MS subtypes to recognize the differences in molecular signal transduction and propose possible combinational therapies (CombiMS FP7 project http://combims.eu).

Chapter 3. Kinetic model of the IFN-beta signaling pathway in macrophages

One of the main interests in MS pathway studies is IFNbeta pathway due to wide usage of IFNbeta as a first choice drug for MS. The response to IFNbeta by MS patients is very limited and biomarkers and combinations are necessary to increase effectiveness of the treatment. For improving understanding on the IFNbeta pathway we developed a dynamic ODE model, which is focused on the implication of different parameters in the pathway dynamics.

In order to identify the critical elements of the signaling pathway that are responsible for the transient oscillatory behavior observed in our experiments in macrophages upon IFN-beta stimulation, we built an ODE model based in biological knowledge and experimental data. To minimize its complexity, we pursued the minimal system explaining the experimental observations, instead of a full descriptive system [92]. The model was not used to reproduce sustained endogenous IFN activation after viral infection, although it could be applied to that scenario. We developed the model of IFN-beta signaling pathway using a systems biology approach and finding the key pathway bottlenecks, which could be proposed as possible IFN-beta treatment response markers [48].

In order to analyze the effects of microbial infection in the type I IFN pathway, we stimulated the murine macrophage-like cell line RAW 264.7 with the lipopolysaccharide (LPS) endotoxin, and measured the release of IFN-beta at different time points by ELISA. We observed (fig. 32A, blue line) that IFN-beta release

increases shortly after LPS stimulation, fluctuating around a markedly non-zero level, which is sustained for long times. The initial increase in the release of IFN-beta is accompanied by a significant increase in the levels of phosphorylated Stat1 (fig. 32B). We also simulated the effects of viral infections in the endogenous IFN production, stimulating RAW cells with poly (I:C). We observed that poly (I:C) induced also an increase in the levels of IFN-beta in RAW 264.7 cells, although to a lower level than LPS (fig. 32A, red line).

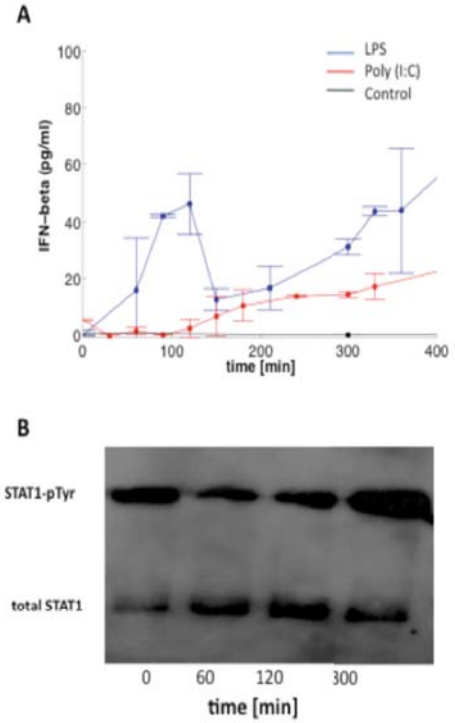

Figure 32 IFN-beta induction after microbial or viral trigger in macrophage cell line. IFN-beta levels in Raw cell culture supernatants after stimulation with LPS (15 μg/ml) (blue) or Poly (I:C) (25μg/ml) (red) versus non-stimulated control (black line) in the first 6 h and in some later times from 12 h (A); B) Western-blot showing phosphorylated and total Stat1 levels after LPS stimulation (15 μg/ml) of Raw cell line analyzed by Western-blot and

quantified by densitometry. All experiments were performed in triplicates and repeated at least two times independently.

We built a dynamic model of the IFN-beta signaling pathway using experimental data of protein and mRNA concentration measurements in vitro and previous biological knowledge. The model is based on ordinary differential equations (ODE) and predicts the behavior of the IFN-beta signaling pathway during time. The simple model included the main and most important parts of the pathway, such as Stat1 phosphorylation, Socs1 inhibition of Stat1 phosphorylation and others. The model was focused on the self-regulatory events in the pathway. We verified the model with the experiments with macrophage-like murine RAW cell line.

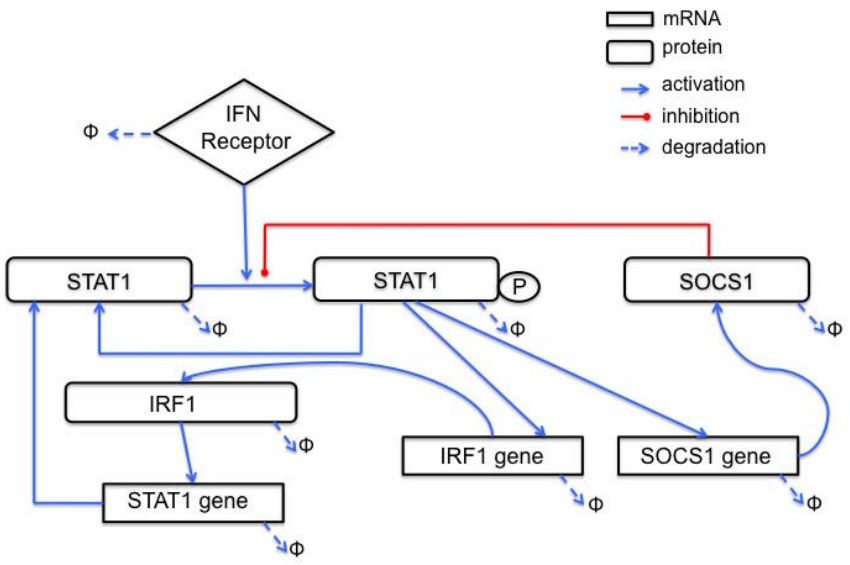

Figure 33 Mathematical model of type I IFN signaling pathway. Graphical representation of the mathematical model of type I IFN signaling pathway.

The ordinary differentiation equations for the model showed on fig. 33 are:

$$dS/dt = b_s - \lambda_s S$$

$$dA/dt = b_{\exp} A_{pn} + b_{deph} A_{pc} + b_A a - \frac{b_{ph} S A/k_A}{1 + A/k_A + (R/k_I)^q} - \lambda_{STAT} A$$

$$dA_{pc}/dt = \frac{b_{ph} S A/k_A}{1 + A/k_A + (R/k_I)^q} - b_{imp} A_{pc} - b_{deph} A_{pc} - \lambda_{STAT} A_{pc}$$

$$dA_{pn}/dt = b_{imp} A_{pc} - b_{\exp} A_{pn} - \lambda_{STAT} A_{pn}$$

$$dr/dt = b_r \frac{(A_{pn}/k_r)^n}{1 + (A_{pn}/k_r)^n} - \lambda_r r$$

$$dR/dt = b_R r - \lambda_R R$$

$$df/dt = b_f \frac{(A_{pn}/k_f)^m}{1 + (A_{pn}/k_f)^m} - \lambda_f f$$

$$dF/dt = b_F f - \lambda_F F$$

$$da/dt = b_a \frac{(F/k_F)^u}{1 + (F/k_F)^u} - \lambda_a a + B_{STAT}$$

We performed time series analysis of the phosphorylation of Stat1 and levels of total Stat1 and Socs1 by Luminex assays and Elisa (fig. 35) and levels of Stat1, IRF1 and Socs1 mRNA after IFN-beta stimulation by RT-PCR (fig. 34). We observed that phosphorylated Stat1 levels increased rapidly after IFN-beta induction (fig. 35A). The increase was significant as soon as 2 min after stimulation and reached a maximum at 10–15 min after stimulation, followed by a decrease that correlates with a substantial increase in the concentration of the SOCS1 protein (fig.

35C). A second, smaller peak was visible at around 180 min, followed by a subsequent decrease back to the baseline level after around 360 min. The quick decrease of phosphorylated Stat1 levels is in agreement with previous studies pointing to the activation of the negative feedback loop mediated by SOCS1 protein, which suppresses the phosphorylation of Jak1 and TYK2 proteins and prevents the formation of Stat-dimers [93]. The total level of Stat1 protein, on the other hand, is maintained practically constant until around 200 min after stimulation, after which it starts to increase slowly until the end of the experiments (fig. 35B). Stat1 mRNA levels grew quickly and continuously, starting sharply at around 75 min and leveling off after 200 min (fig. 34A). This increase in the mRNA level of Stat1, as soon as 1 hour after the induction of response by IFN-beta, agrees with the influence of the positive feedback loop IRF1 – Stat1 [94] and confirms the importance of this circuit for the pathway dynamics.

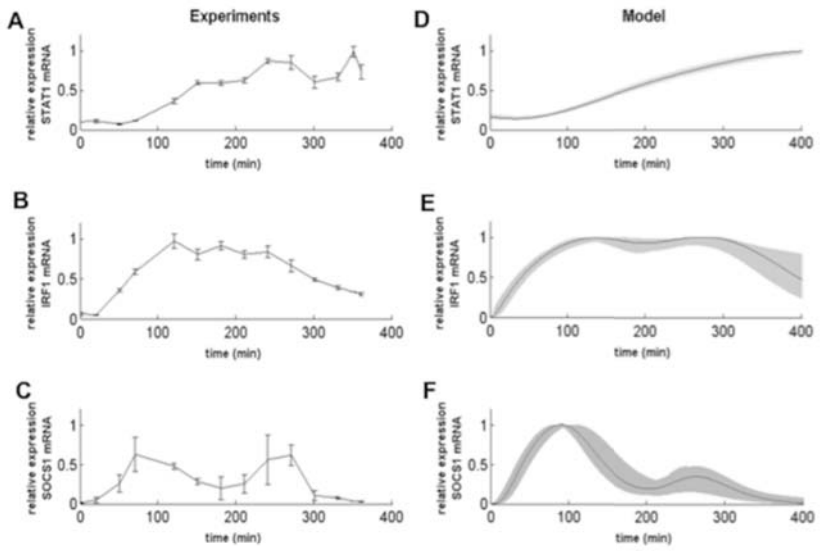

Figure 34 Gene expression levels of Stat1, IRF1 and Socs1 after IFN-beta stimulation and the corresponding simulations from the ODE model. A-C) Stat1, IRF1 and Socs1 RNA concentration in cell lysates were measured by RT-PCR in the Raw cells stimulated with IFN-beta (1000 units/ml); A) Stat1 RNA levels in the Raw cells stimulated with IFN-beta; B) IRF1 RNA levels in the Raw cells stimulated with IFN-beta; C) Socs1 RNA levels in the Raw cells stimulated with IFN-beta. We plot here one out of three independent experiments, which were performed in duplicates. D-F) Model simulation and sensitivity analysis with ± 20% change for all parameters (shaded areas) for Stat1 (D), IRF1 (E), and Socs1 (F) RNA levels.

To analyze the expression of regulatory genes of the type I IFN pathway, we measured the levels of two downstream Stat1 genes, SOCS1 (responsible of the negative feedback) and IRF1 (mediator of the positive feedback). We observed an oscillatory behavior of SOCS1 mRNA during the first 360 minutes after stimulation, with clear peaks at around 90 min and 250 min, before returning to baseline levels (fig. 34C). On the other hand, IRF1 shows different dynamics, with its concentration raising quickly

between 30 and 120 min, then reaching a plateau and decreasing more slowly after 250 min (fig. 34B). We also quantified the expression levels of other downstream effector IFN-induced genes, such as MX1 and OAS1b, but did not identify any activation of their transcription in the RAW 264.7 cell line after IFN-beta stimulation. Our observations show that in the RAW 264.7 cell line the main activated genes were the ones controlled by the Stat1-Stat1 homodimer (IRF1 and SOCS1) and containing GAS elements in their promoter region. These genes are mainly responsible for the antimicrobial activity of the cells [95].

Then, we compared experimental results with mathematical model simulations in order to assess the agreement of the dynamics at the qualitative level. Experiments uncovered several important features of Jak/Stat signaling dynamics during the first eight hours after treatment with IFN-beta. For example, our results showed the transient oscillatory nature of Stat1 activation (pStat1), with a fast increase in cytosol concentration early after stimulation (within the first hour), followed by a secondary concentration peak at around 200 min. A key Stat1 transcription target such as Socs1 also showed two peaks of expression (correlated in time to the pStat peaks) at around 90 min and 250 min after stimulation, whereas another important target, namely IRF1, exhibited a more bell-shaped plateau signal.

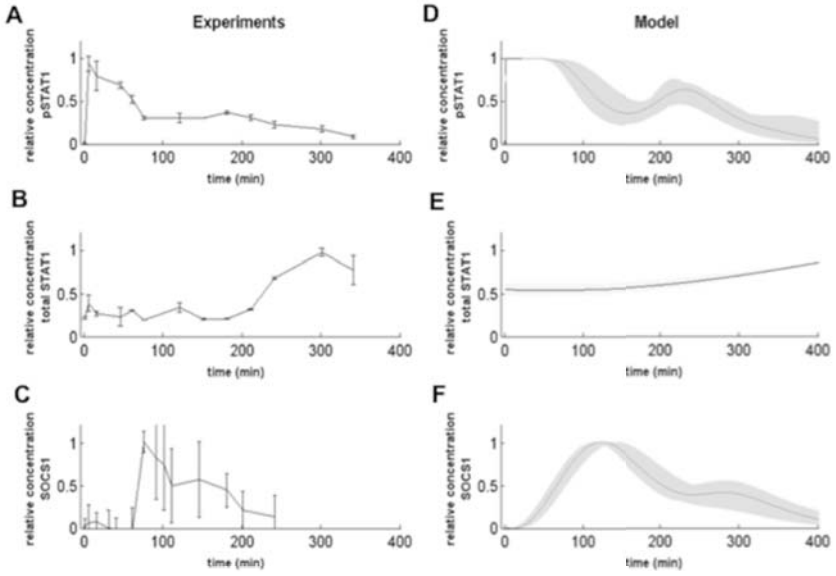

Figure 35 Activation of type I IFN pathway by IFN-beta in Raw cell line and the corresponding simulations from the ODE model. A-C) pStat1, Stat1 and Socs1 protein concentration in cell lysates were measured by Luminex, Flow cytometry or ELISA after stimulation with IFN-beta (1000 units/ml). The data was normalized to the maximum level. A) pStat1 protein concentration in the Raw cells stimulated with IFN-beta; (B) Total Stat1 protein concentration in the Raw cells stimulated with IFN-beta; C) Socs1 protein concentration in the Raw cells stimulated with IFN-beta. We plot here one out of three independent experiments, which were performed in duplicates. D-F) Model simulation and sensitivity analysis with ± 20% change for all parameters (shaded areas) (D: pStat1; E: Stat1; F: Socs1).

Chapter 4. IFNbeta model analysis and nuclear translocation as a modulator of the IFNbeta pathway kinetics

We performed computer simulations using different conditions and parameters as well as sensitivity and bifurcation analysis of the developed IFNbeta ODE model. The bifurcation analysis indicated the possible implication of nuclear translocation of pStat1 for the correct oscillatory activity of the cells upon the IFNbeta stimulation in vitro. This finding led us to the hypothesis of alteration of the nuclear translocation process in the response to IFNbeta therapy.

The model allows us to interpret the second peak observed experimentally in pStat1 and SOCS1-mRNA levels in terms of an underlying damped oscillatory dynamics. We now ask which are the mechanisms that lead to oscillations, on the one hand, and to damping, on the other hand. A well-known gene circuit architecture that leads to oscillatory behavior is a combination of positive and negative feedback loops. As mentioned above, our model contains a negative feedback loop mediated by SOCS1. We can examine in the model the effect of not having this feedback by eliminating SOCS1 signaling from the model. The results show that this negative feedback is required for the oscillatory behavior to arise: its absence leads to a transient plateau of high pStat1 levels during the first 4–5 h of IFN treatment (fig. 36B), which contrasts with the relaxation oscillator behavior obtained for our basal parameter values (fig. 36A), which is a closer match to the experimental observations (fig. 35-35). The model also contains a positive feedback loop mediated by IRF1. This loop, however, does

not appear to be crucial for the oscillatory behavior of pStat1 (fig. 36C), and is only necessary to reproduce the experimentally observed increase of Stat1 expression (fig. 34).

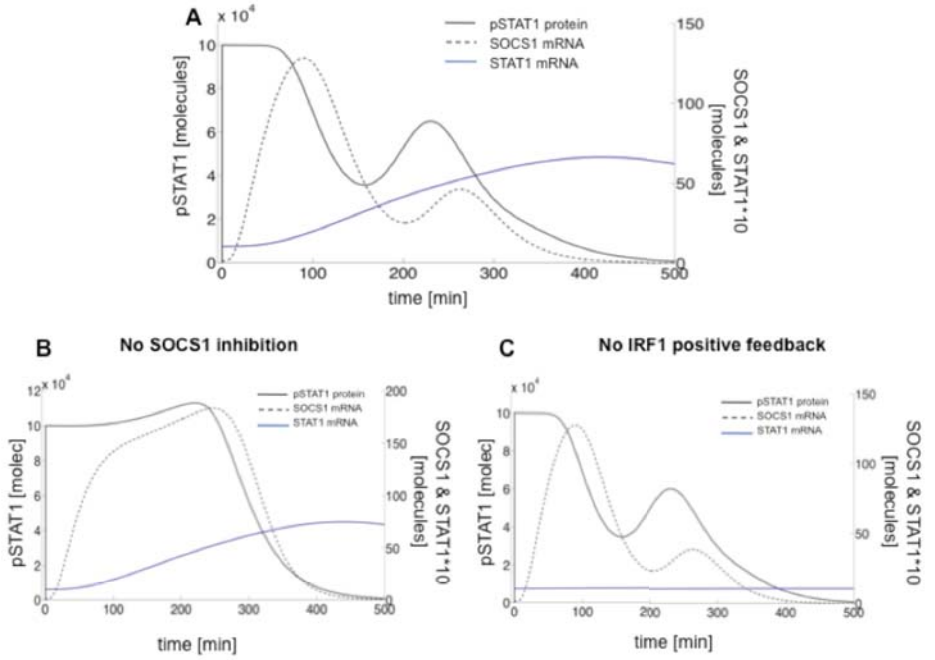

Figure 36 Type I IFN pathway model simulations during the first 8 hours after IFN-beta stimulation. (A) Model simulations showing oscillations of total (nuclear plus cytoplasmic) pStat1 protein, Socs1 mRNA expression (dashed line) and Stat1 mRNA expression (dotted line). (B) Corresponding simulations where the Socs1-mediated negative feedback is disrupted by assuming an infinite value of the repression threshold kI. (C) Corresponding simulations not including the IRF1-mediated positive feedback, by assuming a zero value of the Stat1 activation threshold kF (which leads to saturation of the corresponding Hill function, so that the dependence of an expression on F is removed).

The temporal evolution of the phosphorylation of Stat1 can be crucial for understanding the response to IFN-beta therapy, and may provide an explanation of the lack of response to this therapy in some cases [96]. In particular, transient oscillatory dynamics could provide a way for the Stat1 pathway to increase the duration of its response to IFN-beta in a physiological manner (i.e. without a period of sustained constant activation as in fig. 36B). In order to

establish the conditions under which this transient dynamics exists, we analyzed the behavior of the system for combinations of two-parameter pairs, distinguishing between the parameter values for which pStat dynamics is overdamped (and thus non-oscillatory) and those for which the oscillations are underdamped (which corresponds to the experimental situation reported above). We focused on the phosphorylation and dephosphorylation rates (b_{ph} and b_{deph}) and export and import rates (b_{exp} and b_{imp}). These parameters represent crucial steps to regulate the nuclear availability of transcription factors such as pStat dimers, and thus also the expression of downstream genes.

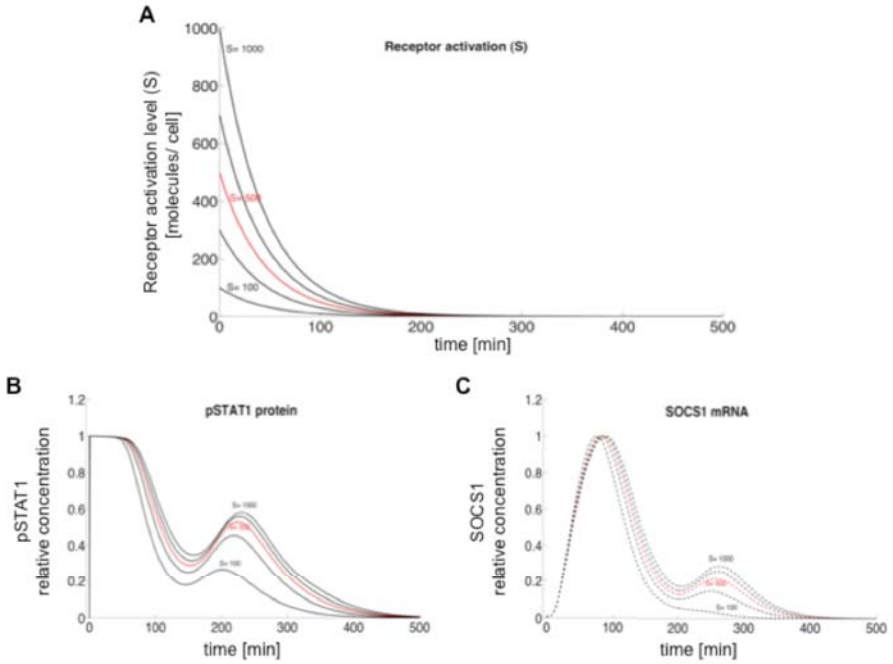

Figure 37 Influence of activated receptor level on the transient oscillatory dynamics. (A). Time evolution of the activation level of type I IFN receptors in the model (S) by stimulation with IFN-beta (added at t = 0) for different initial levels (in red, S = 500 molecules at t = 0). (B, C) pStat1 (B) and Socs1 mRNA (C) dynamic responses for varying levels of initial receptor activation as in panel A (lower lines in B and C correspond to lower lines in A).

In order to identify mathematically the two different dynamical regimes mentioned above, we examined the stability properties of the steady state of the ODE system for a constant activated receptor level (S) equal to its initial value. In that context, the underdamped/oscillatory regime is characterized by a steady state that takes the form of an unstable focus (i.e. the stability eigenvalue with maximum real part has negative imaginary part), whereas the steady state in the overdamped/non-oscillatory regime is a node (the stability eigenvalue with maximum real part has no imaginary component). In that way, by calculating the imaginary part of the stability eigenvalue of the steady state with maximum real part, we can identify the parameter regions in which the pathway exhibits a transient oscillatory response to IFN-beta. The result, for the parameter space formed by the phosphorylation and dephosphorylation rates b_{ph} and b_{deph}, is shown in fig. 37A. This figure shows, on the one hand, the prevalence of oscillations for a wide range of these parameters, and on the other hand it tells us the conditions for which transient oscillations exist. For instance, increasing sufficiently the dephosphorylation rate can transform an oscillatory regime into a non-oscillatory one, and reversely, by making the phosphorylation rate large enough the system can be made to exhibit transient oscillations. Figure 38B shows examples of these two dynamical regimes for two specific

parameter sets within this phase diagram.

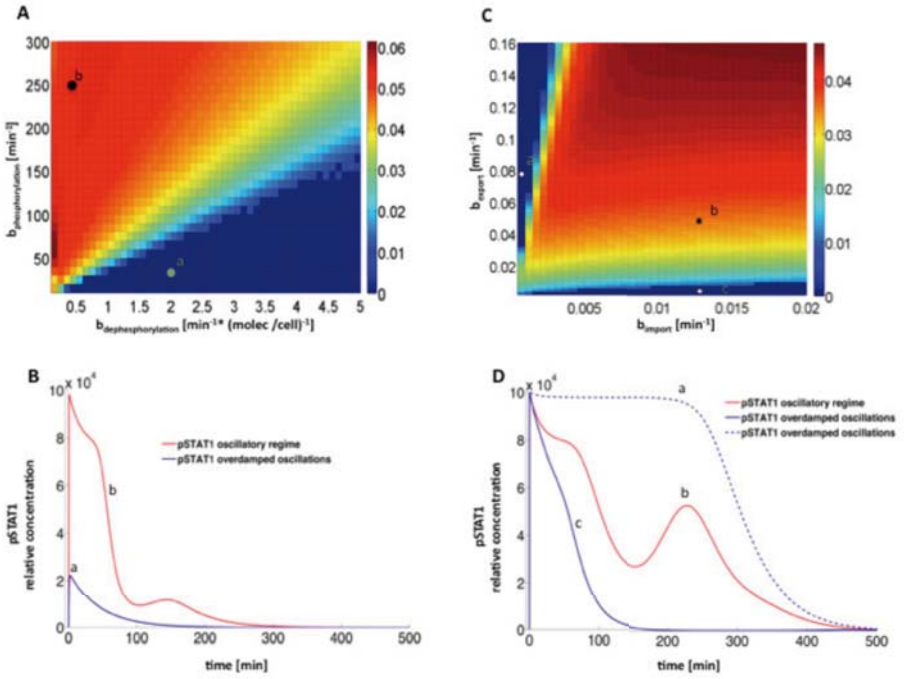

Figure 38 Stability analysis of the steady state solution in two 2D parameter spaces. (A, C) The color scale represents the absolute value of the imaginary part of the stability eigenvalue with maximum real part, corresponding to the steady state of the system after IFN stimulation, for varying phospho/ dephosphorylation rates (bph and bdeph, panel A), and nuclear export/import rates (bexp and bimp, panel B). Two distinct dynamic regimes can be identified with this analysis: the damped oscillatory regime (shifted to red) and the overdamped/ non-oscillatory regime (blue). (B, D) Examples of pStat1 time evolution in both regimes (damped and over-damped in red/blue lines, respectively) corresponding to parameter position of circle markers for the two diagrams shown in panels A and B, respectively.

We also tested the influence of the import rate of pStat1 molecules into the nucleus, and of the export rate of Stat1 from the nucleus into the cytosol. By tuning both parameters (b_{exp} and b_{imp}) simultaneously, we observed again that the transient oscillatory regime is prevalent in this system (fig. 38C). We found that the oscillatory regime is associated with high nuclear import rates in

combination with high export rates. For high export rates but low import rates, the pathway exhibits an overdamped (non-oscillatory) response, showing a sustained plateau in the transient level of pStat1 (discontinuous blue line in fig. 38D). Conversely, for high import rates and low export rates the response is also overdamped, but with a faster decay (continuous blue line in fig. 38D). We conclude that bifurcation analysis of the Stat1 pathway model identifies translocation to the nucleus as a critical step

To check the hypothesis that nuclear translocation process is critical for the response to IFNbeta therapy in Multiple Sclerosis patients, we assessed Stat1 nuclear translocation after IFNbeta treatment in MS patients using ImageStreamX imaging platform (see methods). We adjusted the flow cytometry standard protocol using PBMCs from healthy controls (fig. 39).

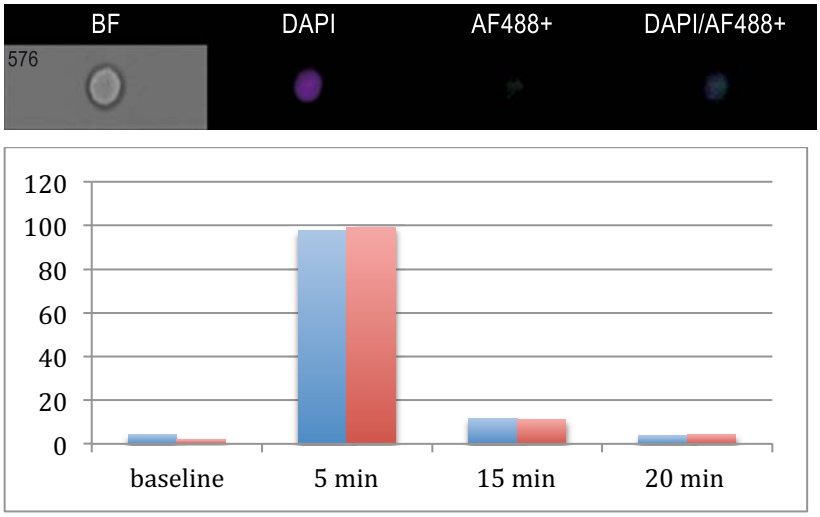

Figure 39 Nuclear translocation measured by ISX technology. UP: The example of nuclear localization of pStat1 visualized by ImageStreamX. DOWN: the quantification of PBMCs from a healthy control in vitro stimulated with 1000 un/ml of IFNbeta. Blue – the percent of pStat1+ cells from the total population, red – percent of pStat1+ cells with pStat1 localized in the nucleus from a total population of pStat1+ cells.

We obtained PBMCs from controls (n=2) and patients treated with IFNbeta (n=2) at different times after injection (fig. 39-40). The PBMCs from controls were used for in vitro studies (fig. 39) The control in vitro stimulations of PBMCs from healthy individuals show very quick response with nearly all pStat1 translocating to the nucleus at 5 minutes and shuttling back in just 15 minutes after stimulation.

The PBMCs from MS patients were obtained in different time after the injection of IFNbeta (in vivo conditions).

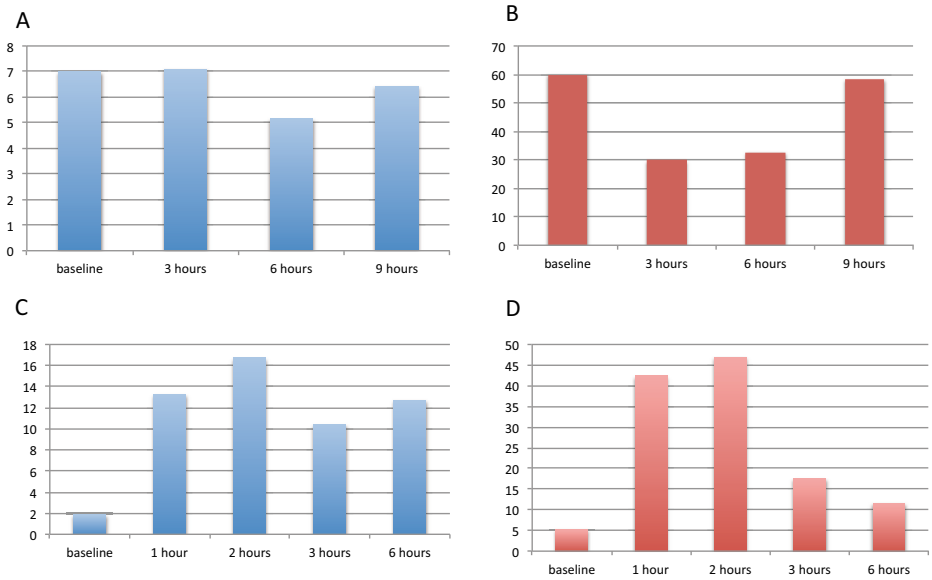

Figure 40 Nuclear translocation measured by ISX technology. The quantification of PBMCs from an MS patients treated with IFNbeta - Extavia (A and B) and Avonex (C and D). The time shows the time of blood withdrawal after injection. Blue: the percent of pStat1+ cells from the total population, Red: percent of pStat1+ cells with pStat1 localized in the nucleus from a total population of pStat1+

The results from MS patients show significant differences in the nuclear translocation pattern between individuals. On fig. 40 in blue we see the percent of pStat1+ cells from the total number of cells at different times after in vivo injection. While for Extavia

patient this level stays nearly the same around 5-7%, the Avonex patient shows a sharp increase in pStat1+ PBMCs after 1-2 hours peaking at 17% and a slow decrease at 3-6 hours. The fig. 40B and 40D shows the percent of translocated to the nucleus pStat1 in the Stat1+ cells in the same patients. While Extavia patient has a high level of nuclear Stat1 at a baseline and unexplainable decrease after the injection, the Avonex patient shows nearly no nuclear Stat1 at a baseline and quick translocation to up to 50% after 1-2 hours post-injection with a decrease at later timepoints.

While these results are promising, the sample size is too small to determine the translocation of Stat1 to the nucleus after in vivo injections of IFNbeta and a study with a bigger cohort of responders and non-responders to IFNbeta is needed to determine if pStat1 translocation rate can determine the response to therapy and serve as a clinical biomarker of the response.

Chapter 5. Nuclear translocation dynamics of Foxo3a orchestered by Sgk/Akt balance

In order to model the Akt/Sgk-Foxo3a pathway (Foxo pathway), we have developed an ODE model based in previous knowledge and experimental data. The core feature of our model is the nuclear export and phosphorylation of pFoxo3a by pAkt and pSgk after activation of IGF1 pathway. The phosphorylation of Foxo3a in the 3 main phosphosites leads to its deactivation and arrest in the cytoplasm. Other post-translational modifications may lead to its ubiquitination and degradation (fig. 41).

Our model shows the importance of the mechanism of inhibition of Foxo3a for the noise resistance of the system.

In our model we consider following key points:

- First mechanism: Activation of Akt (phosphorylation) by IGF1 or other growth factor leads to phosphorylation of Foxo3 in 3 conserved sites. pFoxo3 transfers to the cytoplasm
- Second mechanism: Sgk is activated either by PI3K pathway or by stress sensors and phosphorylates Foxo3a
- pFoxo3a has three main phosphosites. pSgk and pAkt has different affinity to different pFoxo3a phosphosites but both lead to the phosphorylation of all three of them
- Both mechanisms lead to export from the nucleus and inhibition of Foxo3a action as a TF
- Dephosphorylation is induced by PP2A and allows Foxo3 to come back to the nucleus and bind specific binding sites restoring the pro-apoptosis gene expression pattern (this term should influence the kinetics of the system as well)

• Ubiquitination of Foxo3a targets it for degradation, which has influence in the kinetics of the system

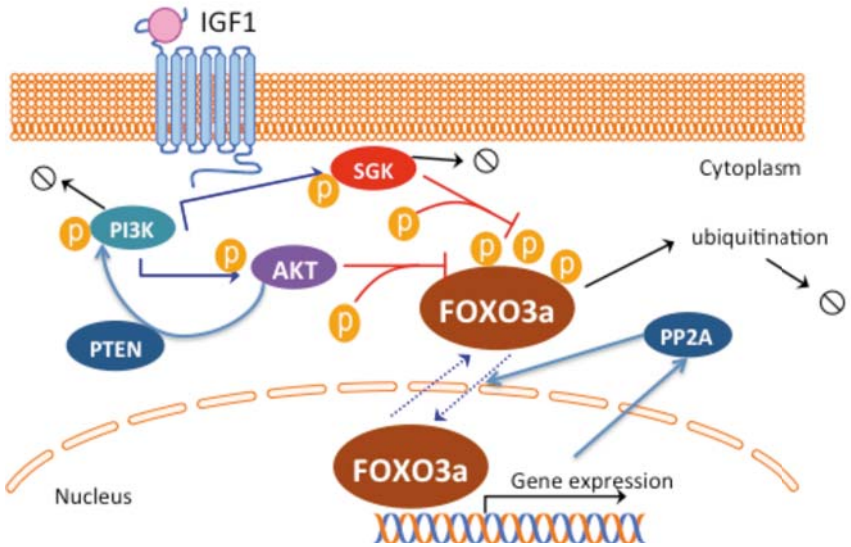

Figure 41 The model of Akt-Foxo3 signaling and Foxo3 nuclear shuttling

The model is represented on the fig. 41 and consists of the following events and elements: IGF1 growth factor signal, phosphorylation and dephosphorylation of Sgk, phosphorylation and dephosphorylation of Akt, phosphorylation of Foxo3a in 3 phosphosites by pSgk, phosphorylation of Foxo3a in 3 phosphosites by pAkt, export of Foxo3a to the cytoplasm, dephosphorylation and import of pFoxo3a to the nucleus, activation of transcription of apoptotic genes by Foxo3a (non-phosphotylated). We also included degradation of pFoxo3a, Akt and Sgk.

On the top at the moment there are included several additional points: the negative regulation of pAkt by Pten (this includes inhibition of phosphorylation of pAkt by Pten) and active dephosphorylation of Foxo3a by PP2A

PTEN should be considered as a constant growing function and PP2A is considered to be constant for the moment

The model can be represented as the following system of equations

$$\frac{dS}{dt} = r_1 S_p - \frac{k_{sp} * I * \left(\frac{S}{k_S}\right)^n}{1 + \left(\frac{S}{k_S}\right)^n} - \lambda_S S$$

$$\frac{dS_p}{dt} = \frac{k_{sp} * I * \left(\frac{S}{k_S}\right)^n}{1 + \left(\frac{S}{k_S}\right)^n} - r_1 S_p$$

$$\frac{dA}{dt} = r_{10} A_p - \frac{k_{ap} * I * \left(\frac{A}{k_A}\right)^m}{1 + \left(\frac{A}{k_A}\right)^m + \frac{P}{k_{inh}}} - \lambda_A A$$

$$\frac{dA_p}{dt} = \frac{k_{ap} * I * \left(\frac{A}{k_A}\right)^m}{1 + \left(\frac{A}{k_A}\right)^m + \frac{P}{k_{inh}}} - r_{10} A_p$$

$$\frac{dF_c}{dt} = k_{\exp} F_n - \frac{k_{deph\_c} * \left(\frac{F_c}{k_c}\right)^c}{1 + \left(\frac{F_c}{k_c}\right)^c + \frac{D}{k_d}} - r_8 F_c$$

$$\frac{dF_n}{dt} = \frac{k_a A_p * \left(\frac{F}{k_f}\right)^j}{1 + \left(\frac{F}{k_f}\right)^j} + \frac{k_s S_p * \left(\frac{F}{k_f}\right)^q}{1 + \left(\frac{F}{k_f}\right)^q} - k_{exp} F_n - k_{deph\_n} F_n$$

$$\frac{dF_{dc}}{dt} = \frac{k_{deph\_c} * \left(\frac{F_c}{k_c}\right)^c}{1 + \left(\frac{F_c}{k_c}\right)^c + \frac{D}{k_d}} - k_{imp} F_{dc}$$

$$\frac{dF_{dn}}{dt} = k_{deph} F_n - \frac{k_a A_p * \left(\frac{F}{k_f}\right)^j}{1 + \left(\frac{F}{k_f}\right)^j} - \frac{k_s S_p * \left(\frac{F}{k_f}\right)^q}{1 + \left(\frac{F}{k_f}\right)^q} + k_{imp} F_{dc}$$

$$\frac{dg}{dt} = \frac{k_g * F_{dn} * \left(\frac{g}{k_e}\right)^t}{1 + \left(\frac{g}{k_e}\right)^t} - r_{18} * g$$

$$\frac{dP}{dt} = c * P$$

$$\frac{dD}{dt} = x + \frac{k_{inh} * \frac{F_{dn}}{k_{dn}}}{1 + \frac{F_{dn}}{k_{dn}}} - r_5 * D$$

where

S is non-phosphorylated Sgk, S_p – phosphorylated Sgk, A - non-phosphorylated Akt, A_p – phosphorylated Akt, F - non-phosphorylated Foxo3a, F_{n_akt} – phosphorylated in 3 phosphosites by

Akt Foxo3a in the nucleus, F_{n_sgk} – phosphorylated in 3 phosphosites by Sgk Foxo3a in the nucleus, F_{c_akt} – phosphorylated in 3 phosphosites by Akt Foxo3a in the cytoplasm, F_{n_sgk} – phosphorylated in 3 phosphosites by Sgk Foxo3a in the nucleus, F_{dc} – nonphosphorylated Foxo3a in cytoplasm, F_{dn} – nonphosphorylated Foxo3a in the nucleus, g – downstream genes, P - active PTEN molecules, D - active PP2A molecules

The parameters are explained in the supplementary table 6.

While this work is still in process we have preliminary promising results. From experimental perspective, we challenged the SH-Sy5 cell line with a new compound. The compound is in preclinical development as a potential drug for MS. We observed the oscillations in the nuclear translocation of Foxo3a during the first 2 hours after in vitro stimulation with the compound. The results were obtained by IHC.

In order to understand this experimental observation we performed the analysis of the parameter space of our model and identified the set of parameters capable to produce oscillations with the same period. We are performing further experiments and simulations to validate the hypothesis of oscillatory behavior of the nuclear translocation of Foxo3a and its possible implication in drug discovery.

Discussion

In this thesis I tried to assess the signal transduction molecular system in different levels of detail. Watching from hierarchical upper and lower levels I was able to identify different questions and examine the answers. As a result we examine several hypothesis from hierarchical perspective:

1. The oscillatory dynamics of IL6 pathway in populations
2. The connection between pathways in different cell lines (T cell and macrophage-like human cell lines)
3. In-deep understanding of single pathway dynamics
4. Exploration of a concrete dynamical feature: the translocation in two different pathways

This top down approach brought us from general theoretical questions to possible clinical implication of Systems Biology. In the discussion we'll follow this logic from higher to lower hierarchy and compare the approaches and their outcomes. During the journey we developed new approaches and methods to combine Systems biology and Translational medicine and apply standard Systems biology approaches to clinical questions.

Populations exhibit important dynamical features, which can be overwatched in traditional Systems biology dynamical approaches

The behavior of populations and single-cell variability is a challenge for Systems biology approach with different methods developed to model the real populations

Different cell types provide different responses to external signals due to their network constructions

In RAW cell line, Socs1 and IRF1 genes expression change during early IFN response, but there are no significant expression of some commonly used reference genes (Mx1 and OAS1a). Jak-Stat pathway activation by IFN-beta activates the phosphorylation of Stat1, Stat2 and some other proteins. These activated proteins mainly form 2 different complexes: Stat1-Stat1 (AAF complex) and Stat1-Stat2-IRF9 (ISGF complex). Both complexes activate many genes in the nucleus binding to the specific regulation elements in the promoters. AAF complex binds to GAS elements and ISGF complex binds to ISRE elements. GAS-containing genes (Incl. Socs1 and IRF1) are responsible for the antibacterial response of the cells and ISRE-containing genes are activating an antiviral response of the cells [95]. Based on this background and our results we hypothesized that macrophages form mainly AAF complexes which activates the antibacterial route (GAS sequences) but in T cells the situation is opposite, activation ISFG3 elements and therefore the antiviral response (Figure 16). For example, it was recently shown that the response to IFN-beta differs between immune cells, and an analysis of non-responders to IFN-beta therapy indicates an impairment of the type I IFN pathway differentially in the monocytes of those patients [52].

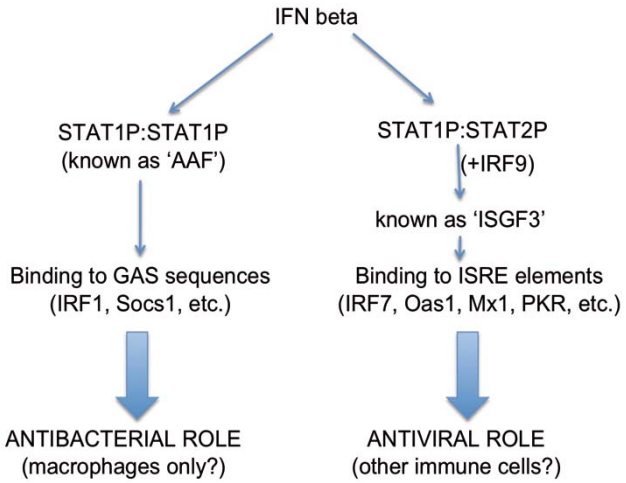

Figure 42 Possible explanation of the difference in RAW macrophages cell line IFNbeta signaling and classical Jak-Stat pathway.

The IFN signaling network affects different complex pathways, involving processes such as differentiation, proliferation, survival and cell death. Importantly, it is a canonical pathway involved in different complex pathways, involving processes such as differentiation, proliferation or survival and cell death [97, 98] and also as a therapy for autoimmune [99]. IFN-beta is the most common treatment for MS [100], exerting a pleiotropic immunomodulatory activity not well understood. IFN-beta treatment decreases activation, proliferation, cytokine release, and migratory properties of activated T cells, diminishing their ability to enter and damage the brain tissue. In spite of these properties, up to 40% of patients do not respond to IFN-beta therapy, which represents a significant health problem [96]. Previous genomic studies have identified certain genes belonging to the IFN pathway that are associated with a lack of response to IFN-beta, suggesting that the genetic background of certain individuals may

modulate this pathway, and consequently the response to therapy, by specific transcriptional profiles [101].

This considerations led us to the idea of studying the difference in type I and type II IFN signaling in macrophages and T cells. We chose the Boolean modeling approach to be able to explore more extended networks. We found significant differences between 2 networks including differences in IFNbeta-Stat1-Stat2 connections and IFNgamma-Stat1-Stat2 connections we expected from our hypothesis of Stat1-Stat2 and Stat1-Stat2 dimers formation theory explained above.

In-depth understanding of IFNbeta signaling pathway dynamics in RAW 264.7 macrophage-like cell line

We analyzed the type I IFN-beta signaling pathway in macrophages, showing that the response of this pathway to IFN-beta stimulation takes the form of transient oscillations in Stat1 phosphorylation. We characterized and identified the critical elements governing the transient dynamics of IFN activation, and examined the influence of this dynamical regime in the response to IFN-beta. To that end, we quantified in a time-resolved manner the level of certain pathway components after IFN-beta activation, and implemented a mathematical model of the Jak/Stat pathway.

Dynamical models of IFN induction of the Jak/Stat signaling pathway based on nonlinear ordinary differential equations, have been previously used to study the effect of IFN pre-treatment on the response of the immune system to virus infection [44, 45] and the robustness of the pathway to noise and parameter fluctuations [46], among other problems. Systems biology approaches have also been applied to this pathway in order to examine its role in certain

pathological mechanisms underlying the behavior of cancer cells [102], and its interaction with other key signaling pathways [44, 103]. Here we combine our theoretical model with experimental observations, in order to study the role of the pathway architecture on the immediate molecular response of the pathway to IFN-beta stimulation. Our results show that a combination of positive and negative feedback loops, together with the eventual degradation of the IFN signal in the medium, leads to a transient oscillatory response in several components of the pathway. This behavior is consistent with previous numerical results found in pure modeling studies [104], and goes beyond previous observations that indicate a simpler transient response [37, 85, 98]. We interpret the transient oscillatory response of the pathway in terms of the potential effectiveness of IFN-beta treatment in MS patients.

Jak-Stat signaling pathway regulation appears to be more complex than it was thought before. It is tightly regulated and highly connected with other pathways [105]. Moreover, type I IFNs are commonly used as treatment in several chronic diseases such as hepatitis C, leukemia and Multiple Sclerosis (MS). Improving our understanding on how this signaling pathway works, processes information and participates in the pathogenesis of these diseases or in the response to therapy would improve our ability to manage such diseases.

One of the aims of this work was to characterize the dynamics of the key components of the type I IFN-beta signaling pathway in macrophage RAW 264.7 cells. This system robustly translates extracellular chemical signals through cell membrane receptors, leading to phosphorylation of the Stat transcription

factors, which induce gene expression of multiple targets. Jak/Stat signaling directly regulates the immune system response under viral or bacterial infection, and is also important in autoimmune diseases and cancer treatments. The IFN signaling network affects different complex pathways, involving processes such as differentiation, proliferation, survival and cell death. Importantly, it is a canonical pathway involved in first-line treatments of multiple sclerosis as a main target of the IFN system [99] but, also, affects different complex pathways, involving processes such as differentiation, proliferation or survival and cell death [90, 91].

Our IFNbeta model simulations exhibit a transient oscillatory behavior in pStat1 concentration, and reveal that the oscillations require the presence of a negative feedback loop on Stat1, mediated by its phosphorylation inhibitor Socs1. Previous mathematical models of the type I and type II IFN pathways have suggested the possibility that Stat1 pathway has an oscillatory behavior [36, 97] and indicated the importance of the Socs1 negative feedback [85, 100]. Another factor that has been proposed to be important in defining the response to IFN is the basal level of receptors of the Jak/Stat pathway[106]. In our model this aspect was also taken into account, showing clear effects on the dynamics of the pathway response. Going beyond previous models, our theoretical results show that the physiological regime of the pathway's response to IFN-beta takes the form of damped oscillations that can be identified by means of a stability analysis of the model's steady state solution. This analysis shows that processes such as the phosphorylation and dephosphorylation of pStat1, and the transport of Stat1 between the nuclear and cytosol

compartments, can make the pathway switch between underdamped and overdamped oscillatory regimes [107].

Limitations

There are several limitations in this research.

From the experimental point of view we used cell lines in most of our studies. Cell lines is a simple and powerful tool to explore signaling pathway dynamics but may differ significantly from in vivo conditions. For the validation of the translocation of Stat1 as a potential biomarker we used PBMCs from MS patients in a small cohort. The clinical findings have to be validated on a much bigger cohort of patients. The design of the in vivo study doesn't allow the comparison with healthy controls and patients due to injection of a prescribed drug.

For Boolean modeling we used al limited phosphoproteins dataset so we couldn't see some of the possibly presented links due to the lack of the clinical data.

The main limitation of the ODE modeling is the unknown parameters in most of the cases. Many parameters con't be derived from the experimental or don't have direct biological meaning. We overcome this limitation by comparing our model to experimental data but can't reject possible biases due to manual parameter fit.

Sgk/Akt-Foxo3a model lack experimental validation, which is the next step planned in this project and should be available soon.

Implications of the type I IFN and Sgk/Akt-Foxo3a signaling dynamics in autoimmune diseases

IFN-beta is the most common treatment for MS [100], exerting a pleiotropic immunomodulatory activity not well understood [99]. IFN-beta treatment decreases activation, proliferation, cytokine release, and migratory properties of activated T cells, diminishing their ability to enter and damage the brain tissue. In spite of these properties, up to 40% of patients do not respond to IFN-beta therapy, which represents a significant health problem [96]. Previous genomic studies have identified certain genes belonging to the IFN pathway that are associated with a lack of response to IFN-beta, suggesting that the genetic background of certain individuals may modulate this pathway, and consequently the response to therapy, by specific transcriptional profiles [101]. For example, it was recently shown that the response to IFN-beta differs between immune cells, and an analysis of non-responders to IFN-beta therapy indicates an impairment of the type I IFN pathway in the monocytes of those patients [52][108].

Our study indicates the importance of identifying the temporal dynamics of the concentration of certain key components of the Jak-Stat pathway, such as the phosphorylated form of the Stat1 protein, and of the expression of interferon-stimulated transcription genes like Socs1 and IRF1, within the first 8 hours of IFN-beta administration. Cataloguing these dynamics could provide us with early molecular biomarkers that allow us to distinguish the lack of response to IFN-beta therapy of certain MS patients.

Our models indicate the crucial role of nuclear translocation of Stat1 and Foxo3a molecules for the correct dynamics of the whole pathway. The alterations in the translocation features of Stat1 prevail over the rates of phosphorylation and dephosphorylation in determining the oscillatory dynamics of IFNbeta signaling pathway. On a small group of MS patients we showed that the rate of translocation differs a lot between individuals and may determine the response to therapy or disease progression. The levels of Stat1 translocation may be potential biomarkers of IFNbeta treatment response and require further research.

Another example of the importance of nuclear shuttling characteristics in signal transduction is Foxo3a transcription factor. Foxo3a can be considered as a master regulator of the PI3K-Akt pathway, which determines the survival or apoptotic scenario of cell decision [109]. In this case the quality and versatility of the network structure (inhibition by phosphorylation in the nucleus and further transfer to the cytosol) as well as the numerous possible post-transcriptional modifications [56] make Foxo3a an example of the key node protein tightly regulated to prevent misconducted decisions of the cell. The model of Akt-Foxo3a signaling is an interesting tool from both theoretical and practical point of view. From the theoretical side, the Akt-Foxo3a signaling is an example of a larger group of signal transduction pathways involved in cell decisions, which share number of common patterns of behavior. The kinetics of Akt-Foxo3a and its regulation and crosstalk may be a common trend in the whole class of signaling pathways. The reason for the phosphorylation-

inhibition-nuclear export structure is the resistance to noise of such mechanism of action and easy tuning possibilities and constantly changing behavior.

From the practical point of view, Foxo3a is an emerging target in immunology and neurology [65, 110]. The new promising neuroprotective drug for MS BN201 targets Sgk, the upstream kinase of Foxo3a, and modifies Foxo3a activity. The understanding of the Sgk-Akt balance and communication as well as Foxo3a behavior in human cells in different conditions let us predict the effects of the new emerging treatments of MS.

Conclusions

1. The population of cells has an ability to coordinate and synchronize their activity in response to IL-6 stimulation. This ability is a necessary attribute of the cell signaling, which allows correct response to the external systems and provides a more robust response to the environment.

2. T cells and macrophages respond different to IFNbeta, IFNgamma or infectious agents due to the qualitative difference in their signaling networks. These differences lead to a complex repertoire of behaviors of immune system cells in response to different challenges as well as to the response to IFNbeta treatment in autoimmune diseases.

3. The IFN-beta signaling in macrophages takes the form of transient oscillatory dynamics of the Jak-Stat pathway, whose specific relaxation properties determine the lifetime of the cellular response to the cytokine, which has implication for the outcome of the immune response.

4. The nuclear translocation of pStat1 modulates the dynamics of Jak-Stat signaling system and leads to the switch between damped/overdamped oscillatory regimes. Individuals with different clinical response to IFNbeta therapy showed differences in the dynamics of nuclear translocation of pStat1, becoming a promising biomarker for monitoring the response to this therapy.

5. The inhibition through phosphorylation of pFoxo3a is a molecular switch, which allows tighter regulation of the Foxo3a transcriptional activity. Nuclear shuttling of Foxo3a is a kinetic buffer of Foxo3 activity and keeps the equilibrium between

survival and tumor repression mechanism. This Foxo3a switch mechanism is controlled by the coordinated activation of Akt and Sgk in the PI3K pathway.

List of figures

Figure 1 A simplified hierarchical structure of a living system. The system is composed by the components with increasing complexity. On one edge of the pyramid are the physical entities and on the other their functional properties. 4

Figure 2 The interconnection between different layers of cellular system. This figure represents only the connections between different layers of signaling. The interconnections create increasing complexity systems of intersections and relationships between subsystems in the same layer and between different layers of the hierarchical system..... 6

Figure 3 Basic graph models representing different combinations of both modular and hub characteristics from [12]. Most real Systems are both modular and contain hubs (central nodes), e.g. D or F graphs of the figure. 7

Figure 4 Most common network motifs. A – regulatory chain (left) and single input (right); B – feed-forward motif; C – Feedback loops: positive (left) and negative (right). 10

Figure 5 Multi-component negative-feedback oscillator. A. Negative feedback between mRNA and protein, as described by kinetic equations in the text. B. Representative solutions (dashed curves) of equations in the text, for parameter values: $p = 2$, $K_m/K_d = 1$, $S/K_d = 1$, $k = k = 0.1$ min^{-1}, $k = k\ E\ /K = 1$ min^{-1}. Notice that every trajectory spirals into the stable steady state located at the grey circle. C. The negative-feedback loop, taking into account transport of macromolecules between the nucleus and the cytoplasm. D. Sustained oscillations for the four-component loop in panel. From [17] 11

Figure 6 The circuits, which may produce bistability: mutual activation (on the left) and mutual inhibition (on the right). From [18] 12

Figure 7 Data sets can dictate the computational approaches used in systems biology. (Left) Omics technologies generate extremely large data sets that can be analyzed and organized into networks by using statistical modeling techniques. This strategy can be considered "top-down" modeling. (Right) When high-quality data are available, smaller-scale systems can be represented by dynamical models, and simulations with these models can generate quantitative predictions of system behavior. This strategy is sometimes called "bottom-

up" modeling. Both approaches are important in systems biology, and a few cutting-edge studies combine the positive aspects of both. From [22] 13
Figure 8 The 2-dimensional parameter space vs model fitness to the data. Most of the algorithms search for the combination of parameters to maximize model fitness. 17
Figure 9 Examples of single cell behaviors that produce the same average population behavior. Individual cells are shown as circles with each cell's signaling activity denoted by its color; black denotes 100% signaling and white denotes 0% signaling. The population average for each panel is 50%. In panel A, each cell signals at 50%. In panel B, half of the cells are in the 100% state and half of the cells are in the 0% state. In panel C, cells are as in panel B, but individual cells may switch states in time without affecting the population average. The switching may occur stochastically, or result from oscillatory signaling activity whose phase and frequency vary from cell to cell. In panel D, cell signaling is distributed between 0 and 100%. In panel E, signaling within a cell is spatially heterogeneous such that the average signaling within each cell is 50%. From [34] 18
Figure 10 Different types of MS produce different clinical course.20
Figure 11 The inflammatory phase of multiple sclerosis. T cells, B cells and antigen-presenting cells (APCs), including macrophages, enter the central nervous system (CNS), where they secrete certain chemicals known as cytokines that damage the oligodendroglial cells. These cells manufacture the myelin that insulates the neuronal axon. The injured myelin cannot conduct electrical impulses normally, just as a tear in the insulation of a wire leads to a short circuit [37] 21
Figure 12 The main events of IL6 signaling and pathway self-regulation. Schematic representation of the circuit. Cytokines bind their membrane receptors, causing a cascade of phosphorylation reactions that triggers Stat activation. Active Stats upregulated the transcription of the repressors SOCS, which inhibit Stat phosphorylation 23
Figure 13 The canonical type I and type II IFN signaling pathways. The plot represents the canonical IFN pathways and the cross-talk between them, including the different pStat dimers formed after stimulation. [48] 26
Figure 14 Some of Foxo3 inhibition mechanism from [64]. Note the alternative IGF1 activator - Sgk 30

Figure 15 Fundamental reaction types of Foxo translocation (from [67])..... 31
Figure 16 Regulation of Foxos is conserved between Caenorhabditis elegans, Drosophila melanogaster, and mammals. Activation of the insulin receptor (DAF-2) activates PI3K (AGE-1) resulting in the formation of PIP_3. These phosphorylated lipids form docking sites for PDK1 and PKB (AKT) resulting in their activation. PKB phosphorylates and inhibits Foxo transcription factors. While C. elegans and D. melanogaster have a single Foxo isoform, in mammals three distinct Foxos are regulated by PKB: Foxo1, Foxo3, and Foxo4. From [69])..... 33
Figure 17 ImageStreamX technology. The method allows to quantify the nuclear translocation in single cells. 45
Figure 18 The simplified workflow to obtain the specific logic model based on the experimental data. See details in the text. 46
Figure 19 The PKN used for the Boolean modeling of immune response network in THP1 and Jurkat cell lines. Stimulus marked in green, measured phosphoproteins – in purple, inhibited proteins in red rounds, transcription factors in yellow, measured total proteins - in light blue. The analytes are labeled as following Green – stimulus: IFNbeta, IFNgamma, LPS, polyC, Blue – phosphoproteins: p38, Mekk, Stat1, Stat2, mTor, AKT, Jak1, Yellow – Lueferase reporter assay targets: GAS, ISRE, IRF-E, Red circles – the proteins to inhibitor: Stat1, p38, PKCa, AKT, Jak1, TYK1..... 47
Figure 20 The example of the experimental data visual representation by DataRail. Rows - measured phosphoproteins. Columns: up - stimulus, down - inhibitors used during the experiment. The graph inside represents the change in the signal over time (from 0 to 15 minutes) 48
Figure 21 Population versus single cells oscillations. The second peak may be present in single cells, but missing in populational level due to desynchronization. 51
Figure 22 Median levels of phosphorylated Stat3 (A) in mouse 3T3 fibroblasts measured by flow cytometry in the absence of stimulation (grey), stimulated with IL-6 (1 ng/ml: blue, 10 ng/ml: green, 100 ng/ml: red). Standard errors (SE) are smaller than 0.02 in all cases, therefore error bars have been omitted. Mean fold change in the expression of Socs3 (B) in response to IL-6 is also shown, as measured by RT-PCR, with

error bars corresponding to the SE of two experimental replicates. 53
Figure 23 The single-cell distribution histogram for pStat3 after IL6 stimulation of 3T3 fibroblasts. Based on single-cell flow cytometry results 54
Figure 24 Graphical reppresentation of IL6 signaling pathway model 55
Figure 25 Model simulations versus experimental data for pStat3. Fold change of phosphorylation levels (on the left) and coeffecient of variation (right). Green lines correspond to experimental data and black – to the simulation of the model. 57
Figure 26 Experimental results and model fit for Jurkat cell line. Fit of model predictions (dashed blue lines) to data. The color of cells represents the quality of fit (green - perfect fit, red - the model couldn't explain the data). 59
Figure 27 Experimental results and model fit for THP1 cell line. Fit of model predictions (dashed blue lines) to data. The color of cells represents the quality of fit (green - perfect fit, red - the model couldn't explain the data). 60
Figure 28 Logic model fitting the data from Jurkat cell line. Confirmed links are in green and blue. 61
Figure 29 Logic model fitting the data from THP1 cell line. Confirmed links are in green and blue. 61
Figure 30 Scaffolds obtained from logic models for Jurkat cell line (up) and THP1 cell line (down) 62
Figure 31. Differences between two average networks of simulated patients cohorts 64
Figure 32 IFN-beta induction after microbial or viral trigger in macrophage cell line. IFN-beta levels in Raw cell culture supernatants after stimulation with LPS (15 μg/ml) (blue) or Poly (I:C) (25μg/ml) (red) versus non-stimulated control (black line) in the first 6 h and in some later times from 12 h (A); B) Western-blot showing phosphorylated and total Stat1 levels after LPS stimulation (15 μg/ml) of Raw cell line analyzed by Western-blot and quantified by densitometry. All experiments were performed in triplicates and repeated at least two times independently. 68
Figure 33 Mathematical model of type I IFN signaling pathway. Graphical representation of the mathematical model of type I IFN signaling pathway. 69

Figure 34 Gene expression levels of Stat1, IRF1 and Socs1 after IFN-beta stimulation and the corresponding simulations from the ODE model. A-C) Stat1, IRF1 and Socs1 RNA concentration in cell lysates were measured by RT-PCR in the Raw cells stimulated with IFN-beta (1000 units/ml); A) Stat1 RNA levels in the Raw cells stimulated with IFN-beta; B) IRF1 RNA levels in the Raw cells stimulated with IFN-beta; C) Socs1 RNA levels in the Raw cells stimulated with IFN-beta. We plot here one out of three independent experiments, which were performed in duplicates. D-F) Model simulation and sensitivity analysis with ± 20% change for all parameters (shaded areas) for Stat1 (D), IRF1 (E), and Socs1 (F) RNA levels. 72
Figure 35 Activation of type I IFN pathway by IFN-beta in Raw cell line and the corresponding simulations from the ODE model. A-C) pStat1, Stat1 and Socs1 protein concentration in cell lysates were measured by Luminex, Flow cytometry or ELISA after stimulation with IFN-beta (1000 units/ml). The data was normalized to the maximum level. A) pStat1 protein concentration in the Raw cells stimulated with IFN-beta; (B) Total Stat1 protein concentration in the Raw cells stimulated with IFN-beta; C) Socs1 protein concentration in the Raw cells stimulated with IFN-beta. We plot here one out of three independent experiments, which were performed in duplicates. D-F) Model simulation and sensitivity analysis with ± 20% change for all parameters (shaded areas) (D: pStat1; E: Stat1; F: Socs1). 74
Figure 36 Type I IFN pathway model simulations during the first 8 hours after IFN-beta stimulation. (A) Model simulations showing oscillations of total (nuclear plus cytoplasmic) pStat1 protein, Socs1 mRNA expression (dashed line) and Stat1 mRNA expression (dotted line). (B) Corresponding simulations where the Socs1-mediated negative feedback is disrupted by assuming an infinite value of the repression threshold kI. (C) Corresponding simulations not including the IRF1-mediated positive feedback, by assuming a zero value of the Stat1 activation threshold kF (which leads to saturation of the corresponding Hill function, so that the dependence of an expression on F is removed). 76
Figure 37 Influence of activated receptor level on the transient oscillatory dynamics. (A). Time evolution of the activation level of type I IFN receptors in the model (S) by stimulation

with IFN-beta (added at t = 0) for different initial levels (in red, S = 500 molecules at t = 0). (B, C) pStat1 (B) and Socs1 mRNA (C) dynamic responses for varying levels of initial receptor activation as in panel A (lower lines in B and C correspond to lower lines in A).....77
Figure 38 Stability analysis of the steady state solution in two 2D parameter spaces. (A, C) The color scale represents the absolute value of the imaginary part of the stability eigenvalue with maximum real part, corresponding to the steady state of the system after IFN stimulation, for varying phospho/ dephosphorylation rates (bph and bdeph, panel A), and nuclear export/import rates (bexp and bimp, panel B). Two distinct dynamic regimes can be identified with this analysis: the damped oscillatory regime (shifted to red) and the overdamped/ non-oscillatory regime (blue). (B, D) Examples of pStat1 time evolution in both regimes (damped and over-damped in red/blue lines, respectively) corresponding to parameter position of circle markers for the two diagrams shown in panels A and B, respectively.....79
Figure 39 Nuclear translocation measured by ISX technology. UP: The example of nuclear localization of pStat1 visualized by ImageStreamX. DOWN: the quantification of PBMCs from a healthy control in vitro stimulated with 1000 un/ml of IFNbeta. Blue – the percent of pStat1+ cells from the total population, red – percent of pStat1+ cells with pStat1 localized in the nucleus from a total population of pStat1+ cells.....80
Figure 40 Nuclear translocation measured by ISX technology. The quantification of PBMCs from an MS patients treated with IFNbeta - Extavia (A and B) and Avonex (C and D). The time shows the time of blood withdrawal after injection. Blue: the percent of pStat1+ cells from the total population, Red: percent of pStat1+ cells with pStat1 localized in the nucleus from a total population of pStat1+ 81
Figure 41 The model of Akt-Foxo3 signaling and Foxo3 nuclear shuttling.....84
Figure 42 Possible explanation of the difference in RAW macrophages cell line IFNbeta signaling and classical Jak-Stat pathway.....89

References

1. Jacob F: *The Logic of Life*. 1974.
2. Filippi M: **Multiple sclerosis in 2010: Advances in monitoring and treatment of multiple sclerosis.** *Nat Rev Neurol* 2011, **7**:74–5.
3. Jacques Loeb: *The Mechanistic Conception of Life*. 1912.
4. Smuts Hon J.C.: *Holism And Evolution*. 1927.
5. Roger Williams: *Biochemical Individuality*. 1956.
6. Trewavas A: **A brief history of systems biology.** *Plant Cell* 2006, **18**:2420–30.
7. Wilson; White.: *Hierarchical Structures*. 1969.
8. Polanyi M: **Life's Irreducible Structure: Live mechanisms and information in DNA are boundary conditions with a sequence of boundaries above them**. *Science (80-)* 1968, **160**:1308–1312.
9. Von Bertalanffy L: *General System Theory: Foundations, Development, Applications*. George Braziller Inc.; Revised edition; 1969:296.
10. Barabasi A, Frangos J: *Linked: The New Science of Networks*. Perseus Books Group; 1st edition; 2002:256.
11. Westerhoff H V, Palsson BO: **The evolution of molecular biology into systems biology.** *Nat Biotechnol* 2004, **22**:1249–52.
12. Müller-Linow M, Hilgetag CC, Hütt M-T: **Organization of excitable dynamics in hierarchical biological networks.** *PLoS Comput Biol* 2008, **4**:e1000190.
13. Karr JR, Sanghvi JC, Macklin DN, Gutschow M V, Jacobs JM, Bolival B, Assad-Garcia N, Glass JI, Covert MW: **A whole-cell computational model predicts phenotype from genotype.** *Cell* 2012, **150**:389–401.
14. Alon U: *An Introduction to Systems Biology: Design Principles of Biological Circuits*. 2006.
15. Milo R, Shen-Orr S, Itzkovitz S, Kashtan N, Chklovskii D, Alon U: **Network motifs: simple building blocks of complex networks.** *Science* 2002, **298**:824–7.
16. Solé R V, Valverde S: **Are network motifs the spandrels of cellular complexity?** *Trends Ecol Evol* 2006, **21**:419–22.
17. Novák B, Tyson JJ: **Design principles of biochemical oscillators.** *Nat Rev Mol Cell Biol* 2008, **9**:981–91.
18. Ferrell JE: **Self-perpetuating states in signal transduction: positive feedback, double-negative feedback and bistability.** *Curr Opin Cell Biol* 2002, **14**:140–8.
19. Sobie E a: **Bistability in biochemical signaling models.** *Sci Signal* 2011, **4**:tr10.

20. Smits WK, Kuipers OP, Veening J-W: **Phenotypic variation in bacteria: the role of feedback regulation.** *Nat Rev Microbiol* 2006, **4**:259–71.
21. Bhalla US, Iyengar R: **Emergent properties of networks of biological signaling pathways.** *Science* 1999, **283**:381–7.
22. Sobie E, Lee Y, Jenkins S, Iyengar R: **Systems biology—biomedical modeling**. *Sci Signal* 2011, **4**(September).
23. Morris MK, Saez-Rodriguez J, Sorger PK, Lauffenburger D a: **Logic-based models for the analysis of cell signaling networks.** *Biochemistry* 2010, **49**:3216–24.
24. Wynn ML, Consul N, Merajver SD, Schnell S: **Logic-based models in systems biology: a predictive and parameter-free network analysis method.** *Integr Biol (Camb)* 2012, **4**:1323–37.
25. Terfve C, Cokelaer T, Henriques D, MacNamara A, Goncalves E, Morris MK, van Iersel M, Lauffenburger DA, Saez-Rodriguez J: **CellNOptR: a flexible toolkit to train protein signaling networks to data using multiple logic formalisms.** *BMC Syst Biol* 2012, **6**:133.
26. Forero IM: **Reaction network analysis in biochemical signaling pathways**. 2009:1–119.
27. Neves SR: **Obtaining and estimating kinetic parameters from the literature.** *Sci Signal* 2011, **4**:tr8.
28. Nim TH, Luo L, Clément M-V, White JK, Tucker-Kellogg L: **Systematic parameter estimation in data-rich environments for cell signalling dynamics.** *Bioinformatics* 2013, **29**:1044–51.
29. Liang H, Wu H: **Parameter Estimation for Differential Equation Models Using a Framework of Measurement Error in Regression Models.** *J Am Stat Assoc* 2008, **103**:1570–1583.
30. Ghasemi O, Lindsey ML, Yang T, Nguyen N, Huang Y, Jin Y-F: **Bayesian parameter estimation for nonlinear modelling of biological pathways.** *BMC Syst Biol* 2011, **5 Suppl 3**:S9.
31. Apgar JF, Witmer DK, White FM, Tidor B: **Sloppy models, parameter uncertainty, and the role of experimental design.** *Mol Biosyst* 2010, **6**:1890–900.
32. Gomez-Cabrero D, Compte A, Tegner J: **Workflow for generating competing hypothesis from models with parameter uncertainty.** *Interface Focus* 2011, **1**:438–49.
33. Givan AL: **Flow cytometry: an introduction.** *Methods Mol Biol* 2004, **263**:1–32.
34. Cheong R, Paliwal S, Levchenko A: **Models at the single cell level.** *Wiley Interdiscip Rev Syst Biol Med* , **2**:34–48.

35. Kampen N: *Stochastic Processes in Physics and Chemistry*. North Holland; 3 edition; 2007:464.
36. Steinman L: **Multiple sclerosis: a two-stage disease.** *Nat Immunol* 2001, **2**:762–4.
37. Steinman L, Zamvil S: **Transcriptional analysis of targets in multiple sclerosis.** *Nat Rev Immunol* 2003, **3**:483–92.
38. Beecham AH, Patsopoulos N a, Xifara DK, Davis MF, Kemppinen A, Cotsapas C, Shah TS, Spencer C, Booth D, Goris A, Oturai A, Saarela J, Fontaine B, Hemmer B, Martin C, Zipp F, D'Alfonso S, Martinelli-Boneschi F, Taylor B, Harbo HF, Kockum I, Hillert J, Olsson T, Ban M, Oksenberg JR, Hintzen R, Barcellos LF, Agliardi C, Alfredsson L, Alizadeh M, et al.: **Analysis of immune-related loci identifies 48 new susceptibility variants for multiple sclerosis.** *Nat Genet* 2013(September):1–10.
39. Naka T, Nishimoto N, Kishimoto T: **The paradigm of IL-6: from basic science to medicine.** *Arthritis Res* 2002, **4 Suppl 3**:S233–42.
40. Murray PJ: **The Jak-Stat signaling pathway: input and output integration.** *J Immunol* 2007, **178**:2623–9.
41. Rawlings JS, Rosler KM, Harrison DA: **The Jak/Stat signaling pathway.** *J Cell Sci* 2004, **117**(Pt 8):1281–3.
42. Imada K, Leonard WJ: **The Jak-Stat pathway.** *Mol Immunol* 2000, **37**:1–11.
43. Levy DE DE, Darnell JE: **StatS : TRANSCRIPTIONAL CONTROL AND BIOLOGICAL IMPACT**. *Nat Rev Mol Cell Biol* 2002, **3**:651–62.
44. Raza S, Robertson K a, Lacaze P a, Page D, Enright AJ, Ghazal P, Freeman TC: **A logic-based diagram of signalling pathways central to macrophage activation.** *BMC Syst Biol* 2008, **2**:36.
45. Qiao L, Phipps-Yonas H, Hartmann B, Moran TM, Sealfon SC, Hayot F, Cells VHD: **Immune Response Modeling of Interferon b-Pretreated Influenza Virus-infected Human Dendritic Cells**. *Biophysj* 2010, **98**:505–514.
46. Smieja J, Jamaluddin M, Brasier AAR, Kimmel M: **Model-based analysis of interferon-β induced signaling pathway**. *Bioinformatics* 2008, **24**:2363–2369.
47. Horvath CM: **Stat proteins and transcriptional responses to extracellular signals.** *Trends Biochem Sci* 2000, **25**:496–502.
48. Pertsovskaya I, Abad E, Domedel-Puig N, Garcia-Ojalvo J, Villoslada P: **Transient oscillatory dynamics of interferon beta signaling in macrophages**. *BMC Syst Biol* 2013, **7**:59.

49. Qin H, Wilson C a, Lee SJ, Benveniste EN: **IFN-beta-induced SOCS-1 negatively regulates CD40 gene expression in macrophages and microglia.** *FASEB J* 2006, **20**:985–7.
50. Van Boxel-Dezaire AHH, Zula JA, Xu Y, Ransohoff RM, Jacobberger JW, Stark GR: **Major Differences in the Responses of Primary Human Leukocyte Subsets to {IFN-\${\$beta\$}$}**. *J Immunol* 2010, **185**:5888.
51. Hervas-Stubbs S, Perez-Gracia JL, Rouzaut A, Sanmamed MF, Le Bon A, Melero I: **Direct effects of type I interferons on cells of the immune system.** *Clin Cancer Res* 2011, **17**:2619–27.
52. Oliver-Martos B, Órpez T, Pinto-Medel MJ, Mayorga C, García-León J a, Maldonado-Sanchez R, Suardíaz M, Guerrero M, Luque G, Leyva L, Fernández O: **Gene expression in IFNß signalling pathway differs between monocytes, CD4 and CD8 T cells from MS patients.** *J Neuroimmunol* 2011, **230**:153–9.
53. Starr R, Hilton DJ: **SOCS: suppressors of cytokine signalling.** *Int J Biochem Cell Biol* 1998, **30**:1081–5.
54. Brunet A, Park J, Tran H, Hu LS, Hemmings BA, Greenberg ME: **Protein kinase SGK mediates survival signals by phosphorylating the forkhead transcription factor FKHRL1 (Foxo3a).** *Mol Cell Biol* 2001, **21**:952–65.
55. Greer EL, Brunet A: **Foxo transcription factors at the interface between longevity and tumor suppression.** *Oncogene* 2005, **24**:7410–25.
56. Glauser D a, Schlegel W: **The emerging role of Foxo transcription factors in pancreatic beta cells.** *J Endocrinol* 2007, **193**:195–207.
57. Biggs WH, Meisenhelder J, Hunter T, Cavenee WK, Arden KC: **Protein kinase B/Akt-mediated phosphorylation promotes nuclear exclusion of the winged helix transcription factor FKHR1.** *Proc Natl Acad Sci U S A* 1999, **96**:7421–6.
58. Brunet A, Bonni A, Zigmond MJ, Lin MZ, Juo P, Hu LS, Anderson MJ, Arden KC, Blenis J, Greenberg ME: **Akt promotes cell survival by phosphorylating and inhibiting a Forkhead transcription factor.** *Cell* 1999, **96**:857–68.
59. Essers MAG, Weijzen S, de Vries-Smits AMM, Saarloos I, de Ruiter ND, Bos JL, Burgering BMT: **Foxo transcription factor activation by oxidative stress mediated by the small GTPase Ral and JNK.** *EMBO J* 2004, **23**:4802–12.
60. Matsumoto M, Accili D: **All roads lead to FoxO.** *Cell Metab* 2005, **1**:215–6.

61. Lehtinen MK, Yuan Z, Boag PR, Yang Y, Villén J, Becker EBE, DiBacco S, de la Iglesia N, Gygi S, Blackwell TK, Bonni A: **A conserved MST-Foxo signaling pathway mediates oxidative-stress responses and extends life span.** *Cell* 2006, **125**:987–1001.
62. Wang Q, Li L, Xu E, Wong V, Rhodes C, Brubaker PL: **Glucagon-like peptide-1 regulates proliferation and apoptosis via activation of protein kinase B in pancreatic INS-1 beta cells.** *Diabetologia* 2004, **47**:478–87.
63. Vogt PK, Jiang H, Aoki M: **Triple layer control: phosphorylation, acetylation and ubiquitination of Foxo proteins.** *Cell Cycle* 2005, **4**:908–13.
64. Calnan DR, Brunet a: **The FoxO code.** *Oncogene* 2008, **27**:2276–88.
65. Yeo H, Lyssiotis C a, Zhang Y, Ying H, Asara JM, Cantley LC, Paik J-H: **FoxO3 coordinates metabolic pathways to maintain redox balance in neural stem cells.** *EMBO J* 2013, **32**:2589–602.
66. Mojsilovic-Petrovic J, Nedelsky N, Boccitto M, Mano I, Georgiades SN, Zhou W, Liu Y, Neve RL, Taylor JP, Driscoll M, Clardy J, Merry D, Kalb RG: **Foxo3a is broadly neuroprotective in vitro and in vivo against insults implicated in motor neuron diseases.** *J Neurosci* 2009, **29**:8236–47.
67. Smith GR, Shanley DP: **Modelling the response of Foxo transcription factors to multiple post-translational modifications made by ageing-related signalling pathways.** *PLoS One* 2010, **5**:e11092.
68. Vos KE van der, Coffer PJ: **The Extending Network of Foxo Transcriptional Target Genes**. *Antioxid Redox Signal* 2011:579–92.
69. Vos KE van der, Coffer PJ: **The Extending Network of Foxo Transcriptional Target Genes**. *Antioxid Redox Signal* 2011:579–92.
70. Wu Z, Zhao X-M, Chen L: **A systems biology approach to identify effective cocktail drugs.** *BMC Syst Biol* 2010, **4 Suppl 2**(Suppl 2):S7.
71. Lindholm EM, Krohn M, Iadevaia S, Kristian A, Mills GB, Mælandsmo GM, Engebraaten O: **Proteomic characterization of breast cancer xenografts identifies early and late bevacizumab-induced responses and predicts effective drug combinations.** *Clin Cancer Res* 2014, **20**:404–12.
72. Pritchard JR, Bruno PM, Gilbert LA, Capron KL, Lauffenburger DA, Hemann MT: **Defining principles of combination drug mechanisms of action.** *Proc Natl Acad Sci U S A* 2013, **110**:E170–9.
73. Villoslada P, Baranzini S: **Data integration and systems biology approaches for biomarker discovery: challenges and**

opportunities for multiple sclerosis. *J Neuroimmunol* 2012, **248**:58–65.
74. Palacios R, Goni J, Martinez-Forero I, Iranzo J, Sepulcre J, Melero I, Villoslada P: **A network analysis of the human T-cell activation gene network identifies JAGGED1 as a therapeutic target for autoimmune diseases.** *PLoS One* 2007, **2**:e1222.
75. Livak KJ, Schmittgen TD: **Analysis of relative gene expression data using real-time quantitative PCR and the 2(-Delta Delta C(T)) Method.** *Methods San Diego Calif* 2001, **25**:402–408.
76. Saez-Rodriguez J, Simeoni L, Lindquist J a, Hemenway R, Bommhardt U, Arndt B, Haus U-U, Weismantel R, Gilles ED, Klamt S, Schraven B: **A logical model provides insights into T cell receptor signaling.** *PLoS Comput Biol* 2007, **3**:e163.
77. Terfve C, Cokelaer T, MacNamara A, Saez-Rodriguez J: **Training of boolean logic models of signalling networks using prior knowledge networks and perturbation data with CellNOptR**. 2012:1–15.
78. Haspel RL, Salditt-Georgieff M, Darnell JE: **The rapid inactivation of nuclear tyrosine phosphorylated Stat1 depends upon a protein tyrosine phosphatase.** *EMBO J* 1996, **15**:6262–8.
79. Gao C, Guo H, Mi Z, Grusby MJ, Kuo PC: **Osteopontin induces ubiquitin-dependent degradation of Stat1 in RAW264.7 murine macrophages.** *J Immunol* 2007, **178**:1870–81.
80. Qin H, Niyongere S a, Lee SJ, Baker BJ, Benveniste EN: **Expression and functional significance of SOCS-1 and SOCS-3 in astrocytes.** *J Immunol* 2008, **181**:3167–76.
81. Wong LH, Sim H, Chatterjee-Kishore M, Hatzinisiriou I, Devenish RJ, Stark G, Ralph SJ: **Isolation and characterization of a human Stat1 gene regulatory element. Inducibility by interferon (IFN) types I and II and role of IFN regulatory factor-1.** *J Biol Chem* 2002, **277**:19408–17.
82. Sharova L V, Sharov A a, Nedorezov T, Piao Y, Shaik N, Ko MSH: **Database for mRNA half-life of 19 977 genes obtained by DNA microarray analysis of pluripotent and differentiating mouse embryonic stem cells.** *DNA Res* 2009, **16**:45–58.
83. Wenta N, Strauss H, Meyer S, Vinkemeier U: **Tyrosine phosphorylation regulates the partitioning of Stat1 between different dimer conformations.** *Proc Natl Acad Sci U S A* 2008, **105**:9238–43.
84. Killion JJ, Fishbeck R, Bar-Eli M, Chernajovsky Y: **Delivery of interferon to intracellular pathways by encapsulation of**

interferon into multilamellar liposomes is independent of the status of interferon receptors. *Cytokine* 1994, **6**:443–9.
85. Andrejeva J, Young DF, Goodbourn S, Randall RE: **Degradation of Stat1 and Stat2 by the V proteins of simian virus 5 and human parainfluenza virus type 2, respectively: consequences for virus replication in the presence of alpha/beta and gamma interferons.** *J Virol* 2002, **76**:2159–67.
86. Nakagawa K, Yokosawa H: **Degradation of transcription factor IRF-1 by the ubiquitin-proteasome pathway. The C-terminal region governs the protein stability.** *Eur J Biochem* 2000, **267**:1680–6.
87. FuJITA T, Reis L: **Induction of the transcription factor IRF-1 and and interferon-beta mrnas by cytokines and activators of second-messenger pathways**. *Proc …* 1989, **86**(December):9936–9940.
88. Yoshiura S: **Ultradian oscillations of stat, smad, and hes1 expression in response to serum.** *Proc Natl Acad Sci U S A* 2007, **104**:292–297.
89. Alexopoulos LG, Melas IN, Chairakaki AD, Saez-Rodriguez J, Mitsos A: **Construction of signaling pathways and identification of drug effects on the liver cancer cell HepG2.** *Conf Proc IEEE Eng Med Biol Soc* 2010, **2010**:6717–20.
90. Saez-rodriguez J: **The use of logic modeling methods to determine the alterations in TCR signaling network in Multiple Sclerosis patients**. .
91. MacNamara A, Terfve C, Henriques D, Bernabé BP, Saez-Rodriguez J: **State-time spectrum of signal transduction logic models.** *Phys Biol* 2012, **9**:045003.
92. Yamada S, Shiono S, Joo A, Yoshimura A: **Control mechanism of Jak/Stat signal transduction pathway**. *FEBS Lett* 2003, **534**:190–196.
93. Endo TA, Masuhara M, Yokouchi M, Suzuki R, Sakamoto H, Mitsui K, Matsumoto A, Tanimura S, Ohtsubo M, Misawa H, Miyazaki T, Leonor N, Taniguchi T, Fujita T, Kanakura Y, Komiya S, Yoshimura A: **A new protein containing an SH2 domain that inhibits Jak kinases.** *Nature* 1997, **387**:921–4.
94. Nguyen H, Lin R, Hiscott J: **Activation of multiple growth regulatory genes following inducible expression of IRF-1 or IRF/RelA fusion proteins.** *Oncogene* 1997, **15**:1425–35.
95. Sadler AJ, Williams BRG: **Interferon-inducible antiviral effectors.** *Nat Rev Immunol* 2008, **8**:559–68.

96. Villoslada P, Oksenberg JR, Rio J, Montalban X: **Clinical characteristics of responders to interferon therapy for relapsing MS.** *Neurology* 2004, **62**:1653; author reply 1653.
97. Samuel C: **Antiviral Actions of Interferons**. *Clin Microbiol Rev* 2001, **14**.
98. Lohoff M, Mak TW: **Roles of interferon-regulatory factors in T-helper-cell differentiation.** *Nat Rev Immunol* 2005, **5**:125–35.
99. Javed A, Reder AT: **Therapeutic role of beta-interferons in multiple sclerosis.** *Pharmacol Ther* 2006, **110**:35–56.
100. Marta M, Giovannoni G: **Disease modifying drugs in multiple sclerosis: mechanisms of action and new drugs in the horizon.** *CNS Neurol Disord Drug Targets* 2012, **11**:610–23.
101. Río J, Comabella M, Montalban X: **Predicting responders to therapies for multiple sclerosis.** *Nat Rev Neurol* 2009, **5**:553–60.
102. Vera J, Rateitschak K, Lange F, Kossow C, Wolkenhauer O, Jaster R: **Systems biology of Jak-Stat signalling in human malignancies.** *Prog Biophys Mol Biol* 2011, **106**:426–34.
103. Swameye I, Muller TG, Timmer J, Sandra O, Klingmuller U: **Identification of nucleocytoplasmic cycling as a remote sensor in cellular signaling by databased modeling.** *Proc Natl Acad Sci U S A* 2003, **100**:1028–33.
104. Soebiyanto RP, Sreenath SN, Qu C-K, Loparo KA, Bunting KD: **Complex systems biology approach to understanding coordination of Jak-Stat signaling.** *Biosystems* , **90**:830–42.
105. Rani MRS, Ransohoff RM: **Alternative and accessory pathways in the regulation of IFN-beta-mediated gene expression.** *J Interferon Cytokine Res* 2005, **25**:788–98.
106. Zurney J, Howard KE, Sherry B: **Basal expression levels of IFNAR and Jak-Stat components are determinants of cell-type-specific differences in cardiac antiviral responses.** *J Virol* 2007, **81**:13668–80.
107. Takaoka A, Yanai H: **Microreview Interferon signalling network in innate defence**. *Cell Microbiol* 2006, **8**:907–922.
108. Comabella M, Lünemann JD, Río J, Sánchez A, López C, Julià E, Fernández M, Nonell L, Camiña-Tato M, Deisenhammer F, Caballero E, Tortola MT, Prinz M, Montalban X, Martin R: **A type I interferon signature in monocytes is associated with poor response to interferon-beta in multiple sclerosis.** *Brain* 2009, **132**(Pt 12):3353–65.
109. Burgering BMT: **Decisions on life and death : Foxo Forkhead transcription factors are in command when PKB / Akt is off duty**. 2003, **73**(June):689–701.

110. Peng SL: **Forkhead transcription factors in chronic inflammation**. 2011, **42**:482–485.
111. Smith GR, Shanley DP: **Computational modelling of the regulation of Insulin signalling by oxidative stress.** *BMC Syst Biol* 2013, **7**:41.

Supplementary data

Supplementary Table 1. Parameters for Stat3 ODE model [units/ cell]

Name	Symbol	Value	Unit
Active IL6 receptors	S	[0-500]	#
Transcription rate for Socs3	b_r	11.3	min^{-1}
Translation rate for Socs3	b_R	$1.0 \cdot 10^2$	min^{-1}
Phosphorylation Stat3 rate	b_{ph}	[40-80]	min^{-1}
Dephosphorylation Stat3 rate	b_{deph}	0.1	min^{-1}
Import to the nucleus rate (pStat3)	b_{imp}	0.03	min^{-1}
Export from the nucleus rate (Stat3)	b_{exp}	0.09	min^{-1}
Dephosphorylation Stat3 rate in nucleus	$b_{deph\_nucleus}$	0.046	min^{-1}
Stat3 phosphorylation activation (Hill's constant; half maximal activation)	k_A	17040	molecules
Dissociation constant for the enzyme-inhibitor by Socs3 (Hill's constant; half maximal activation)	k_I	82680	molecules
Socs3 transcription activation by nuclear pStat1 (Hill's constant; half maximal activation)	k_r	34000	molecules
Cooperativity of Socs1 protein over Stat1 dimers	q	4	
Cooperativity of Stat1 on Socs1 gene promoter	n	4	

Socs1 RNA degradation rate	λ_r	0.02	min^{-1}
Socs1 protein degradation rate	λ_R	0.017	min^{-1}
Stat1 protein degradation rate	λ_{Stat}	$1.0 \cdot 10^{-5}$	min^{-1}

Supplementary table **2. Initial conditions for Stat3 model simulations**

Name	Symbol	Value
IL6 active receptors	S	600-700 molecules
U-phosphorylated cytoplasmic Stat3	A_c	$7.5 \cdot 10^4$ molecules
Phosphorylated cytoplasmic Stat3	Ap_c	1 molecule
Phosphorylated nuclear Stat3	Ap_n	1 molecule
U-Phosphorylated nuclear Stat3	An	$2.5 \cdot 10^4$ molecules
Socs3 mRNA	r	1 molecule
Socs3 protein	R	1 molecule

Supplementary table 3. Parameters for type I IFN ODE model

Name	Symbol	Value	Unit
Translation rate for Stat1	b_A	65	min^{-1}
Receptor production rate	b_S	0	min^{-1}
Basal Stat1 RNA	B_{Stat1}	0.0062	min^{-1}
Transcription rate for Stat1	b_a	0.1	min^{-1}
Transcription rate for Socs1	b_r	12.8	min^{-1}
Transcription rate for IRF1	b_f	2.7	min^{-1}
Translation rate for IRF1	b_F	$1.0 \cdot 10^1$	min^{-1}
Translation rate for Socs1	b_R	$1.0 \cdot 10^2$	min^{-1}

Phosphorylation Stat1 rate	b_{ph}	$1.3 \cdot 10^{3}$	min^{-1}
Dephosphorylation Stat1 rate	b_{deph}	0.036	min^{-1}
Import to the nucleus rate (pStat1)	b_{imp}	0.013	min^{-1}
Export from the nucleus rate (Stat1)	b_{exp}	0.048	min^{-1}
Stat1 phosphorylation activation (Hill's constant; half maximal activation)	k_A	4680	molecules
Dissociation constant for the enzyme-inhibitor by Socs1 (Hill's constant; half maximal activation)	k_I	82680	molecules
Socs1 transcription activation by nuclear pStat1 (Hill's constant; half maximal activation)	k_r	23400	molecules
IRF1 transcriptional activation by pStat1	k_f	7366	molecules
Stat1 transcriptional activation by IRF1	k_F	$1.3 \cdot 10^{5}$	molecules
Cooperativity of Socs1 protein over Stat1 dimers	q	4	
Cooperativity of Stat1 on Socs1 gene promoter	n	3	
Cooperativity of Stat1 on IRF1 gene promoter	m	2	
Cooperativity of IRF1 on Stat1 gene promoter	u	1	
Receptor internalization/degradation rate	λ_s	0.0229	min^{-1}

Socs1 RNA degradation rate	λ_r	0.0347	min^{-1}
Socs1 protein degradation rate	λ_R	0.0231	min-1
IRF1 RNA degradation rate	λ_f	0.0173	min^{-1}
IRF1 protein degradation rate	λ_F	0.0116	min^{-1}
Stat1 RNA degradation rate	λ_a	0.0058	min^{-1}
Stat1 protein degradation rate	λ_{Stat}	0.0007	min^{-1}

Supplementary table 4. Initial conditions for type I IFN ODE model simulations

Name	**Symbol**	**Value**
Non-phosphorylated Stat1	*A*	$1.0 \cdot 10^5$ molecules
IFN activation receptor	*S*	1000 molecules
Phosphorylated nuclear Stat1	*Apn*	1 molecule
Phosphorylated cytoplasmic Stat1	*Apc*	10 molecules
Stat1 mRNA	*a*	1 molecule
IRF1 mRNA	*f*	1 molecule
Socs1 mRNA	*r*	1 molecule
IRF1 protein	*F*	1 molecules
Socs1 protein	*R*	1 molecule

Supplementary table 5. Initial conditions for Foxo3a model dynamics exploration

I	$1*10^5$-$1*10^6$
P	$1*10^5$
A	$1*10^5$
F_{dc}	1000
S	$1*10^5$
A_p	0
S_p	0
F_{n_akt}	0
F_{c_akt}	0
F_{n_sgk}	0
F_{c_sgk}	0
D	$5*10^6$

Supplementary table 6. Parameters for Foxo3a model dynamics exploration (adopted from [111])

Symbol	Biological and mathematical explanation	fixed parameters
r_1	dephosphorylation rate of Sgk	
k_{sp}	phosphorylation rate of Sgk	0,055
I	number of signal molecules	
k_s	Hill's coefficient	
r_{10}	dephosphorylation rate of Akt	0,5
k_{ap}	phosphorylation rate of Akt	
k_A	Hill's coefficient	
k_{exp}	Foxo3a export from the nucleus to the cytoplasm	
k_{imp}	Foxo3a import from the cytoplasm to the nucleus	0,182
r_g	Foxo3a degradation rate	0,1
k_a	rate of phosphorylation of Foxo3a by pAkt	0,5
k_f	Hill's coefficient	
k_{deph}	dephosphorylation rate of Foxo3a	1×10^{-6}
k_s	rate of phosphorylation of Foxo3a by pSgk	
k_g	target gene transcription rate	0,95
k_c	Hill's coefficient	
r_{18}	target gene degradation rate	

λ_s	degradation rate of Sgk	
λ_A	degradation rate of Akt	
n	Cooperativity of the activation of Sgk	
m	Cooperativity of the activation of Akt	
j	Cooperativity of the pAkt on the Foxo3a phosphosites	6
q	Cooperativity of the pSgk on the Foxo3a phosphosites	
t	Cooperativity of Foxo3a on the promoter of the target gene	

Resumen en castellano

Modelos de vías de señalización de citoquinas para el estudio de enfermedades autoinmunes

Resumen

La biología de sistemas abre nuevas fronteras en el estudio de enfermedades complejas como la Esclerosis Múltiple (EM). Las preguntas que era imposible contestar antes por falta de entendimiento y de una base metodológica adecuada, tales como el mecanismo molecular de acción de múltiples fármacos en las vías de señalización, son resueltas ahora mediante el uso del punto de vista de la Biología de Sistemas. Dichas vías de señalización tienen tanto un componente matemático como un componente biológico. La Biología de Sistemas moderna ha desarrollado diversos métodos para modelar las vías de señalización y predecir sus comportamientos en diferentes condiciones.

Esta disertación se centra en algunos de los mecanismos moleculares clave en la transducción de señales durante el desarrollo y la progresión de la EM, elementos clave para lograr explicar el mecanismo de acción de los fármacos más usados en la EM.

Mis principales hipótesis se basan en la presunción de que el principio más relevante de los sistemas biológicos son las conexiones entre las moléculas en lugar de las moléculas per se (p.e.: los bordes en lugar de los nodos en los modelos gráficos). Un ejemplo de esto se encuentra en los subtipos de células inmunes, que tienen distintas respuestas a los estímulos externos dado que interactúan entre ellas dentro de las células más que por sus componentes sean distintos. Otros ejemplos de esto son las cargas cinéticas conducidas por los cambios en la actividad tanslocalizadora de la proteína Stat1.

Para probar mi hipótesis, he desarrollado dos modelos matemáticos distintos de la vía de señalización de IFNbeta: Booleano y ODE. La combinación de los dos modelos nos permite observar la vía de señalización desde dos puntos de vista distintos: en conexión con otras vías de señalización relacionadas y como un sistema cinético.

Hemos detectado regímenes oscilatorios en la señalización de IFNbeta y sus parámetros clave, que determinan los cambios en los regímenes. Ambos

modeles fueron validados experimentalmente y nos condujeron a diversas predicciones que podrían ser clave para el desarrollo de nuevos fármacos o combinaciones de fármacos. Por ejemplo, el análisis de bifurcación del modelo cinético reveló la importancia de las propiedades de la translocación nuclear de la proteína Stat1 para el correcto funcionamiento de la vía de señalización.

La translocación nuclear es un elemento clave conocido de este sistema pero nos focalizamos en los circuitos de conexión y desconexión y la importancia de la combinación de diferentes lugares de fosforilación para la transducción de señales.

Los principales resultados de este trabajo son:

1. Nuevos modelos de vías de señalización de IFNbeta y Akt/Sgk
2. Predicción de prevalencia de los parámetros de translocación sobre las tasas de fosforilación de la vía de señalización IFNbeta
3. Un nuevo método de aplicación del modelo Booleano a datos clínicos

Concluyendo, la Biología de Sistemas es una herramienta poderosa para predecir nuevas propiedades de sistemas biológicos, que pueden ser usados en la práctica clínica, como biomarcadores dinámicos o señales de transducción diferenciales.

Introducción

Las vías de señalización en las enfermedades autoinmunes

Las moléculas extracelulares, como las citoquinas, juegan un rol crucial en la transducción de señales. Una de las vías de señalización prototípicas más estudiadas es la del interferón tipo I. Ésta es una vía de señalización conducida por señales Jak-Stat. Los interferones tipo I (IFNalfa e IFNbeta) se combinan con el mismo receptor, llamado IFNAR y activan la vía de señalización Jak-Stat: Los IFNs tipo I se combinan con receptores IFNAR1, la fosforilación de las proteínas Jak1 y TYK2 transmiten la señal, la fosforilación de las proteínas Stat1 y Stat2 permite la formación del compuesto ISGF3 (pStat1-pStat2-IRF9) que se combina con los receptores ISRE en el núcleo. Se probó que al mismo tiempo que el compuesto ISGF3 se forma, su estimulación también forma otros factores de transcripción que contienen Stat1 activado. El principal de ellos es GAF (homodimero Stat1-Stat1), el principal compuesto para la vía de señalización IFN tipo II (fig. 1). Existen distintas moléculas activadoras e inhibidoras, que

regulan la fosforilación de tirosina de Stat1. Su expresión se regula mediante el factor de transcripción GAF (pStat1-pStat1) al enlazarse con elementos GAS, que son presentados en el promotor Socs1.

Dado que los interferones tipo I juegan un rol clave en la inmunidad innata y adaptativa, son usados frecuentemente como una terapia en el tratamiento de la EM. Interpretamos la respuesta transiente oscilatoria de la vía de señalización para evaluar la efectividad potencial del tratamiento con IFN-beta en pacientes con EM.

Aproximaciones a los modelos en biomedicina

Los modelos dinámicos de inducción de IFN en la vía de señalización Jak/Stat basados en ecuaciones diferenciales ordinarias no lineares han sido usados previamente para estudiar el efecto del pre tratamiento con IFN en la respuesta del sistema inmune a la infección vírica [1][2] y la robustez de la vía de la señalización frente al ruido y las fluctuaciones de parámetros [3] entre otros problemas. Las aproximaciones a través de la Biología de Sistemas también han sido aplicadas a esta vía de señalización para estudiar su rol en ciertos mecanismos patológicos subyacentes en el comportamiento de las células cancerígenas [4] y su interacción con otras vías de señalización clave [1][5]. Estudios anteriores sugieren una combinación de espirales de feedback positivas y negativas, junto con la eventual degradación de la señal de IFN en el médium, lo que lleva a una respuesta transitiva oscilatoria en diversos componentes de la vía de señalización. Este comportamiento es constante con anteriores resultados numéricos encontrados en modelos puros [6], y va más allá de observaciones previas que indicaban una respuesta transitiva simple [3][7][8].

La regulación de la vía de señalización Jak-Stat parece ser más compleja de lo que se suponía previamente. Esta íntimamente regulada y conectada a través de otras vías de señalización [9]. Los IFNs de tipo 1 son usados comúnmente como tratamiento en diversas enfermedades crónicas como la hepatitis C, la leucemia y la EM. Mejorar nuestro entendimiento sobre el funcionamiento de esta vía de señalización, su procesamiento de información y su participación en la patogénesis de estas enfermedades o en sus respuestas a las distintas terapias mejoraría nuestra capacidad de gestionar dichas enfermedades.

Otra vía de señalización crítica bien conocida para factores de señalización tróficos es PI3K. La vía de señalización PI3K-Akt es clave en la apoptosis que juega un papel clave en la longevidad y el cáncer. Es activada mediante factores de crecimiento como el Factor de Crecimiento de Insulina IGF1. IGF1 se enlaza con el dominio externo de los receptores RTK. La fosforilación del dominio interno del receptor conlleva el enlace de PI3K. Una vez activado, PI3K se enlaza con el fosfolípido de membrana PIP2, transformándolo en su forma activada PIP3. PIP3 activa la vía de señalización Akt mediante su fosforilación. pAkt activa muchos procesos celulares distintos promoviendo el crecimiento celular y previniendo la muerte celular. El principal mecanismo de PI3K-Akt es la activación de la síntesis de proteína mTOR y su translación. El otro mecanismo es la inhibición de la actividad apoptótica de Foxo3 mediante su fosforilación.

La vía de señalización PI3K-Akt es crítica para los factores de crecimiento que promueven la supervivencia celular a través de la fosforilación de Foxo3. En esta vía, la translocación nuclear de Foxo3 después de su fosforilación es un paso clave para modular la expresión genética. La familia de factores de transcripción (TFs) Foxo (Forkhead Box, type O) causan cambios en la expresión génica, implementando un programa de respuesta al estrés celular, y un incremento en su actividad lleva a las intervenciones genéticas que extienden la longevidad en modelos de organismos. Foxo se conserva en todos los animales, desde los gusanos a los humanos. La fosforilación de proteínas Foxo en respuesta a los factores de crecimiento como IGF-I, eritropoyetina, factor de crecimiento de la epidermis o el factor de crecimiento de nervios causa la exclusión del núcleo [10]. Para muchas quinasas proteicas activadas por factores de crecimiento, los lugares específicos de fosforilación son conocidos. Éstas incluyen Akt y serum y quinasa inducible glucocorticoide (Sgk), que son activadas principalmente a través de la vía de señalización PI3K [11][12]. La fosforilación de Foxos en respuesta al estrés oxidativo envuelve a JNK y resulta en la importación de Foxo en el núcleo.

Objetivos

El objetivo general de la tesis es desarrollar un método para modelar vías de señalización y mejorar el entendimiento sobre como la información se transmite a través de ellas. Un objetivo secundario es usar estas vías para la

investigación traslacional, para lograr entender como los fármacos apuntan a estas vías e identificar biomarcadores sobre la respuesta a la terapia. Los objetivos específicos son:

1. Construir, validar y comparar redes Booleanas de vías de señalización de IFN en células T y macrófagos usando líneas celulares humanas
2. Desarrollar un modelo cinético de la vía de señalización de IFN tipo I y validarlo mediante datos experimentales obtenidos con líneas celulares de macrófagos de ratones
3. Evaluar el papel de la traslación nuclear de Stat1 en la cinética de las vías de señalización, sus dinámicas y como responden a estímulos
4. Desarrollar un modelo cinético de la vía de señalización Akt-Foxo3a y validarla usando datos obtenidos mediante la experimentación

Materiales y métodos

Líneas celulares y muestras de sangre:

Usamos la línea celular RAW 264.7 para obtener datos experimentales para la validación del modelo ODE. Para el modelo Booleano usamos líneas celulares Jurkat y humanas obtenidas de un banco de células ATCC. Los PBMCs de controles sanos fueron obtenidos en el Hospital Clínico de Barcelona.

ELISA y citometría de flujo:

Usamos la técnica de ELISA para medir la concentración de IFNbeta en el medio. Usamos ELISA intra celular para analizar las concentraciones de proteínas SOCS1 durante LPS y la estimulación mediante IFNbeta de células RAW en cultivos.

qRT-PCR:

Para medir los niveles de SOCS1 en mRNA usamos RT-PCR, y para validar los resultados de la citometría de flujo y ELISA usamos la técnica western blot estándar.

ImageStreamX imaging system: Para determinar la cantidad de pStat1 transportándose hasta el núcleo tras la inyección de IFNbeta en pacientes con EM utilizamos el sistema de imagen ImageStreamX que permite la visualización de la colocación de dos moléculas distintas usando anticuerpos conjugados con fluorocromo. Los núcleos fueron etiquetados con DAPI y Stat1 con anticuerpo anti humano de ratón Alexa Flúor 488 pStat1 (Y701).

Modelo ODE:

El modelo y las simulaciones fueron diseñados en MATLAB utilizando el solucionador ODE15s (el código de Matlab es proporcionado en el material suplementario). El análisis de estabilidad del sistema dinámico fue realizado a través de códigos Matlab hechos a medida.

Modelo Booleano:

La red de conocimiento previa (PKN) fue construida usando data-mining y bases de datos existentes. Convertimos nuestros datos al formato MIDAS aceptado por datarail y describimos PKN en un fichero sif que puede ser visualizado usando Cytoscape. Utilizamos software CNOptR para encajar el modelo con los datos experimentales. Todos los scripts y las funciones fueron escritas en R. El paquete CellNoptR y otros fueron descargados de Bioconductor. Graphviz y Cytoscape fueron usados para la visualización de los modelos.

Resultados

Capítulo 1. Consideraciones teoréticas sobre las dinámicas de vías de señalización en células individuales y poblaciones de células

Desarrollamos un modelo ODE de la vía de señalización IL6, que muestra las siguientes características: i) el modelo lleva por su propia naturaleza a un límite estable de ciclos con perfiles de periodos y fases que encajan con los valores observados experimentalmente; (ii) el límite de ciclos cuenta con un periodo pronunciadamente robusto para un largo rango de valores de parámetros, como la cantidad de citoquinas y el total de proteínas Stat; (iii) la estimulación de la vía de señalización mediante la adición súbita de inductor lleva a la sincronización de la población de células que ya estaban oscilando de manera dosis-dependiente.

Para entender mejor la naturaleza de la distribución calculamos el coeficiente de variación (CV) de los datos de citometría de un flujo celular único. CV se calcula como la desviación estándar dividida por la mediana para cada punto de tiempo medido. CV es la medida de la diferencia en la respuesta de las células a un estímulo en el mismo punto en el tiempo. Muestra que la desincronización de las células ocurre 15 minutos después de la estimulación. Todas las células son activadas al mismo tiempo, pero en distintos niveles (amplitud de respuesta). Entonces CV decrece para remontar de nuevo. El

segundo mínimo de CV en el minuto 200 corresponde al segundo pico de la respuesta mediana. Eso implica que las células ganan una mayor sincronía en el segundo pico que en el primero. Tras el segundo pico las células se de-sincronizan de nuevo y vuelven a un estado estable. La cinética permanece igual con distintas concentraciones de IL6.

En términos biológicos, la segunda ronda de activación celular corresponde en gran medida a la sincronización celular y a la actividad de la población como un sistema completo más que como células diferentes con respuestas individuales. Puede ser de importancia para generar la correcta respuesta inmune.

Capítulo 2. Modelo booleano de la vía de señalización IFNbeta en humanos

La vía de señalización IFNbeta interactúa con muchas vías de señalización virales y antibacteriales, convirtiéndose en parte de una red mayor. Hemos desarrollado una topología simplificada de dichas interacciones llamada la Red de Conocimiento Preliminar (PKN) en nuestro estudio. En esta PKN hemos etiquetado los estímulos, los mediadores y los genes así como las espirales de feedback y la comunicación entre las distintas vías de señalización en la red. El propósito del modelo Booleano es predecir nuevas interacciones entre las moléculas en la red. Resumiendo, nuestro objetivo ha sido el de construir redes celulares específicas de IFNs de tipo I y vías de señalización en células T y macrófagos. Usamos las células T y las líneas celulares similares a los macrófagos (Jurkat y THP1) para obtener los datos experimentales. Las células fueron testadas entonces con combinaciones de distintos estímulos e inhibidores y distintas fosfoproteínas, que fueron medidas a través de ensayos XMAP bead en estas condiciones.

Los datos obtenidos de las líneas celulares y la adecuación del modelo son mostrados en las figuras suplementarias 1 y 2. Tras aplicar el algoritmo CellNoptR a PKN y los datos experimentales de dos líneas celulares distintas, obtuvimos los modelos lógicos y topológicos para cada línea celular. Los modelos pueden ser representados como scaffolds (fig. 1) que permiten evaluar las diferencias de señalización entre las líneas celulares Jurkat y THP1.

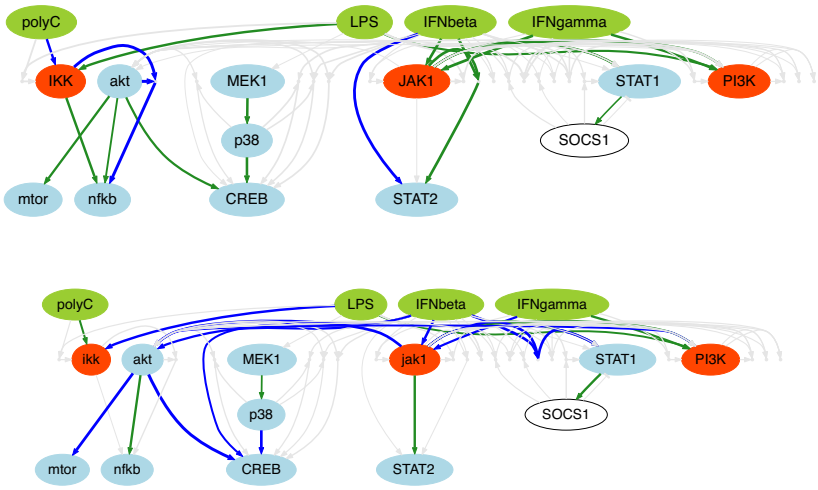

Figura 1. Scaffolds obtenidos desde modelos lógicos para las líneas celulares Jurkat (arriba) y THP1 (abajo)

Dado que muchas de las principales vías de señalización son las mismas (lo cual puede esperarse dada la cercana relación entre todos los subtipos de células inmunes), hay claras diferencias entre los dos andamiajes. Mientras que en THP1 la conexión IFNbeta-Jak1-Stat2 es directa, en Jurkat Jak1 no está directamente activando Stat2. En este caso la activación viene dada por otros intermediarios. También, en THP1 vemos que la activación de CREB viene promovida por IFNbeta, mient4ras que en Jurkat no se aprecia este efecto. Hay otras diferencias en la señalización que podrían explicar algunas de las diferencias en la respuesta de los subtipos de células inmunes in vivo (ver la discusión).

La diferencia en la vía de señalización IFN tipo I entre los subtipos de las células inmunes puede ser crucial para la respuesta celular al tratamiento con IFNbeta. Por esta razón hemos desarrollado un método para aplicar el mismo acercamiento hacia los datos clínicos de pacientes individuales. El reto de los datos clínicos radica en la diversidad entre individuos en la cohorte, lo que produce ruido en los datos. Por este motivo hemos propuesto los siguientes algoritmos para el análisis de las lecturas homogéneas de dos grupos de individuos. Aplicamos el paquete CellNoptR a los resultados estimulados de los experimentos, imitando los datos de los pacientes [13]. PKN y los datos

simulados fueron utilizados entonces para la optimización del método de promedio y comparación las redes topológicas resultantes. El método fue utilizado para promediar cadenas de bits correspondientes a cada modelo generado de cada set de datos.

Capítulo 3. Modelo matemático IFN-beta

Para identificar los elementos críticos de la vía de señalización responsables del comportamiento transitorio oscilatorio observado experimentalmente en macrófagos durante la estimulación con IFN-beta, construimos un modelo ODE basado en conocimiento biológico y datos experimentales (Fig. 2). Para minimizar su complejidad, hemos perseguido el sistema mínimo que explique las observaciones experimentales, en lugar de un sistema descriptivo completo [7].

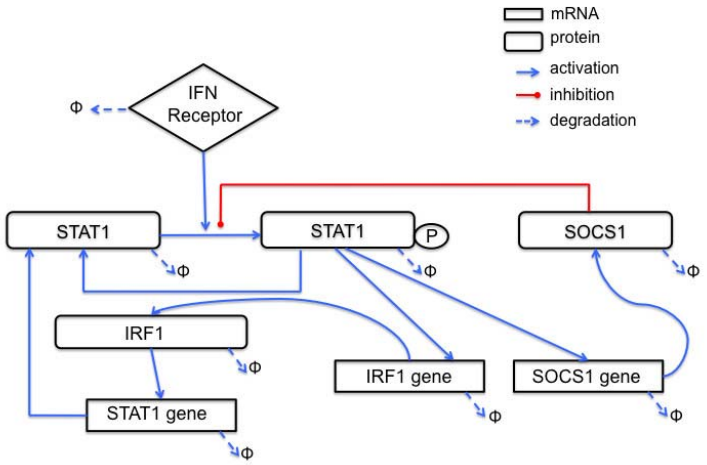

Figura 2. Representación gráfica del modelo matemático de la vía de señalización IFN tipo I

Hemos construido un sistema dinámico de la vía de señalización IFN-beta usando datos experimentales de proteínas y mediciones de concentraciones de mRNA in vitro y conocimiento biológico previo. El modelo esta basado en ecuaciones diferenciales ordinarias (ODE) y predice el comportamiento de la vía de señalización IFN-beta durante el tiempo. El modelo simple incluye las partes principales y más importantes de la vía, como la fosforilación de Stat1, la

inhibición la fosforilación de Stat1 y otras. El modelo se centró en los eventos auto-regulatorios de la vía. Verificamos los modelos mediante los experimentos con líneas celulares murinas RAW similares a macrófagos.

Las ecuaciones diferenciales ordinarias para el modelo mostrado en fig.2 son:

$$
\begin{aligned}
dS/dt &= b_s - \lambda_s S \\
dA/dt &= b_{\exp} A_{pn} + b_{deph} A_{pc} \\
&\quad + b_A a - \frac{b_{ph} S A / k_A}{1 + A/k_A + (R/k_I)^q} - \lambda_{STAT} A \\
dA_{pc}/dt &= \frac{b_{ph} S A / k_A}{1 + A/k_A + (R/k_I)^q} - b_{imp} A_{pc} - b_{deph} A_{pc} \\
&\quad - \lambda_{STAT} A_{pc} \\
dA_{pn}/dt &= b_{imp} A_{pc} - b_{\exp} A_{pn} - \lambda_{STAT} A_{pn} \\
dr/dt &= b_r \frac{\left(A_{pn}/k_r\right)^n}{1 + \left(A_{pn}/k_r\right)^n} - \lambda_r r \\
dR/dt &= b_R r - \lambda_R R \\
df/dt &= b_f \frac{\left(A_{pn}/k_f\right)^m}{1 + \left(A_{pn}/k_f\right)^m} - \lambda_f f \\
dF/dt &= b_F f - \lambda_F F \\
da/dt &= b_a \frac{(F/k_F)^u}{1 + (F/k_F)^u} - \lambda_a a + B_{STAT}
\end{aligned}
$$

Usamos diversos métodos para obtener los parámetros del modelo. Algunos de los parámetros fueron estimados utilizando datos experimentales provenientes de conocimiento previo mientras que otros fueron encajados manualmente.

Hemos realizado análisis de tiempos de serie de la fosforilación de Stat1 y los niveles totales de Stat1 y Socs1 mediante ensayos de Luminex (Fig. 4) y los niveles de Stat1, IRF1 y SOCS1 mRNA tras la estimulación de IFN-beta mediante RT-PCR (Fig. 3). Entonces, comparamos los resultados experimentales con simulaciones de modelos matemáticos para evaluar la concordancia de las dinámicas en un nivel cualitativo

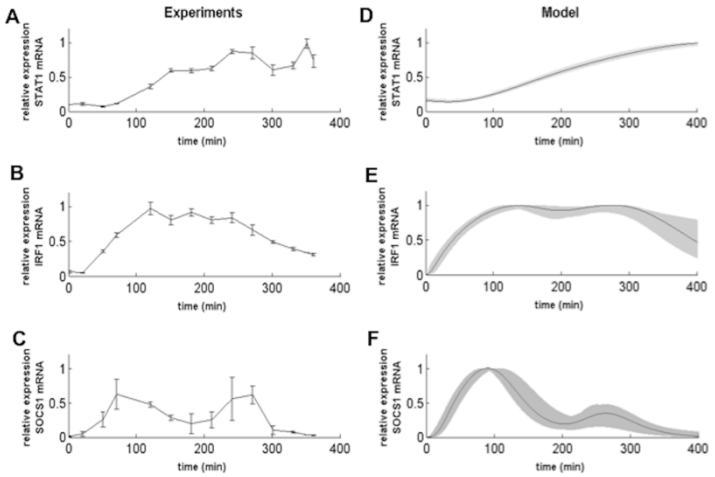

Figura 3. Expresión génica de los niveles de Stat1, IRF1 y Socs1 tras la estimulación con IFN-beta y las correspondientes simulaciones del modelo ODE A-C) Las concentraciones de Stat 1, IRF1 y RNA de SOCS1 en lisados celulares fueron medidas mediante RT-PCR en las células Raw estimuladas con IFN-Beta (1000 unidades/ml)

. Los experimentos descubrieron diversas características importantes de las dinámicas de señalización de Jak/Stat durante las ocho primeras horas después del tratamiento con IFN-beta. Por ejemplo, nuestros resultados mostraron la naturaleza oscilatoria de la activación de Stat1 (pStat1), con un rápido incremento de la concentración de cytosol pronto tras la estimulación (durante la primera hora), seguida por un segundo pico de concentración alrededor del minuto 200. Un objetivo crítico de la transcripción de Stat1 como Socs1 también mostró dos picos de expresión (correlacionados en el tiempo a los picos de pStat) alrededor de tras 90 y 250 mn tras la estimulación, mientras que otro objetivo importante, IRF1, exhibió una señal de plató en forma de campana de Bell.

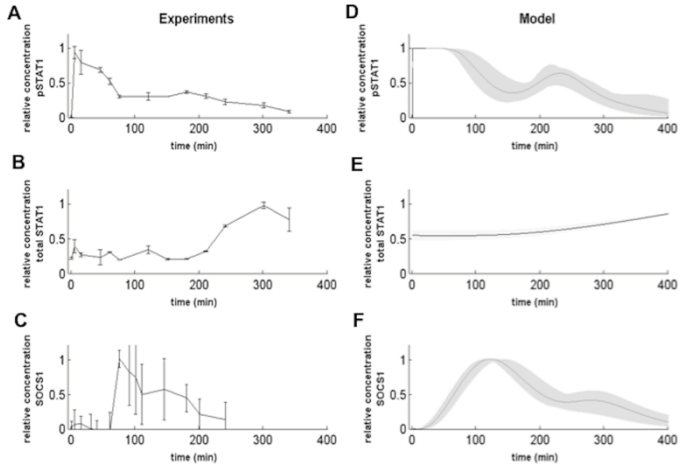

Figura 4. Activación de la vía de señalización de IFN tipo I mediante IFN-beta en líneas celulares Raw y sus correspondientes simulaciones en el modelo ODE A-C) La concentración de proteínas pStat1, Stat1 y Socs1 en lisados celulares fue medida mediante Luminex, citometría de flujo o ELISA tras la estimulación con IFN-beta (1000 unidades/ml).

Capítulo 4. La translocación nuclear modela la cinética de la vía de señalización IFNbeta

Realizamos simulaciones por ordenador usando diferentes condiciones y parámetros así como un análisis de sensibilidad y bifurcación del modelo desarrollado (fig. 5). El análisis de bifurcación indican la posible implicación de la translocación nuclear de pStat1 para la correcta actividad oscilatoria de las células una vez estimuladas in vitro con IFNbeta. Este descubrimiento nos llevó a la hipótesis de la alteración del proceso de translocación nuclear como respuesta a la terapia con IFNbeta. El análisis de bifurcación del modelo de la vía de señalización Stat1 identifica que la translocación al núcleo es un paso crítico.

(A, C) La escala cromática representa el valor absoluto de la parte imaginaria de la ecuación de auto valores con parte máxima real, correspondiente al estado estable del sistema tras estimulación con IFN, para valores variantes de fosfo y defosforilación (bph y bdeph en el panel A), y ratios de importación/exportación nuclear (bexp y bimp en el panel B). Dos distintos

regímenes dinámicos pueden ser identificados con este análisis: el régimen oscilatorio amortiguado (en rojo) y el régimen sobre-amortiguado/no oscilatorio (en azul).

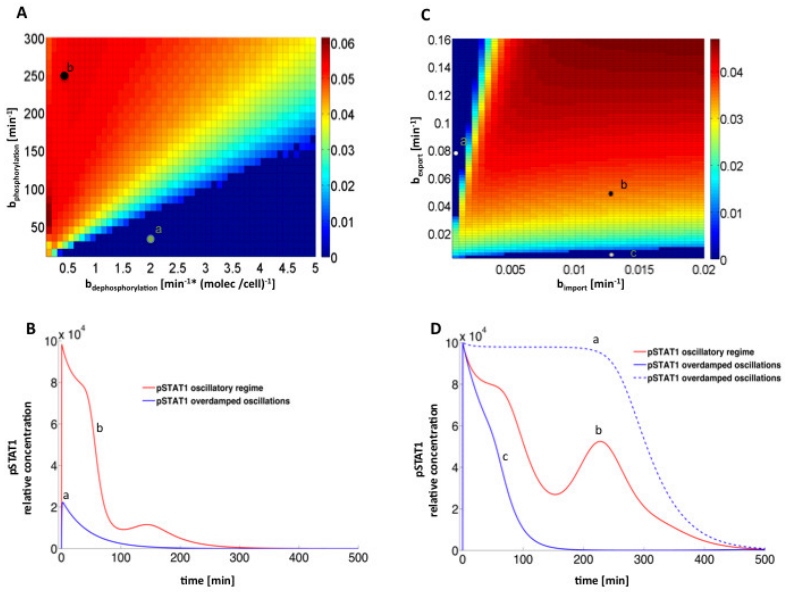

Figura 5. Análisis de estabilidad de la solución en estado estable en espacios con parámetros de 2D

(B, D) Ejemplos de la evolución en el tiempo de pStat1 en ambos regímenes (amortiguado y sobre-amortiguado en las líneas rojas y azules, respectivamente), correspondientes a la posición de los parámetros de marcadores circulares para los dos diagramas mostrados en los paneles A y B, respectivamente.

Para comprobar la hipótesis de que el proceso de translocación nuclear es crítico para la respuesta a la terapia con IFNbeta en pacientes con EM, evaluamos la translocación nuclear de Stat1 tras el tratamiento con IFNbeta en pacientes con EM usando la plataforma de imagen ImageStreamX. Ajustamos el protocolo estándar de la citometría de flujo usando PBMCs de los controles sanos.

Obtuvimos PBMCs de controles y pacientes tratados con IFNbeta (n=4) en tiempos diferentes tras la inyección. Los resultados muestran diferencias significantes en el patrón de translocación nuclear entre individuos.

Capítulo 5. Modelo AKT-Foxo

Para modelar la vía de señalización AKT/Sgk-Foxo3, hemos desarrollado un modelo ODE basado en conocimientos previos y datos experimentales. La característica principal de nuestro modelo es la exportación nuclear y la fosforilación de pFoxo3a mediante pAkt y pSgk tras la activación de la vía IGF1. La fosforilación de Foxo3a en los 3 principales fosfatos nos lleva a su desactivación y arresto en el citoplasma. Otras modificaciones post-translacionales pueden llevar a su ubiquidad y su degradación (fig. 6). Los genes principales, regulados por Foxo3a TF, son Foxa2, las cyclinas D1, D2, D3, los inhibidores de quinasa dependiente de cyclina 1B y 1A, Bcl-6, Catalasa, el ligando Fas y otros. Nuestros modelos muestran la importancia del mecanismo de inhibición de Foxo3a para la reducción de ruido en el sistema.

El gran interés en términos de tratamiento neuroprotectivo es la comunicación cruzada entre la vía de señalización PI3K y la activación de Foxo3a mediante ROS y su actividad apoptótica en condiciones de estrés oxidativo. La transportación nuclear es un parámetro crucial del sistema para mantener el equilibrio entre escenarios de supervivencia y apoptosis.

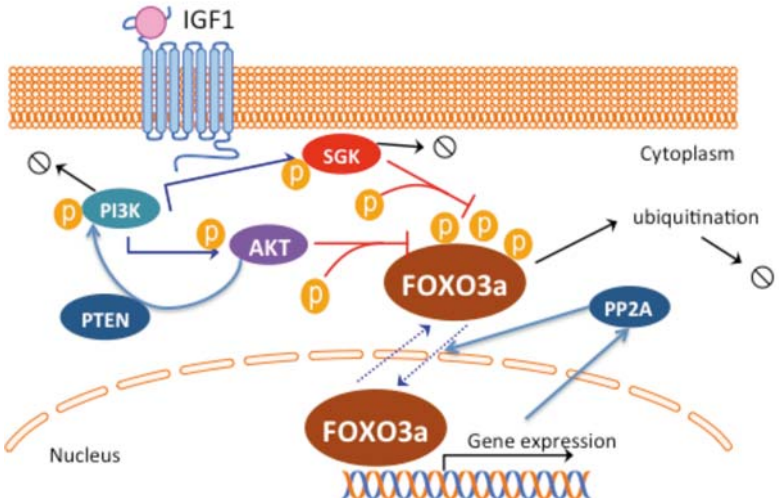

Figura 6. El modelo de señalización Akt-Foxo3 y el transporte nuclear de Foxo3

Discusión

En la línea celular RAW, la expresión de los genes Socs1 y IRF1 cambia durante la primera respuesta al IFN, pero no existe expresión significante de algunos genes usados comúnmente como referencia (Mx1 y OAS1a). La

activación de la vía de señalización Jak-Stat mediante IFN-beta activa la fosforilación de Stat1, Stat2 y algunas otras proteínas. Estas proteínas activadas proceden principalmente de dos compuestos distintos: Stat1-Stat1 (compuesto AAF) y Stat1-Stat2-IRF9 (compuesto ISGF). Ambos compuestos activan numerosos genes en el núcleo, enlazándose a los elementos de regulación específicos en los promotores. El compuesto AAF se enlaza con los elementos GAS y el compuesto ISGF se enlaza con los elementos ISRE. Los genes contenedores de GAS (incluyendo Socs1 y IRF1) son responsables de la respuesta antibacteriana de las células y los genes contenedores de ISRE activan la respuesta antiviral de las células [15]. Basado en el background y nuestros resultados hemos hipotetizado que los macrófagos forman principalmente compuestos AAF que activan la ruta antibacterial (secuencias GAS), mientras que en las células T la situación es la opuesta, activando elementos ISFG3 y, por lo tanto, la respuesta antiviral. Por ejemplo, recientemente se mostró que la respuesta a IFN-beta difiere entre distintas células inmunes, y un análisis de los pacientes que no muestran respuesta a la terapia con IFN-beta indican una anulación diferencial de la vía de señalización IFN tipo I en los monocitos de estos pacientes [16].

La red de señalización de IFN afecta diferentes vías de compuestos, involucrando procesos como la diferenciación, la proliferación, la supervivencia y la muerte celular [17, 18], y además sirve como una terapia autoinmune [19]. IFN-beta es el tratamiento más común para la EM [20], y estudios genómicos previos han identificado ciertos genes pertenecientes a la vía de señalización IFN que están asociados con una falta de respuesta ante IFN-beta, sugiriendo que el background genético de ciertos individuos puede modular esta vía y, consecuentemente, la respuesta a la terapia, mediante perfiles transcripcionales específicos [22].

Nuestro estudio realza la importancia de identificar las dinámicas temporales de la concentración de ciertos elementos clave de la vía Jak-Stat, como la forma fosforilada de la proteína Stat1 y la expresión de los genes de transcripción estimulados con interferón como Socs1 y IRF1 durante las primeras 8 horas de la administración de IFN-beta. Catalogar estas dinámicas puede proveernos con biomarcadores moleculares tempranos que nos permitan

distinguir la falta de respuesta a la terapia con IFN-beta en ciertos pacientes con EM.

Nuestro modelo también indica el rol crucial de la translocación nuclear de las moléculas de Stat1 para la correcta dinámica de la vía de señalización. Las alteraciones en estas características de translocación de Stat1 prevalecen sobre las tasas de fosforilación y defosforilación para determinar las dinámicas oscilatorias de la vía de señalización IFNbeta. En un pequeño grupo de pacientes con EM hemos mostrado que la tasa de translocación difiere substancialmente entre distintos individuos y puede determinar la diferencia de respuesta a la terapia o la progresión de la enfermedad. Los niveles de translocación de Stat1 pueden ser potenciales biomarcadores de la respuesta al tratamiento con IFNbeta y requieren más investigación.

Otro ejemplo de la importancia de las características de transporte nuclear en la transducción de señales es el factor de transcripción Foxo3a. Foxo3a puede ser considerada como un regulador maestro de la vía PI3K-Akt, que determina la supervivencia o un escenario en el que la célula opta por la apoptosis. El modelo de señalización de Akt-Foxo3a es una herramienta interesante desde un punto de vista teorético y práctico.

Desde el punto de vista teorético, la señalización de Akt-Foxo3a es un ejemplo de un grupo mayor de vías de señalización de transducción que tienen que ver con la toma de decisiones a nivel celular y que comparten un amplio número de pautas de comportamiento corrientes. La cinética de Akt-Foxo3a y su regulación y comunicación puede ser una tendencia común en toda la clase de vías de señalización. La razón de la estructura de inhibición y fosforilación nuclear es la resistencia al ruido de estos mecanismos de acción y múltiples posibilidades de ajuste y un cambio de comportamiento constante.

Desde el punto de vista práctico, Foxo3a es cada vez más un blanco de investigación en la inmunología y la neurología [24, 25]. El nuevo fármaco neuroprotectivo prometedor, MS BN201, apunta a Sgk la quinasa de emisión de Foxo3a, modificando la actividad de Foxo3a. El entendimiento del comportamiento de Foxo3a en las células humanas en diferentes condiciones nos llevará a predecir los efectos de los nuevos tratamientos para la EM.

Conclusiones

1. La población de células tiene la habilidad de coordinar y sincronizar su actividad en respuesta a la estimulación con IL-6. Esta habilidad es un atributo necesario de la señalización celular, que permite una correcta respuesta a los sistemas externos y provee una respuesta más robusta al entorno.

2. Las células T y los macrófagos responden de manera diferente a IFNbeta, IFNgamma o a agentes infecciosos por las diferencias cualitativas en sus redes de señalización. Estas diferencias llevan a un amplio abanico de comportamientos de las células del sistema inmune en respuesta a distintos retos y al tratamiento con IFNbeta en enfermedades autoinmunes.

3. La señalización de IFNbeta en los macrófagos toma la forma de dinámicas oscilatorias transitorias en la vía JAK-Stat, cuyas propiedades específicas de relajación determinan la longitud de la respuesta celular a la citoquina, lo cual tiene una implicación en el resultado de la respuesta inmune.

4. La translocación nuclear de pStat1 modela las dinámicas del sistema de señalización JAK-Stat y lleva al cambio entre sistemas oscilatorios amortiguados y sobre-amortiguados. Individuos con distintas respuestas clínicas al tratamiento con IFNbeta mostraron diferencias en las dinámicas de traslocación nuclear de pStat1, convirtiéndolo en un biomarcador muy prometedor sobre la respuesta a esta terapia.

5. La inhibición mediante fosforilación de pFoxo3a es un interruptor molecular, que constriñe la regulación de la actividad transcripcional de Foxo3a. El transporte nuclear de Foxo3a es un buffer cinético de la actividad de Foxo3 y mantiene el equilibrio entre los mecanismos de supervivencia celular y represión de tumor. Este mecanismo de cambio está controlado por la acción coordinada de Akt y Sgk en la vía de señalización PI3K.

Referencias

1. Raza S, Robertson K a, Lacaze P a, Page D, Enright AJ, Ghazal P, Freeman TC: **A logic-based diagram of signalling pathways central to macrophage activation.** *BMC Syst Biol* 2008, **2**:36.

2. Qiao L, Phipps-Yonas H, Hartmann B, Moran TM, Sealfon SC, Hayot F, Cells VHD: **Immune Response Modeling of Interferon b-Pretreated Influenza Virus-infected Human Dendritic Cells**. *Biophysj* 2010, **98**:505–514.

3. Smieja J, Jamaluddin M, Brasier AAR, Kimmel M: **Model-based analysis of interferon-β induced signaling pathway**. *Bioinformatics* 2008, **24**:2363–2369.

4. Vera J, Rateitschak K, Lange F, Kossow C, Wolkenhauer O, Jaster R: **Systems biology of JAK-STAT signalling in human malignancies.** *Prog Biophys Mol Biol* 2011, **106**:426–34.

5. Swameye I, Muller TG, Timmer J, Sandra O, Klingmuller U: **Identification of nucleocytoplasmic cycling as a remote sensor in cellular signaling by databased modeling.** *Proc Natl Acad Sci U S A* 2003, **100**:1028–33.
6. Soebiyanto RP, Sreenath SN, Qu C-K, Loparo KA, Bunting KD: **Complex systems biology approach to understanding coordination of JAK-STAT signaling.** *Biosystems* , **90**:830–42.
7. Yamada S, Shiono S, Joo A, Yoshimura A: **Control mechanism of JAK/STAT signal transduction pathway**. *FEBS Lett* 2003, **534**:190–196.
8. Shudo E, Yang J, Yoshimura A, Iwasa Y: **Robustness of the signal transduction system of the mammalian JAK/STAT pathway and dimerization steps.** *J Theor Biol* 2007, **246**:1–9.
9. Rani MRS, Ransohoff RM: **Alternative and accessory pathways in the regulation of IFN-beta-mediated gene expression.** *J Interferon Cytokine Res* 2005, **25**:788–98.
10. Glauser D a, Schlegel W: **The emerging role of FOXO transcription factors in pancreatic beta cells.** *J Endocrinol* 2007, **193**:195–207.
11. Biggs WH, Meisenhelder J, Hunter T, Cavenee WK, Arden KC: **Protein kinase B/Akt-mediated phosphorylation promotes nuclear exclusion of the winged helix transcription factor FKHR1.** *Proc Natl Acad Sci U S A* 1999, **96**:7421–6.
12. Brunet A, Bonni A, Zigmond MJ, Lin MZ, Juo P, Hu LS, Anderson MJ, Arden KC, Blenis J, Greenberg ME: **Akt promotes cell survival by phosphorylating and inhibiting a Forkhead transcription factor.** *Cell* 1999, **96**:857–68.
13. MacNamara A, Terfve C, Henriques D, Bernabé BP, Saez-Rodriguez J: **State-time spectrum of signal transduction logic models.** *Phys Biol* 2012, **9**:045003.
14. Pertsovskaya I, Abad E, Domedel-Puig N, Garcia-Ojalvo J, Villoslada P: **Transient oscillatory dynamics of interferon beta signaling in macrophages**. *BMC Syst Biol* 2013, **7**:59.
15. Sadler AJ, Williams BRG: **Interferon-inducible antiviral effectors.** *Nat Rev Immunol* 2008, **8**:559–68.
16. Oliver-Martos B, Órpez T, Pinto-Medel MJ, Mayorga C, García-León J a, Maldonado-Sanchez R, Suardíaz M, Guerrero M, Luque G, Leyva L, Fernández O: **Gene expression in IFNß signalling pathway differs between monocytes, CD4 and CD8 T cells from MS patients.** *J Neuroimmunol* 2011, **230**:153–9.
17. Samuel C: **Antiviral Actions of Interferons**. *Clin Microbiol Rev* 2001, **14**.
18. Lohoff M, Mak TW: **Roles of interferon-regulatory factors in T-helper-cell differentiation.** *Nat Rev Immunol* 2005, **5**:125–35.
19. Javed A, Reder AT: **Therapeutic role of beta-interferons in multiple sclerosis.** *Pharmacol Ther* 2006, **110**:35–56.
20. Marta M, Giovannoni G: **Disease modifying drugs in multiple sclerosis: mechanisms of action and new drugs in the horizon.** *CNS Neurol Disord Drug Targets* 2012, **11**:610–23.
21. Villoslada P, Oksenberg JR, Rio J, Montalban X: **Clinical characteristics of responders to interferon therapy for relapsing MS.** *Neurology* 2004, **62**:1653; author reply 1653.
22. Río J, Comabella M, Montalban X: **Predicting responders to therapies for multiple sclerosis.** *Nat Rev Neurol* 2009, **5**:553–60.
23. Burgering BMT: **Decisions on life and death : FOXO Forkhead transcription factors are in command when PKB / Akt is off duty**. 2003, **73**(June):689–701.

24. Yeo H, Lyssiotis C a, Zhang Y, Ying H, Asara JM, Cantley LC, Paik J-H: **FoxO3 coordinates metabolic pathways to maintain redox balance in neural stem cells.** *EMBO J* 2013, **32**:2589–602.
25. Peng SL: **Forkhead transcription factors in chronic inflammation**. 2011, **42**:482–485.

Annex 1. Curriculum vitae

Inna Pertsovskaya

Business address Neuroimmunology Group, Department of Neurosciences, Institut Biomedical Research August Pi Sunyer, Hospital Clinic, Casanova, 143

Edificio CELLEX 08036 Barcelona, Spain

Phone: 93 227 54 00 ext 4802

E-mail: inna.perts@gmail.com

Education:

11/2009 – present PhD student, University of Barcelona, Barcelona, Spain

2002 - 2007 M.S. Bioengineering and bioinformatics, Moscow State University, Moscow, Russia

Career History:

05/2012 - present Researcher, IDIBAPS - Hospital clinic, Barcelona, Spain

05/2009 – 05/2012 Early Stage Researcher, Marie Curie Trainee Program UEPHA-MS, IDIBAPS - Hospital clinic, Barcelona, Spain

10/2007 – 05/2009 Ph.D. student, Dept. of Bioengineering and Bioinformatics, Moscow State University, Moscow, Russia. Specialization in molecular biology

01/2008 – 05/2009 School teacher (biology), State school, Moscow, Russia

Past projects:

Reconstruction of the tankyrase protein family evolution

Analysis of senescence mechanisms on stationary cell cultures

Computational identification of *cis*-regulatory modules in vertebrates

MS thesis: “CpG islands in mammalian genomes”

UEPHA*MS FP7 ITN. Systems biology for predicting biomarkers

Current projects:

Modeling kinetics of type I IFN pathway using ordinary differential equations

Boolean models of signaling pathways for data-specific networks

Sybilla (Systems biology of T-cell activation in health and disease) FP7. Modelling T cell activation in Multiple Sclerosis patients and healthy controls

CombiMS

Skills:

Molecular biology techniques: western blot, real-time RT-PCR, ELISA, flow cytometry, Luminex xMap

Cell culturing, experimantal animals manipulations

Perl, SQL, Matlab programming, public database analysis

Bioinformatics research (Clustal, Blast, Genome Browser, MiRanda and other tools)

Computer skills (Word, Excel, PowerPoint, CorelDRAW, Photoshop)

User of Linux/Unix operating systems

Systems biology tools: Cytoscape, Wikipathways, DataRail and CNO

Mathematical methods: ordinary differential equations, stochastic simulations, Boolean logic, Statistics

Grants and awards:

Award for the best oral presentation on the XIV International Moscow Lomonosov's Conference, 2007

UEPHA-MS (United Europeans dor the Development of Pharmacogenomics in Multiple Sclerosis) Grant Agreement Number 212877 (PITN-GA-2008-212877) support for training and career development of researchers (Marie Curie) Networks for Initial Training (ITN)

60th Meeting of Nobel Laureates (3rd Interdisciplinary Meeting) in 2010. Participant

Research interests:

Systems biology and mathematical modeling of biological processes

Synthetic biology and artificial genetic circuits

Neuroimmunology, autoimmunity disorders

Signal transduction pathways modeling

Bioinformatics methods of eukaryotic genome analysis,

Evolution of regulatory systems

Epigenetics, comparative genomic analysis

Courses and short stages:

Model thinking online course, Mechigan university, April 2012

Experimental animals manipulations and care for researchers, February 2010

ESNI course, November 2010

Ascertaining the Genetic Architecture of Disease, October 2011

Toulouse UEPHA Summer school "Biomarkers in Multiple Sclerosis and pharmacogenomics research"

Barcelona UEPHA Summer school "Systems biology and career development"

Berlin UEPHA Summer school "The clinical validation process. Entrepreneurship"

CITI online Ethics course, August 2010

Rotation in Vall d'Hebron Hospital (Barcelona) "Flow cytometry for human samples analysis", June 2010

Rotation in GosNIIGenetika (Moscow) "Bioinformatics and statistics for clinical research", August 2010

Rotation in EBI - EMBL (Hinxton, UK) "Boolean models for phosphoproteomics data", August 2011

Publications:

Pertsovskaya I, Abad E, Domedel-Puig N, Garcia-Ojalvo J, Villoslada P: **Transient oscillatory dynamics of interferon beta signaling in macrophages**. *BMC Syst Biol* 2013, **7**:59.

Domedel-Puig N PJ, Pertsovskaya I, Volkov EI, Nolan G, Villoslada P, Garcia-Ojalvo J: **Cytokine-Driven Stat Oscillations are Generated by an Activator-Repressor Module**. *(in preparation)*

Pertsovskaya I, Abad E, Kiani N, Tegner J, Garcia-Ojalvo J, Villoslada P: **The dynamical influnce of Sgk and Akt on the translocation of Foxo3a transciption factor** *(in preparation)*

Key conferences:

Pertsovskaya I.M., Kourchashova S.Y., Sidorova N.N., Kuimov A.N. **Tankyrase – a novel regulator of human telomeres.** The Second Moscow International Congress

"Biotechnology: State of the Art and Prospects of Development", 2004 (poster presentation)

Pertsovskaya I.M., Nikulova A.A. **Computational identification of *cis*-regulatory modules in vertebrates.** XIII International Moscow Lomonosov's Conference. P. 38-39. April 12-15, 2006, Moscow, Russia (oral presentation)

I.M.Pertsovskaya, A.A.Mironov. **Evolution of CpG islands in mammalian genomes** 3rd Int. Moscow Conference on Computational Molecular Biology MCCMB'07 Moscow, Russia, July 2007) (poster presentation) p. 250

I.M.Pertsovskaya. **Evolution of CpG islands in mammalian genomes**, Information Technology and Systems Conference (ITaS), Zvenigorod, Russia, September 2007 (oral presentation)

Pertsovskaya I, Oparina N, Vinogradov D, Mironov A, Favorov. **An evidence of the role of selection pressure in CpG islands stability: new approach.** Grand Challenges In Computational Biology, Barcelona, Spain, June 2008. p. 19 (poster presentation)

I. Pertsovskaya, N. Oparina, D. Vinogradov, A. Favorov, A. Mironov **CpG islands evolution: CpG dinucleotides death and birth probabilities in different genome regions.** The Sixth International Conference on Bioinformatics of Genome Regulation and Structure (BGRS'2008) Novosibirsk, Russia, June 2008. (oral presentation)

I. Pertsovskaya, N. Domodel - Puig, J. Garcia-Ojalvo, P. Villoslada **Modeling type I IFN pathway in macrophages: implications for immunotherapy**

10th International congress of neuroimmunology (ISNI 2010) (Barcelona, 27-30.10.2010) (poster presentation)

I. Pertsovskaya, N. Domodel - Puig, J. Garcia-Ojalvo, P. Villoslada **Modeling cytokine signaling pathways for the study of Multiple Sclerosis**

Systems Biology: Bridging the gaps between disciplines (Barcelona, 9-10.12.2010) (oral presentation)

I. Pertsovskaya, N. Domodel - Puig, J. Garcia-Ojalvo, P. Villoslada **Modeling Type I interferon pathway for the study of Multiple Sclerosis**

Moscow Conference on Computational Molecular Biology (MCCMB'11) (Moscow, 21-24.07.2011) (poster presentation)

I. Pertsvoskaya, J. Saez-Rodriguez, P. Villoslada. **Modelling cell-specific response to interferon beta by different immune cell subtypes.** RECOMB - RICCI (Barcelona, October 2011)

Annex 2. Published work

Pertsovskaya I, Abad E, Domedel-Puig N, Garcia-Ojalvo J, Villoslada P. **Transient oscillatory dynamics of interferon beta signaling in macrophages.** BMC Syst Biol. 2013 Jul 9;7(1):59.

Pertsovskaya et al. BMC Systems Biology 2013, 7:59
http://www.biomedcentral.com/1752-0509/7/59

BMC Systems Biology

RESEARCH ARTICLE Open Access

Transient oscillatory dynamics of interferon beta signaling in macrophages

Inna Pertsovskaya[1†], Elena Abad[2,3†], Núria Domedel-Puig[3], Jordi Garcia-Ojalvo[2,3] and Pablo Villoslada[1*]

Abstract

Background: Interferon-beta (IFN-beta) activates the immune response through the type I IFN signaling pathway. IFN-beta is important in the response to pathogen infections and is used as a therapy for Multiple Sclerosis. The mechanisms of self-regulation and control of this pathway allow precise and environment-dependent response of the cells in different conditions. Here we analyzed type I IFN signaling in response to IFN-beta in the macrophage cell line RAW 264.7 by RT-PCR, ELISA and xMAP assays. The experimental results were interpreted by means of a theoretical model of the pathway.

Results: Phosphorylation of the STAT1 protein (pSTAT1) and mRNA levels of the pSTAT1 inhibitor SOCS1 displayed an attenuated oscillatory behavior after IFN-beta activation. In turn, mRNA levels of the interferon regulatory factor IRF1 grew rapidly in the first 50–90 minutes after stimulation until a maximum value, and started to decrease slowly around 200–250 min. The analysis of our kinetic model identified a significant role of the negative feedback from SOCS1 in driving the observed damped oscillatory dynamics, and of the positive feedback from IRF1 in increasing STAT1 basal levels. Our study shows that the system works as a biological damped relaxation oscillator based on a phosphorylation-dephosphorylation network centered on STAT1. Moreover, a bifurcation analysis identified translocation of pSTAT1 dimers to the nucleus as a critical step for regulating the dynamics of type I IFN pathway in the first steps, which may be important in defining the response to IFN-beta therapy.

Conclusions: The immunomodulatory effect of IFN-beta signaling in macrophages takes the form of transient oscillatory dynamics of the JAK-STAT pathway, whose specific relaxation properties determine the lifetime of the cellular response to the cytokine.

Keywords: Type I interferon pathway, Interferon-beta, Ordinary differential equation, Oscillations, Multiple sclerosis, Immunotherapy

Background

Type I interferons, such as interferon alfa and beta, are cytokines that represent a first-line endogenous defense mechanism in response to viruses and bacterial infections, are secreted by many cell types (e.g. lymphocytes, macrophages and endothelial cells) and they are used as a therapy in Multiple Sclerosis (MS).

The canonical type I interferon (IFN) pathway involves different signaling cascades, one of which is the JAK/STAT pathway. This pathway is composed by several steps, which include receptor binding (IFNR1 and 2), transformation of the latent transcription factor (a protein of the STAT family) into its active form by phosphorylation, nuclear migration of the transcription factor (TF), binding of the TF to target promoters, and expression of their corresponding genes [1] (Figure 1). Previous studies have shown that phosphorylated STAT1 forms other TF complexes in response to type II interferons, the most important of which is a STAT1-STAT1 homodimer, known as GAF, that binds to IFN Gamma-activated sequence (GAS) elements [2].

The target genes of the IFN-beta pathway can be divided into three categories according to the type of activating transcription factor: 1) the ISGF3 complex activates genes containing an ISRE binding site in their promoter (e.g. ISG15, Mx1, OAS1, IRF7). 2) The GAF complex activates genes containing a GAS binding site

* Correspondence: pvilloslada@clinic.ub.es
†Equal contributors
[1]Center of Neuroimmunology, Institut d'Investigacions Biomèdiques August Pi i Sunyer (IDIBAPS), Hospital Clinic of Barcelona, Barcelona, Spain
Full list of author information is available at the end of the article

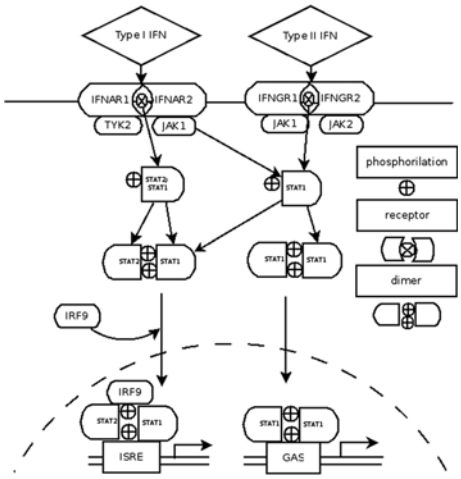

Figure 1 The canonical type I and type II IFN signalling pathways. The plot represents the canonical IFN pathways and the cross-talk between them, including the different pSTAT dimers formed after stimulation.

in their promoter, such as SOCS1 and IRF1 [3,4]. 3) A third class of STAT protein complexes activates other canonical pathways that exhibit crosstalk with the JAK/STAT pathway (such as PI3K, NFkB, MAPK) [5]. Recently it was shown that different immune cell subtypes respond differently to IFN-beta induction through activation of these different types of genes [6].

Different proteins regulate STAT1 phosphorylation. Importantly, a negative feedback loop upon STAT1 activation coexists with a positive feedback mechanism. First, the phosphorylation of STAT1 is inhibited by its inhibitor SOCS1 [7]. The SOCS1 protein then inhibits STAT1 phosphorylation at the kinase level. Besides this negative loop based on SOCS1, STAT1 is a subject to positive regulation via the TF IRF1, whose transcription is induced by activated STAT1. IRF1 promotes the expression of the STAT1 gene at the transcriptional level. Given the existence of these multiple feedback loops, a mathematical modeling of the system would help provide an understanding of the response to type I IFN-beta.

Here we analyzed the type-I IFN-beta signaling pathway in macrophages, showing that the response of this pathway to IFN-beta stimulation takes the form of transient oscillations in STAT1 phosphorylation. We characterized and identified the critical elements governing the transient dynamics of IFN activation, and examined the influence of this dynamical regime in the response to IFN-beta.

Dynamical models of IFN induction of the JAK/STAT signaling pathway based on nonlinear ordinary differential equations, have been previously used to study the effect of IFN pre-treatment on the response of the immune system to virus infection [8,9] and the robustness of the pathway to noise and parameter fluctuations [10], among other problems. Systems biology approaches have also been applied to this pathway in order to examine its role in certain pathological mechanisms underlying the behavior of cancer cells [11], and its interaction with other key signaling pathways [8,12]. Here we combine our theoretical model with experimental observations. Our results show that a combination of positive and negative feedback loops, together with the eventual degradation of the IFN signal in the medium, leads to a transient oscillatory response in several components of the pathway. This behavior is consistent with previous numerical results found in pure modeling studies [13], and goes beyond previous observations that indicate a simpler transient response [10,14,15]. We interpret the transient oscillatory response of the pathway in terms of the potential effectiveness of IFN-beta treatment in MS patients.

Results

IFN-beta induces a transient oscillatory activation of the STAT1 pathway

It is well known that microbial and viral infections induce endogenous IFN-beta release by macrophages as part of the immune cell system response. We could observe IFN-beta production accompanied with significant increases in levels of phosphorylated STAT1 in the murine macrophage-like cell line RAW 264.7 stimulated with lipopolysaccharide (LPS) endotoxin and also, with viral fragments (poly(I:C)) (data not shown). In this study we focused on STAT1 signaling by IFN-beta stimulation in macrophages by challenging the RAW cell line with increasing concentrations of mouse IFN-beta.

We observed that phosphorylated STAT1 levels increased rapidly after IFN-beta induction (Figure 2A). The increase was significant as soon as 2 min after stimulation and reached a maximum at 10–15 min after stimulation, followed by a decrease that correlates with a substantial increase in the concentration of the SOCS1 protein (Figure 2C). A second, smaller peak was visible at around 180 min, followed by a subsequent decrease back to the baseline level after around 360 min. The quick decrease of phosphorylated STAT1 levels is in agreement with previous studies pointing to the activation of the negative feedback loop mediated by SOCS1 protein, which suppresses the phosphorylation of JAK1 and TYK2 proteins and prevents the formation of STAT-dimers [16]. The total level of STAT1 protein, on the other hand, is maintained practically constant until around 200 min after which it starts to increase slowly until the end of the experiments (Figure 2B). STAT1 mRNA levels grew quickly and continuously, starting sharply at around 75 min and leveling off after 200 min (Figure 3A). This increase in the mRNA level of STAT1, as soon as 1 hour after the induction of response by IFN-beta, agrees with the influence of the positive feedback loop IRF1 – STAT1

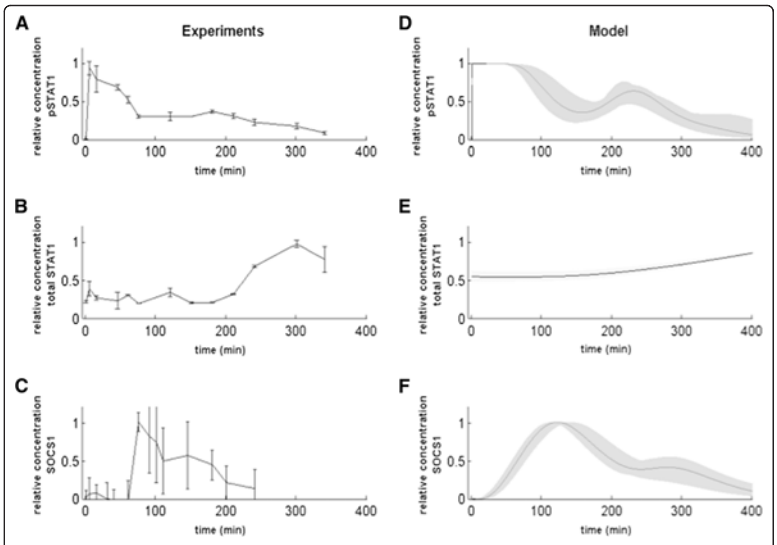

Figure 2 Activation of type I IFN pathway by IFN-beta in Raw cell line and the corresponding simulations from the ODE model. A-C) pSTAT1, STAT1 and SOCS1 protein concentration in cell lysates were measured by Luminex, Flow cytometry or ELISA after stimulation with IFN-beta (1000 units/ml). The data was normalized to the maximum level. **A)** pSTAT1 protein concentration in the Raw cells stimulated with IFN-beta; **(B)** Total STAT1 protein concentration in the Raw cells stimulated with IFN-beta; **C)** SOCS1 protein concentration in the Raw cells stimulated with IFN-beta. We plot here one out of three independent experiments, which were performed in duplicates. **D-F)** Model simulation and sensitivity analysis with ± 20% change for all parameters (shaded areas) **(D**: pSTAT1; **E**: STAT1; **F**: SOCS1**)**.

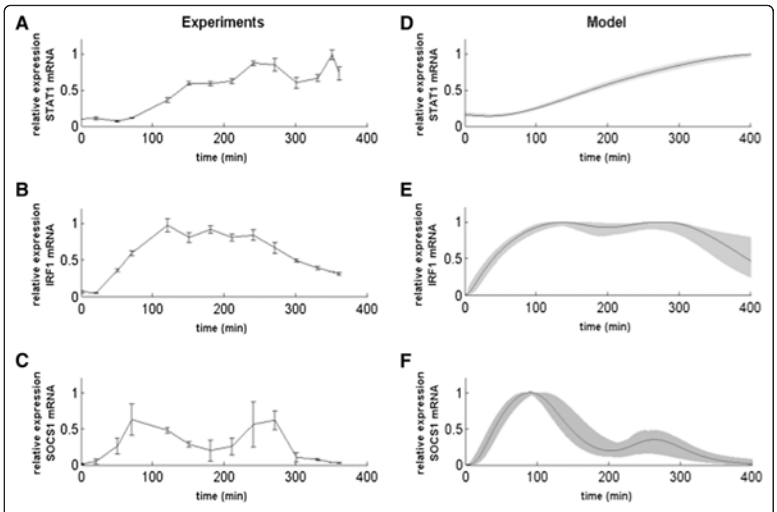

Figure 3 Gene expression levels of STAT1, IRF1 and SOCS1 after IFN-beta stimulation and the corresponding simulations from the ODE model. **A-C)** STAT1, IRF1 and SOCS1 RNA protein concentration in cell lysates were measured by RT-PCR in the Raw cells stimulated with IFN-beta (1000 units/ml); **A)** STAT1 RNA levels in the Raw cells stimulated with IFN-beta; **B)** IRF1 RNA levels in the Raw cells stimulated with IFN-beta; **C)** SOCS1 RNA levels in the Raw cells stimulated with IFN-beta. We plot here one out of three independent experiments, which were performed in duplicates. **D-F)** Model simulation and sensitivity analysis with ± 20% change for all parameters (shaded areas) for STAT1 **(D)**, IRF1 **(E)**, and SOCS1 **(F)** RNA levels.

[17] and confirms the importance of this circuit for the pathway dynamics.

To analyze the expression of regulatory genes of the type I IFN pathway, we measured the levels of two downstream STAT1 genes, SOCS1 (responsible of the negative feedback) and IRF1 (mediator of the positive feedback). We observed an oscillatory behavior of SOCS1 mRNA during the first 360 minutes after stimulation, with clear peaks at around 90 min and 250 min, before returning to baseline levels (Figure 3C). On the other hand, IRF1 shows different dynamics, with its concentration raising quickly between 30 and 120 min, then reaching a plateau and decreasing more slowly after 250 min (Figure 3B). We also quantified the expression levels of other downstream effector IFN-induced genes, such as MX1 and OAS1b, but did not identify any activation of their transcription in the RAW 264.7 cell line after IFN-beta stimulation (data not shown). These observations are in agreement with a differential signal transduction mechanism in macrophages when compared to canonical JAK-STAT pathway in lymphocytes [4,18]. Our observations show that in the RAW 264.7 cell line the main activated genes were the ones controlled by the STAT1-STAT1 homodimer (IRF1 and SOCS1) and containing GAS elements in their promoter region. These genes are mainly responsible for the antimicrobial activity of the cells [19].

Modeling the oscillatory signaling of type I IFN pathway

In order to identify the critical elements of the signaling pathway that are responsible for the transient oscillatory behavior observed experimentally in macrophages upon IFN-beta stimulation, we built an ODE model based in biological knowledge and experimental data (Figure 4). To minimize its complexity, we pursued the minimal system explaining the experimental observations, instead of a full descriptive system [14]. The model was not used to reproduce sustained endogenous IFN activation after viral infection, although it could be applied to that scenario.

The first ingredient of our model is the binding of IFN-beta to the receptor (with the concentration of activated receptor being represented by the variable S below). The activated receptor induces phosphorylation

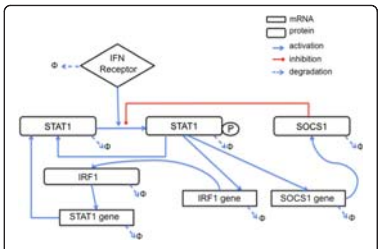

Figure 4 Mathematical model of type I IFN signaling pathway. Graphical representation of the biological processes modeled.

of the STAT1 protein (represented by A). Phosphorylated STAT1 translocates from the cytoplasm (A_{pc}) to the nucleus (A_{pn}) (Figure 4). In the nucleus, pSTAT1 complexes activate the transcription of SOCS1 and IRF1 genes. SOCS1 mRNA (r) is translated into SOCS1 protein (R), which inhibits further phosphorylation of STAT1. IRF1 mRNA (f) is translated to IRF1 protein (F), which activates the transcription of the STAT1 gene (with STAT1 mRNA being denoted by a). Each of the species has a certain linear degradation rate. We also introduced receptor internalization through an effective degradation (or deactivation) term, consistent with the literature [20]. With those ingredients, the model reads:

$$dS/dt = b_s - \lambda_s S$$

$$dA/dt = b_{\exp} A_{pn} + b_{deph} A_{pc} + b_A a - \frac{b_{ph} S A/k_A}{1 + A/k_A + (R/k_I)^q} - \lambda_{STAT} A$$

$$dA_{pc}/dt = \frac{b_{ph} S A/k_A}{1 + A/k_A + (R/k_I)^q} - b_{imp} A_{pc} - b_{deph} A_{pc} - \lambda_{STAT} A_{pc}$$

$$dA_{pn}/dt = b_{imp} A_{pc} - b_{\exp} A_{pn} - \lambda_{STAT} A_{pn}$$

$$dr/dt = b_r \frac{(A_{pn}/k_r)^n}{1 + (A_{pn}/k_r)^n} - \lambda_r r$$

$$dR/dt = b_R r - \lambda_R R$$

$$df/dt = b_f \frac{(A_{pn}/k_f)^m}{1 + (A_{pn}/k_f)^m} - \lambda_f f$$

$$dF/dt = b_F f - \lambda_F F$$

$$da/dt = b_a \frac{(F/k_F)^u}{1 + (F/k_F)^u} - \lambda_a a + B_{STAT}$$

The parameters correspond to transcription rates, including basal transcription of STAT (b_a, b_s, b_f, B_{STAT}), translation rates (b_A, b_R, b_F), cooperativity indexes (Hill coefficients, n, m, q, u), degradation rates (λ_i), receptor activation (b_S) and deactivation (λ_S) rates, phosphorylation and dephosphorylation rates (b_{ph}, b_{deph}), and nucleo-cytoplasmic transport rates (b_{imp}, b_{exp}). We adjusted some of the parameters using published data sources (Table 1), and the rest were estimated by manual fit of the model dynamics to the experimental data (Table 2) [21]. Initial conditions are listed in Table 3. The model implements the SOCS1-mediated negative feedback loop on pSTAT1 by means of a competitive inhibition term in the expression determining the phosphorylation rate of STAT1 in the equation for A_{pc}, with the parameter k_I quantifying the half-maximal inhibition threshold and the exponent q defining the sharpness of the inhibition. Similarly, the positive feedback through IRF1 is described by the transcription activation term of STAT1 mRNA in the equation for a, with k_F representing the half-maximal activation threshold.

The right panels in Figures 2 and 3 show simulation results corresponding to the experimental observations presented in the left panels. For comparative purposes, both the experimental and model variables were shown in relative concentrations dividing by their maximum value along the time series. We also performed a sensitivity analysis by simulating changes of ±20% for every model parameter, leading to deviations from the basal curve falling within the shaded areas shown in Figures 2 and 3.

The model simulations reproduce the main features observed experimentally, such as the first and very fast peak of phosphorylated STAT1 shortly after IFN-beta stimulation, and the second peak of smaller amplitude at around 200 min (Figure 2D). The concentration of total STAT1 protein is almost constant during the first 200 min, after which the protein level increases slowly (Figure 2E), following the increased expression level of STAT1 mRNA, which mRNA grows slowly starting at around 50 min after stimulation (Figure 3D). In turn, SOCS1 mRNA levels

Table 1 Parameter values obtained from the literature

Parameter	Value	Reference
b_{deph}	15 min half-life	[36,37]
n	3	[38]
u	1	[39]
λ_r	2.82 hour half-life	This work
λ_f	1.23 hour half-life	[40]
A initial	10^5 molecules/cell	[41]
S initial	700-900 receptors/cell	[42]
$\lambda_{STAT\ protein}$	24 hour half-life	[43]
λ_F	30 min half-life	[44]
f initial	1 molecule/cell	[45]

Table 2 Parameters for type I IFN ODE model

Name	Symbol	Value	Unity
Translation rate for STAT1	b_A	65	min^{-1}
Receptor production rate	b_S	0	min^{-1}
Basal STAT1 RNA	B_{STAT1}	0.0062	min^{-1}
Transcription rate for STAT1	b_a	0.1	min^{-1}
Transcription rate for SOCS1	b_r	12.8	min^{-1}
Transcription rate for IRF1	b_f	2.7	min^{-1}
Translation rate for IRF1	b_F	$1.0 \cdot 10^1$	min^{-1}
Translation rate for SOCS1	b_R	$1.0 \cdot 10^2$	min^{-1}
Phosphorylation STAT1 rate	b_{ph}	$1.3 \cdot 10^3$	min^{-1}
Dephosphorylation STAT1 rate	b_{deph}	0.036	min^{-1}
Import to the nucleus rate (pSTAT1)	b_{imp}	0.013	min^{-1}
Export from the nucleus rate (STAT1)	b_{exp}	0.048	min^{-1}
STAT1 phosphorylation activation (Hill's constant; half maximal activation)	k_A	4680	molecules
Dissociation constant for the enzyme-inhibitor by SOCS1 (Hill's constant; half maximal activation)	k_I	82680	molecules
SOCS1 transcription activation by nuclear pSTAT1 (Hill's constant; half maximal activation)	k_r	23400	molecules
IRF1 transcriptional activation by pSTAT1	k_f	7366	molecules
STAT1 transcriptional activation by IRF1	k_F	$1.3 \cdot 10^5$	molecules
Cooperativity of SOCS1 protein over STAT1 dimers	q	4	
Cooperativity of STAT1 on SOCS1 gene promoter	n	3	
Cooperativity of STAT1 on IRF1 gene promoter	m	2	
Cooperativity of IRF1 on STAT1 gene promoter	u	1	
Receptor internalization/degradation rate	λ_S	0.0229	min^{-1}
SOCS1 RNA degradation rate	λ_r	0.0347	min^{-1}
SOCS1 protein degradation rate	λ_R	0.0231	min-1
IRF1 RNA degradation rate	λ_f	0.0173	min^{-1}
IRF1 protein degradation rate	λ_F	0.0116	min^{-1}
STAT1 RNA degradation rate	λ_a	0.0058	min^{-1}
STAT1 protein degradation rate	λ_{STAT}	0.0007	min^{-1}

increase from the beginning, showing a first peak at around 90 min and a second smaller peak following the second peak of phosphorylated STAT1 at around 250 min (Figure 3F), in agreement with the experiments. Again similarly to the experiments, IRF1 mRNA levels show a bell-shaped time course (Figure 3E), with an increase resembling that of SOCS1 mRNA levels (Figure 3F) and remaining high from around 90 min to 250 min, when IRF1 mRNA levels decrease to half their maximum value at around 350 min.

Table 3 Initial conditions for type I IFN model simulations

Name	Symbol	Value
Non-phosphorylated STAT1	A	$1.0 \cdot 10^5$ molecules
IFN activation receptor	S	1000 molecules
Phosphorylated nuclear STAT1	Apn	1 molecule
Phosphorylated cytoplasmic STAT1	Apc	10 molecules
STAT1 mRNA	a	1 molecule
IRF1 mRNA	f	1 molecule
SOCS1 mRNA	r	1 molecule
IRF1 protein	F	1 molecules
SOCS1 protein	R	1 molecule

The model allows us to interpret the second peak observed experimentally in pSTAT1 and SOCS1-mRNA levels in terms of an underlying damped oscillatory dynamics. We now ask what are the mechanisms leading to oscillations, on the one hand, and to damping, on the other hand. A well-known gene circuit architecture that leads to oscillatory behavior is a combination of positive and negative feedback loops [22]. As mentioned above, our model contains a negative feedback loop mediated by SOCS1. We can examine in the model the effect of not having this feedback by eliminating SOCS1 signaling from the model. The results show that this negative feedback is required for the oscillatory behavior to arise: its absence leads to a transient plateau of high pSTAT1 levels during the first 4–5 h of IFN treatment (Figure 5B), which contrasts with the relaxation oscillator behavior obtained for our basal parameter values (Figure 5A), which is a closer match to the experimental observations (Figures 2–3). The model also contains a positive feedback loop mediated by IRF1. This loop, however, does not appear to be crucial for the oscillatory behavior of pSTAT1 (Figure 5C), and is only necessary to reproduce the experimentally observed increase of STAT1 expression (Figure 3A D).

The combination of negative and positive feedbacks discussed in the preceding paragraph would naturally lead to sustained oscillatory behavior. The experimental observations shown in Figures 2 and 3, however, reveal a strong damping of the oscillations that lead to their sudden disappearance. This behavior is not consistent with the standard damping undergone by nonlinear oscillations when they become unstable via a Hopf bifurcation, in which case the damping is either slow close to the bifurcation, or the damped oscillations are too weak to begin with far away from the bifurcation. A key distinctive characteristic of our model is the fact that the external input to which the system is subject (mediated by the activated receptors represented by S in the model above) decays monotonously due to receptor inactivation by internalization or degradation [20,23]. Assuming

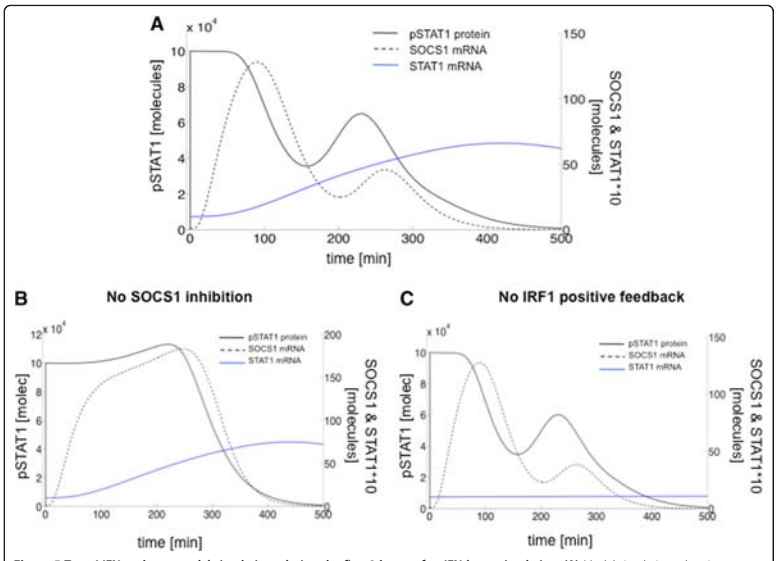

Figure 5 Type I IFN pathway model simulations during the first 8 hours after IFN-beta stimulation. (A) Model simulations showing oscillations of total (nuclear plus cytoplasmic) pSTAT1 protein, SOCS1 mRNA expression (dashed line) and STAT1 mRNA expression (dotted line). **(B)** Corresponding simulations where the SOCS1-mediated negative feedback is disrupted by assuming an infinite value of the repression threshold k_I. **(C)** Corresponding simulations not including the IRF1-mediated positive feedback, by assuming a zero value of the STAT1 activation threshold k_F (which leads to saturation of the corresponding Hill function, so that the dependence of a expression on F is removed).

a linear decay, the external input decreases exponentially (Figure 6A), taking the system quickly out of the oscillatory regime and thus leading to a strong damping of the oscillations, as seen experimentally. Exploring systematically the dependence of the dynamics on the receptor level, we observed that as the initial levels of activated receptor decrease (Figure 6A) the second peak of both pSTAT1 (Figure 6B) and SOCS1 mRNA (Figure 6C) levels diminish, with the SOCS1 expression peak disappearing earlier than the pSTAT1 concentration peak.

Bifurcation analysis of the STAT1 pathway model identifies translocation to the nucleus as a critical step

The temporal evolution of the phosphorylation of STAT1 can be crucial for understanding the response to IFN-beta therapy, and may provide an explanation of the lack of response to this therapy in some cases [24]. In particular, transient oscillatory dynamics could provide a way for the STAT1 pathway to increase the duration of its response to IFN-beta in a physiological manner (i.e. without a period of sustained constant activation as in Figure 5B). In order to establish the conditions under which this transient dynamics exists, we analyzed the behavior of the system for combinations of two-parameter pairs, distinguishing between the parameter values for which pSTAT dynamics is overdamped (and thus non-oscillatory) and those for which the oscillations are underdamped (which corresponds to the experimental situation reported above). We focused on the phosphorylation and dephosphorylation rates (b_{ph} and b_{deph}) and export and import rates (b_{exp} and b_{imp}). These parameters represent crucial steps to regulate the nuclear availability of transcription factors such as pSTAT dimers, and thus also the expression of downstream genes.

In order to identify mathematically the two different dynamical regimes mentioned above, we examined the stability properties of the steady state of the ODE system for a constant activated receptor level (S) equal to its

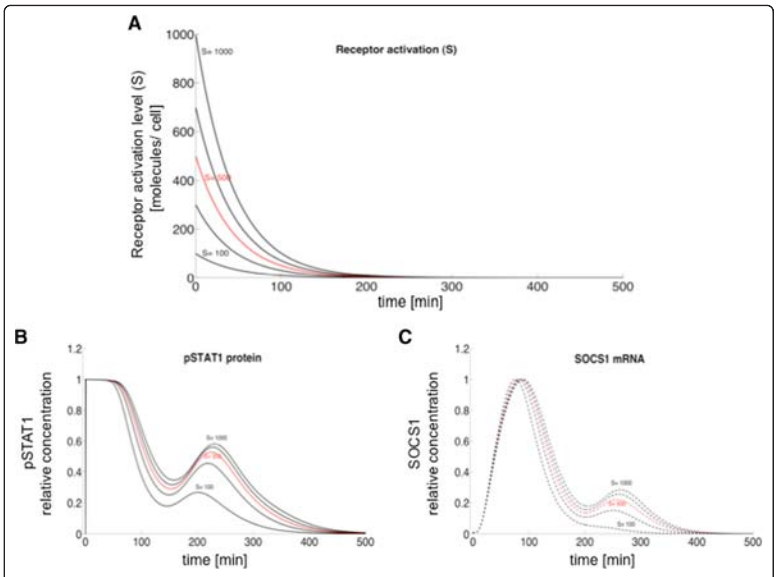

Figure 6 Influence of activated receptor level on the transient oscillatory dynamics. (A) Time evolution of the activation level of type I IFN receptors in the model (*S*) by stimulation with IFN-beta (added at $t = 0$) for different initial levels (in red, $S = 500$ molecules at $t = 0$). **(B, C)** pSTAT1 **(B)** and SOCS1 mRNA **(C)** dynamic responses for varying levels of initial receptor activation as in panel **A** (lower lines in **B** and **C** correspond to lower lines in **A**).

initial value. In that context, the underdamped/oscillatory regime is characterized by a steady state that takes the form of an unstable focus (i.e. the stability eigenvalue with maximum real part has negative imaginary part), whereas the steady state in the overdamped/non-oscillatory regime is a node (the stability eigenvalue with maximum real part has no imaginary component). In that way, by calculating the imaginary part of the stability eigenvalue of the steady state with maximum real part, we can identify the parameter regions in which the pathway exhibits a transient oscillatory response to IFN-beta. The result, for the parameter space formed by the phosphorylation and dephosphorylation rates b_{ph} and b_{deph}, is shown in Figure 7A. This figure shows, on the one hand, the prevalence of oscillations for a wide range of these parameters, and on the other hand it tells us the conditions for which transient oscillations exist. For instance, increasing sufficiently the dephosphorylation rate can transform an oscillatory regime into a non-oscillatory one, and reversely, by making the phosphorylation rate large enough the system can be made to exhibit transient oscillations. Figure 7B shows examples of these two dynamical regimes for two specific parameter sets within this phase diagram.

We also tested the influence of the import rate of pSTAT1 molecules into the nucleus, and of the export rate of STAT1 from the nucleus into the cytosol. By tuning both parameters (b_{exp} and b_{imp}) simultaneously, we observed again that the transient oscillatory regime is prevalent in this system (Figure 7C). We found that the oscillatory regime is associated with high nuclear import rates in combination with high export rates. For high export rates but low import rates, the pathway exhibits an overdamped (non-oscillatory) response, showing a sustained plateau in the transient level of pSTAT1 (discontinuous blue line in Figure 7D). Conversely, for high import rates and low export rates the response is also

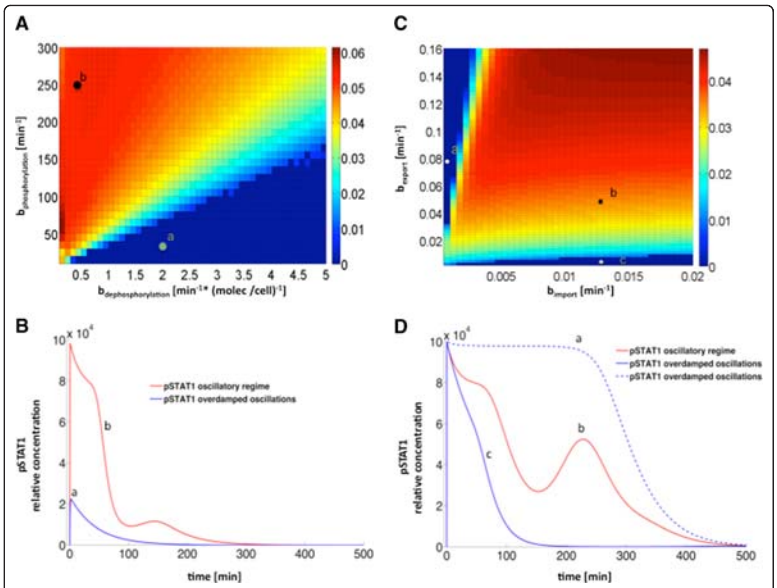

Figure 7 Stability analysis of the steady state solution in two 2D parameter spaces. (A, C) The color scale represents the absolute value of the imaginary part of the stability eigenvalue with maximum real part, corresponding to the steady state of the system after IFN stimulation, for varying phospho/ dephosphorylation rates (b_{ph} and b_{deph}, panel **A**), and nuclear export/import rates (b_{exp} and b_{imp}, panel **B**). Two distinct dynamic regimes can be identified with this analysis: the damped oscillatory regime (shifted to red) and the overdamped/ non-oscillatory regime (blue). **(B, D)** Examples of pSTAT1 time evolution in both regimes (damped and over-damped in red/blue lines, respectively) corresponding to parameter position of circle markers for the two diagrams shown in panels **A** and B, respectively.

overdamped, but with a faster decay (continuous blue line in Figure 7D).

Discussion

The aim of this work was to characterize the dynamics of the key components of the type I IFN-beta signaling pathway in macrophage RAW 264.7 cells. This system robustly translates extracellular chemical signals through cell membrane receptors, leading to phosphorylation of the STAT transcription factors, which induce gene expression of multiple targets. JAK/STAT signaling directly regulates the immune system response under viral or bacterial infection, and is also important in autoimmune diseases and cancer treatments. The IFN signaling network affects different complex pathways, involving processes such as differentiation, proliferation, survival and cell death. Importantly, it is a canonical pathway involved in first-line treatments of multiple sclerosis as a main target of the IFN system [25] but, also, affects different complex pathways, involving processes such as differentiation, proliferation or survival and cell death [26,27].

In this paper, we used a combination of experimental approaches in order to obtain a quantitative picture of the response of the JAK/STAT signaling pathway to IFN-beta stimulation, and to identify the most relevant aspects of its dynamics to be modeled with kinetic equations. Experiments uncovered several important features of JAK/STAT signaling dynamics during the first eight hours after treatment with IFN-beta. For example, our results showed the transient oscillatory nature of STAT1 activation (pSTAT1), with a fast increase in cytosol concentration early after stimulation (within the first hour), followed by a secondary concentration peak at around 200 min. A key STAT1

transcription target such as SOCS1 also showed two peaks of expression (correlated in time to the pSTAT peaks) at around 90 min and 250 min after stimulation, whereas another important target, namely IRF1, exhibited a more bell-shaped plateau signal, respectively (Figures 2 and 3). Our model simulations also exhibit a transient oscillatory behavior in pSTAT1 concentration, and reveal that the oscillations require the presence of a negative feedback loop on STAT1, mediated by its phosphorylation inhibitor SOCS1. Previous mathematical models of the type I and type II IFN pathways have suggested the possibility that STAT1 pathway has an oscillatory behavior [9,13] and indicated the importance of the SOCS1 negative feedback [10,14,28,29]. Another factor that has been proposed to be important in defining the response to IFN is the basal level of receptors of the JAK/STAT pathway [30]. In our model this aspect was also taken into account, showing clear effects on the dynamics of the pathway response (Figure 6). Going beyond previous models, our theoretical results show that the physiological regime of the pathway's response to IFN-beta takes the form of damped oscillations that can be identified by means of a stability analysis of the model's steady state solution. This analysis shows that processes such as the phosphorylation and dephosphorylation of pSTAT1, and the transport of STAT1 between the nuclear and cytosol compartments, can make the pathway switch between underdamped and overdamped oscillatory regimes [31].

Implications of the type I IFN signaling dynamics in autoimmune diseases

IFN-beta is the most common treatment for MS [32], exerting a pleiotropic immunomodulatory activity not well understood [25]. IFN-beta treatment decreases activation, proliferation, cytokine release, and migratory properties of activated T cells, diminishing their ability to enter and damage the brain tissue. In spite of these properties, up to 40% of patients do not respond to IFN-beta therapy, which represents a significant health problem [24]. Previous genomic studies have identified certain genes belonging to the IFN pathway that are associated with a lack of response to IFN-beta, suggesting that the genetic background of certain individuals may modulate this pathway, and consequently the response to therapy, by specific transcriptional profiles [33]. For example, it was recently shown that the response to IFN-beta differs between immune cells, and an analysis of non-responders to IFN-beta therapy indicates an impairment of the type I IFN pathway in the monocytes of those patients [6,34].

Our study indicates the importance of identifying the temporal dynamics of the concentration of certain key components of the JAK-STAT pathway, such as the phosphorylated form of the STAT1 protein, and of the expression of interferon-stimulated transcription genes like SOCS1 and IRF1, within the first 8 hours of IFN-beta administration. Cataloguing these dynamics could provide us with early molecular biomarkers that allow us to distinguish the lack of response to IFN-beta therapy of certain MS patients.

Methods

Materials and reagents

Cells were obtained from ATCC library, mouse recombinant IFN-beta was purchased from Cell sciences, lipopolysaccharide from Escherichia coli and poly(I:C) salt was purchased from Sigma-Albrich, lipofectamine 2000, Hiperfect transfection agent were purchased from QIAGEN, Taqman PCR master mix, VIC-dye GAPDH endogenous control, IRF1, SOCS1, STAT1, STAT2, MX1, OAS1a pre-designed FAM-dye assays were purchased from Applied Biosystems, total STAT1 and STAT1(pTyr701) antibodies and beads, cell detection kit for xMAp assays were purchased from Merck Millipore (Billerica). Alexa Flour 647 STAT1 (pTyr701) and PE STAT1 N-terminal anti-Mouse antibodies and all buffers for cytometry were purchased from BD biosciences. APC-labelled IFNAR1 antibody was purchased from Biolegend.

Cell culture and stimulation

Mouse leukemic monocyte macrophage cell line RAW 264.7 cell line was purchased from ATCC and maintained in DMEM medium complemented with 10% fetal bovine serum and 1% antibiotics at 37°C and 5% CO2. The cells were passed every 2–3 days and maintained in 20-80% surface coverage. One day before the stimulation the cells were seeded in 12 well plates in concentration 1×10^6 cells/well. The cells were stimulated with 1000 units of recombinant mouse IFN-beta, 15 μg of LPS for different times or 15 μg of poly (I:C) solution. At the end of stimulation supernatants or cells were collected for further analysis. The same amount of PBS was added at the corresponding time-points to the control samples.

RT-PCR

Cell lysates were prepared with QiaShredder columns and total RNA was isolated using standard Qiagen Rnaesy Mini kit protocol. Equal amount of total RNA was added to each reverse transcription reaction tube (High-Capacity cDNA Reverse Transcription Kit from Applied Biosystems and cDNA was used for a second step of RT-PCR. Results were analyzed using relative 2CTT method normalized to a GAPDH endogenous control (VIC-dye primer-limited control from Applied Biosystems) as described before [35]. All the qRT-PCR experiments were performed in triplicates and repeated three times independently.

Western blot and quantification

Western blot (WB) was performed using polyclonal rabbit anti-mouse pSTAT1 and STAT1 N-terminal antibodies (Abcam) using standard WB protocol. Western blot results were quantified using ImageJ software (http://rsb.info.nih.gov/ij/index.html) using the method of Luke Miller (http://www.lukemiller.org/journal/2007/08/quantifying-western-blots-without.html)

ELISA and xMAP multiplexing assays

IFN-beta in culture supernatants and SOCS1 protein concentration in cell lysates were measured by standard sandwich ELISA with anti-mouse SOCS1 antibodies (Abcam). IRF1 protein concentration in cell lysates was measured by in-cell ELISA using the kit (Thermo Scientific) STAT1 total protein and phosphorylated state (Tyr701) concentrations (nuclear and cytoplasmic together) were measured using xMAP assays and read in Luminex 201 platform using standard vacuum separation protocol (Millipore). xMAP experiments were repeated twice.

Flow cytometry

Cells for flow cytometry were stimulated with 1,000 μn/ml of IFN-beta as stated before and fixed immediately after stimulation. IFNAR1 receptor on the surface of the RAW 264.7 cells was marked using APC-labelled anti-IFNAR antibody. The mean fluorescent intensity was calculated using FlowJo software. For STAT1 staining cells were fixed immediately after stimulation in order to preserve phosphorylation and then permeabilized using Perm III buffer (BD biosciences). Samples were stained simultaneously with anti-STAT1 (pTyr701) and anti-STAT1 total (N-terminus) antibodies. The mean fluorescent intensity, the percent of staining-positive cells, the medians and the standard deviation were calculated using FlowJo software and the raw single-cell data were extracted to plot the histograms and further analysis.

Mathematical modeling

The model and simulations were run in MATLAB using the ODE15s solver (Matlab codes are provided in the Additional files 1, 2 and 3). The stability analysis of the dynamical system was performed with custom-made Matlab codes.

Availability of supporting data

The model is available as a matlab script in the supporting materials. The raw experimental data are available from the authors upon request.

Additional files

Additional file 1: Type I IFN pathway ODE model equations.

Additional file 2: Type I IFN pathway ODE model as Matlab file.

Additional file 3: Integration and solutions of the Type I IFN pathway ODE model as Matlab file.

Abbreviations

ODE: ordinary differential equations; STAT1: Signal Transducers and Activators of Transcription 1; SOCS1: Suppressor of cytokine signaling 1; IRF1: Interferon regulatory factor 1; AAF: IFNA-activated-factor; ISRE: Interferon-sensitive response element; GAS: Interferon-Gamma Activated Sequence; ISGF3: IFN-stimulated regulatory factor 3; IFNbeta: interferon beta; IFNg: interferon gamma; LPS: Lipopolysaccharide; poly(I:C): Polyinosinic:polycytidylic acid; RT-PCR: quantitative reverse transcription polymerase chain reaction; GAPDH: Glyceraldehyde 3-phosphate dehydrogenase; FAM: Fluorescein amidite; ELISA: Enzyme-Linked Immunosorbent Assay; OAS1a - 2'-5': oligoadenylate synthetase 1 gene; MX1: Interferon-induced GTP-binding protein gene.

Competing interests

The authors declare no competing interests.

Authors' contributions

Study design: IP, PV, JGO, NDP; In vitro experiments: IP; Mathematical model: NDP, EA, IP; Analysis of the data: EA, IP, NDP; Writing article: PV, IP, EA, JGO. All authors read and approved the final manuscript.

Acknowledgements

This work was supported by the EU 6FP ComplexDis project (NEST-043241), the EU 7FP – Marie Curie initial training network UEPHA*MS (ITN-212877) and Fundacion Cellex to PV; by the Spanish network of excellence in MS of the Instituto de Salud Carlos III, Spain to PV and JGO (RD07/0060) and by the Fundación Mutua Madrileña to PV and JGO; by a grant of the Ministerio de Economia y Competitividad and Fondo Europeo de Desarrollo Regional (Spain, project FIS2012-37655) and by the ICREA Academia program to JGO.

Author details

[1]Center of Neuroimmunology, Institut d'Investigacions Biomèdiques August Pi i Sunyer (IDIBAPS), Hospital Clinic of Barcelona, Barcelona, Spain. [2]Department of Experimental and Health Sciences, Universitat Pompeu Fabra, Barcelona, Spain. [3]Department of Physics and Nuclear Engineering, Universitat Politecnica de Catalunya, Spain.

Received: 8 February 2013 Accepted: 5 July 2013
Published: 9 July 2013

References

1. Rawlings JS, Rosler KM, Harrison DA: **The JAK/STAT signaling pathway.** *J Cell Sci* 2004, **117**(Pt 8):1281–1283.
2. Imada K, Leonard WJ: **The Jak-STAT pathway.** *Mol Immunol* 2000, **37**(1–2):1–11.
3. Qin H, Wilson CA, Lee SJ, Benveniste EN: **IFN-beta-induced SOCS-1 negatively regulates CD40 gene expression in macrophages and microglia.** *Faseb J* 2006, **20**(7):985–987.
4. van Boxel-Dezaire AH, Zula JA, Xu Y, Ransohoff RM, Jacobberger JW, Stark GR: **Major differences in the responses of primary human leukocyte subsets to IFN-beta.** *J Immunol* 2010, **185**(10):5888–5899.
5. Hervas-Stubbs S, Perez-Gracia JL, Rouzaut A, Sanmamed MF, Le Bon A, Melero I: **Direct effects of type I interferons on cells of the immune system.** *Clin Cancer Res* 2011, **17**(9):2619–2627.
6. Oliver-Martos B, Orpez T, Pinto-Medel MJ, Mayorga C, Garcia-Leon JA, Maldonado-Sanchez R, Suardiaz M, Guerrero M, Luque G, Leyva L, Fernandez O: **Gene expression in IFNss signalling pathway differs between monocytes, CD4 and CD8 T cells from MS patients.** *J Neuroimmunol* 2011, **230**(1–2):153–159.
7. Starr R, Hilton DJ: **SOCS: suppressors of cytokine signalling.** *Int J Biochem Cell Biol* 1998, **30**(10):1081–1085.
8. Raza S, Robertson KA, Lacaze PA, Page D, Enright AJ, Ghazal P, Freeman TC: **A logic-based diagram of signalling pathways central to macrophage activation.** *BMC Syst Biol* 2008, **2**:36.
9. Qiao L, Phipps-Yonas H, Hartmann B, Moran TM, Sealfon SC, Hayot F: **Immune response modeling of interferon beta-pretreated influenza virus-infected human dendritic cells.** *Biophys J* 2010, **98**(4):505–514.

10. Smieja J, Jamaluddin M, Brasier AR, Kimmel M: **Model-based analysis of interferon-beta induced signaling pathway.** *Bioinformatics* 2008, **24**(20):2363–2369.
11. Vera J, Rateitschak K, Lange F, Kossow C, Wolkenhauer O, Jaster R: **Systems biology of JAK-STAT signalling in human malignancies.** *Prog Biophys Mol Biol* 2011, **106**(2):426–434.
12. Swameye I, Muller TG, Timmer J, Sandra O, Klingmuller U: **Identification of nucleocytoplasmic cycling as a remote sensor in cellular signaling by databased modeling.** *Proc Natl Acad Sci USA* 2003, **100**(3):1028–1033.
13. Soebiyanto RP, Sreenath SN, Qu CK, Loparo KA, Bunting KD: **Complex systems biology approach to understanding coordination of JAK-STAT signaling.** *Biosystems* 2007, **90**(3):830–842.
14. Yamada S, Shiono S, Joo A, Yoshimura A: **Control mechanism of JAK/STAT signal transduction pathway.** *FEBS Lett* 2003, **534**(1–3):190–196.
15. Shudo E, Yang J, Yoshimura A, Iwasa Y: **Robustness of the signal transduction system of the mammalian JAK/STAT pathway and dimerization steps.** *J Theor Biol* 2007, **246**(1):1–9.
16. Endo TA, Masuhara M, Yokouchi M, Suzuki R, Sakamoto H, Mitsui K, Matsumoto A, Tanimura S, Ohtsubo M, Misawa H, Miyazaki T, Leonor N, Taniguchi T, Fujita T, Kanakura Y, Komiya S, Yoshimura A: **A new protein containing an SH2 domain that inhibits JAK kinases.** *Nature* 1997, **387**(6636):921–924.
17. Nguyen H, Lin R, Hiscott J: **Activation of multiple growth regulatory genes following inducible expression of IRF-1 or IRF/RelA fusion proteins.** *Oncogene* 1997, **15**(12):1425–1435.
18. Lucas DM, Lokuta MA, McDowell MA, Doan JE, Paulnock DM: **Analysis of the IFN-gamma-signaling pathway in macrophages at different stages of maturation.** *J Immunol* 1998, **160**(9):4337–4342.
19. Sadler AJ, Williams BR: **Interferon-inducible antiviral effectors.** *Nat Rev Immunol* 2008, **8**(7):559–568.
20. Piganis RA, De Weerd NA, Gould JA, Schindler CW, Mansell A, Nicholson SE, Hertzog PJ: **Suppressor of cytokine signaling (SOCS) 1 inhibits type I interferon (IFN) signaling via the interferon alpha receptor (IFNAR1)-associated tyrosine kinase Tyk2.** *J Biol Chem* 2011, **286**(39):33811–33818.
21. Toni T, Stumpf MP: **Parameter inference and model selection in signaling pathway models.** *Methods Mol Biol* 2010, **673**:283–295.
22. Garcia-Ojalvo J: **Physical approaches to the dynamics of genetic circuits: a tutorial.** *Contemporary Physics* 2011, **52**(5):439–464.
23. Marijanovic Z, Ragimbeau J, van der Heyden J, Uze G, Pellegrini S: **Comparable potency of IFNalpha2 and IFNbeta on immediate JAK/STAT activation but differential down-regulation of IFNAR2.** *Biochem J* 2007, **407**(1):141–151.
24. Villoslada P, Oksenberg JR, Rio J, Montalban X: **Clinical characteristics of responders to interferon therapy for relapsing MS.** *Neurology* 2004, **62**(9):1653. author reply 1653.
25. Javed A, Reder AT: **Therapeutic role of beta-interferons in multiple sclerosis.** *Pharmacol Ther* 2006, **110**(1):35–56.
26. Samuel CE: **Antiviral actions of interferons.** *Clin Microbiol Rev* 2001, **14**(4):778–809. table of contents.
27. Lohoff M, Mak TW: **Roles of interferon-regulatory factors in T-helper-cell differentiation.** *Nat Rev Immunol* 2005, **5**(2):125–135.
28. Rateitschak K, Karger A, Fitzner B, Lange F, Wolkenhauer O, Jaster R: **Mathematical modelling of interferon-gamma signalling in pancreatic stellate cells reflects and predicts the dynamics of STAT1 pathway activity.** *Cell Signal* 2010, **22**(1):97–105.
29. Ramgolam VS, Markovic-Plese S: **Regulation of suppressors of cytokine signaling as a therapeutic approach in autoimmune diseases, with an emphasis on multiple sclerosis.** *J Signal Transduct* 2011, **2011**:635721.
30. Zurney J, Howard KE, Sherry B: **Basal expression levels of IFNAR and Jak-STAT components are determinants of cell-type-specific differences in cardiac antiviral responses.** *J Virol* 2007, **81**(24):13668–13680.
31. Takaoka A, Yanai H: **Interferon signalling network in innate defence.** *Cell Microbiol* 2006, **8**(6):907–922.
32. Marta M, Giovannoni G: **Disease modifying drugs in multiple sclerosis: mechanisms of action and new drugs in the horizon.** *CNS Neurol Disord Drug Targets* 2012, **11**(5):610–623.
33. Rio J, Comabella M, Montalban X: **Predicting responders to therapies for multiple sclerosis.** *Nat Rev Neurol* 2009, **5**(10):553–560.
34. Comabella M, Lunemann JD, Rio J, Sanchez A, Lopez C, Julia E, Fernandez M, Nonell L, Camina-Tato M, Deisenhammer F, Caballero E, Tortola MT, Prinz M, Montalban X, Martin R: **A type I interferon signature in monocytes is associated with poor response to interferon-beta in multiple sclerosis.** *Brain* 2009, **132**(Pt 12):3353–3365.
35. Palacios R, Goni J, Martinez-Forero I, Iranzo J, Sepulcre J, Melero I, Villoslada P: **A network analysis of the human T-cell activation gene network identifies JAGGED1 as a therapeutic target for autoimmune diseases.** *PLoS ONE* 2007, **2**(11):e1222.
36. Haspel RL, Salditt-Georgieff M, Darnell JE Jr: **The rapid inactivation of nuclear tyrosine phosphorylated Stat1 depends upon a protein tyrosine phosphatase.** *Embo J* 1996, **15**(22):6262–6268.
37. Gao C, Guo H, Mi Z, Grusby MJ, Kuo PC: **Osteopontin induces ubiquitin-dependent degradation of STAT1 in RAW264.7 murine macrophages.** *J Immunol* 2007, **178**(3):1870–1881.
38. Qin H, Niyongere SA, Lee SJ, Baker BJ, Benveniste EN: **Expression and functional significance of SOCS-1 and SOCS-3 in astrocytes.** *J Immunol* 2008, **181**(5):3167–3176.
39. Wong LH, Sim H, Chatterjee-Kishore M, Hatzinisiriou I, Devenish RJ, Stark G, Ralph SJ: **Isolation and characterization of a human STAT1 gene regulatory element. Inducibility by interferon (IFN) types I and II and role of IFN regulatory factor-1.** *J Biol Chem* 2002, **277**(22):19408–19417.
40. Sharova LV, Sharov AA, Nedorezov T, Piao Y, Shaik N, Ko MS: **Database for mRNA half-life of 19 977 genes obtained by DNA microarray analysis of pluripotent and differentiating mouse embryonic stem cells.** *DNA Res* 2009, **16**(1):45–58.
41. Wenta N, Strauss H, Meyer S, Vinkemeier U: **Tyrosine phosphorylation regulates the partitioning of STAT1 between different dimer conformations.** *Proc Natl Acad Sci USA* 2008, **105**(27):9238–9243.
42. Killion JJ, Fishbeck R, Bar-Eli M, Chernajovsky Y: **Delivery of interferon to intracellular pathways by encapsulation of interferon into multilamellar liposomes is independent of the status of interferon receptors.** *Cytokine* 1994, **6**(4):443–449.
43. Andrejeva J, Young DF, Goodbourn S, Randall RE: **Degradation of STAT1 and STAT2 by the V proteins of simian virus 5 and human parainfluenza virus type 2, respectively: consequences for virus replication in the presence of alpha/beta and gamma interferons.** *J Virol* 2002, **76**(5):2159–2167.
44. Nakagawa K, Yokosawa H: **Degradation of transcription factor IRF-1 by the ubiquitin-proteasome pathway.** *The C-terminal region governs the protein stability. Eur J Biochem* 2000, **267**(6):1680–1686.
45. Fujita T, Reis LF, Watanabe N, Kimura Y, Taniguchi T, Vilcek J: **Induction of the transcription factor IRF-1 and interferon-beta mRNAs by cytokines and activators of second-messenger pathways.** *Proc Natl Acad Sci USA* 1989, **86**(24):9936–9940.

doi:10.1186/1752-0509-7-59
Cite this article as: Pertsovskaya *et al.*: Transient oscillatory dynamics of interferon beta signaling in macrophages. *BMC Systems Biology* 2013 **7**:59.